CAPITAL UNIVERSITY OF SCIENCE AND
TECHNOLOGY, ISLAMABAD

A Specific Comparative Study of Casson and Carreau Nanofluids

by

Areej Fatima

A thesis submitted in partial fulfillment for the
degree of Master of Philosophy

in the

Faculty of Computing
Department of Mathematics

2019

Dedicated to my beloved Parents, Siblings and dignified Teachers, who have taught me to work diligently for the things that I aspire to achieve.

CERTIFICATE OF APPROVAL

A Specific Comparative Study of Casson and Carreau Nanofluids

by

Areej Fatima

(MMT173022)

THESIS EXAMINING COMMITTEE

S. No.	Examiner	Name	Organization
(a)	External Examiner	Dr. Manshoor Ahmed	COMSATS, Islamabad
(b)	Internal Examiner	Dr. Shafqat Hussain	CUST, Islamabad
(c)	Supervisor	Dr. Muhammad Sagheer	CUST, Islamabad

Dr. Muhammad Sagheer
Thesis Supervisor
September, 2019

Dr. Muhammad Sagheer
Head
Dept. of Mathematics
September, 2019

Dr. Muhammad Abdul Qadir
Dean
Faculty of Computing
September, 2019

Author's Declaration

I, **Areej Fatima** hereby state that my M.Phil thesis titled "**A Specific Comparative Study of Casson and Carreau Nanofluids**" is my own work and has not been submitted previously by me for taking any degree from Capital University of Science and Technology, Islamabad or anywhere else in the country/abroad.

At any time if my statement is found to be incorrect even after my graduation, the University has the right to withdraw my M.Phil Degree.

Areej Fatima

(MMT173022)

Plagiarism Undertaking

I solemnly declare that research work presented in this thesis titled "***A Specific Comparative Study of Casson and Carreau Nanofluids***" is solely my research work with no significant contribution from any other person. Small contribution/help wherever taken has been dully acknowledged and that complete thesis has been written by me.

I understand the zero tolerance policy of the HEC and Capital University of Science and Technology towards plagiarism. Therefore, I as an author of the above titled thesis declare that no portion of my thesis has been plagiarized and any material used as reference is properly referred/cited.

I undertake that if I am found guilty of any formal plagiarism in the above titled thesis even after award of M.Phil Degree, the University reserves the right to withdraw/revoke my M.Phil degree and that HEC and the University have the right to publish my name on the HEC/University website on which names of students are placed who submitted plagiarized work.

Areej Fatima

(MMT173022)

Acknowledgements

First, I would like to thank Almighty Allah for blessing me with knowledge and making it easier for me to pursue M.Phil study.

I am most sincerely and heartily grateful to my honourable supervisor, and my mentor **Dr. Muhammad Sagheer**, for his support throughout this research. I would like to express my deepest appreciation to him for the suggestions he has made to enhance the quality of this thesis. By working under his supervision, I have not just acquired technical knowledge but also learnt about being a good human. I also wish to thank him for always being there for discussions on this thesis despite his extremely busy schedule.

I owe my profound gratitude to **Dr. Shafqat Hussain** for his superb guidance and inexhaustible inspiration throughout this thesis. Without his tireless help, I would have not been able to commence this current research study.

My heartiest and sincere salutations to my Parents and Siblings, whose love and guidance are with me in whatever I pursue and for providing me unending inspiration.

I am truly thankful to my teachers at Capital University of Science and Technology, **Dr. Rashid Ali**, **Dr. Abdul Rehman Kashif**, **Dr. Samina Rashid** and **Dr. Dur e Shehwar**. They are excellent teachers and I learnt alot from them throughout the course of my M.Phil study.

I would also like to thank CUST for the provision of scholarship during my M.Phil study. I also acknowledge the senior management of CUST for maintaining high educational standards.

I am grateful to my fellow researchers at CUST for valuable discussions on this research. I have enjoyed working alongside them in a pleasant working environment.

Areej Fatima

(MMT173022)

Abstract

This thesis proposes the numerical model to investigate the impact of the radiation effects in the presence of heat generation/absorption and the magnetic field on the MHD stagnation point flow past a radially stretching sheet using the Casson and Carreau nanofluids. The non-linear partial differential equations describing the proposed flow problem are reduced to a set of ordinary differential equations via suitable similarity transformations. The shooting method has been used to obtain the numerical results with the help of the computational software MATLAB. The effects of pertinent flow parameters on the non-dimensional velocity, temperature and concentration profiles are presented in tables and graphs. From the results, it has been remarked that the heat transfer rate escalates for the larger values of the radiation paramter for the Casson nanofluid. A similar finding has been observed for the Carreau nanofluid.

Contents

List of Figures

List of Tables

Symbols

a	Constant
ρ	Fluid Density
A	Velocity Ratio Parameter
T_f	Convective Fluid Temperature
k	Thermal Conductivity
σ	Electrical Conductivity
Bi_1	Thermal Biot Number
T_∞	Ambient Temperature
Bi_2	Concentration Biot Number
U_e	Free Stream Velocity
C_f	Concentration at the Surface
U_w	Radial Stretching Velocity
C_∞	Ambient Concentration
k^*	Absorption Coefficient
c_p	Specific Heat
β	Casson Fluid Parameter
D_T	Thermophoresis Diffusion Coefficient
$\theta(\eta)$	Dimensionless Temperature

D_B	Brownian Diffusion Coefficient
$\phi(\eta)$	Dimensionless Concentration
Ec	Eckert Number
$f'(\eta)$	Dimensionless Velocity
M	Magnetic Parameter
δ^*	Stefan-Boltzmann Constant
Nt	Thermophoresis Parameter
ψ	Stream Function
Pr	Prandtl Number
α_f	Thermal Diffusivity of Fluid
Nb	Brownian Motion Parameter
σ	Electrical Conductivity
Rd	Thermal Radiation Parameter
η	Dimensionless Variable
$(\rho c_p)_p$	Effective Heat Capacity of the Nanoparticles
γ	Chemical Reaction Parameter
We	Weissenberg Number
k_f	Thermal Conductivity of Fluid
ρ_p	Nanoparticle Mass Density
h_h	Heat Transfer Coefficient
ρ_f	Fluid Density
Q_0	Rate of Heat Generation/Absorption
$(\rho c_p)_f$	Heat Capacity of the Fluid
q_r	Radiative Heat Flux

Chapter 1

Introduction

1.1 Background

Fluid serves as the basic necessity of life and owing to its significance in the natural and technological processes, scientists have been discovering the various facts and figures about the fluid flow. Fluid dynamics characterizes the flow of fluids and how forces influence them. It illustrates the methodology of understanding the evolution of stars, meteorological phenomena, marine currents as well as the blood circulation. Archimedes was a Greek mathematician, who first examined the statics and buoyancy of the fluid and formulated the Archimedes principle, which was considered to be the first contribution in the area of fluid mechanics. Rapid investigation on this subject began in the fifteenth century. Some crucial engineering applications of fluid dynamics comprise of oil pipelines, rocket engines, air conditioning systems and wind turbines. Casson fluid, being non-Newtonian in nature, exhibits behavior of elastic solids. When stress rate is zero, the Casson fluid can be regarded as a shear thinning liquid, showing an infinite viscosity

whereas the viscosity drops to zero as the stress rate approaches to an infinite value [1]. Jam, tomato ketchup, honey and concentrated fruit syrups are some familiar examples of the Casson fluid. The Casson fluid has been implemented in the preparation of printing ink, silicon suspensions and polymers [2]. During the past few years, a vast range of experiments and investigations have been carried out using the Casson fluid due to its enormous applications in the scientific and engineering domains. Dash et al. [1] examined the flow using a homogeneous porous medium inside a pipe for the Casson fluid. The stagnation point flow for mixed convection and convective boundary conditions using the Casson fluid was analyzed by Hayat et al. [3]. Further to this, Mukhopadhyay et al. [4] investigated the flow past an unsteady stretching surface using the Casson fluid. Moreover, different aspects of such flows using the Casson fluid are presented in the recent studies [5–9]. Furthermore, other types of fluids have been used for describing the different flow problems, which are not non-Newtonian in nature and are regarded as Newtonian fluids. The Carreau fluid can be regarded as a generalization of the Newtonian fluid. The analysis of the peristalic flow [10–13] using Carreau fluid has been the field of focus of numerous researchers because of its usefulness in the scientific and technological fields, neurological and cancer treatment and Phsiology. Furthermore, the stagnation point MHD flow in the light of thermal radiation for Carreau fluid has been discussed by Suneetha et al. [14]. Moreover, numerous significant aspects of the different flow problems using Carreau fluid have been discussed by a number of authors [15–18].

In the past few years, the problem involving stagnation point flow has acquired the considerable attention of many research scientists. Owing to its significant

properties, the study of flow nearby a stagnation point past a stretching/shrinking sheet has a wide range of practical applications, for instance, cooling process of atomic reactors and electronic equipment, the layouts of thrust bearings, and several hydrodynamics processes. Moreover, the analysis of the magnetohydrodynamic flow is highly significant in the fluid dynamics owing to the reason that the impact of the magnetic field on the viscous flow using a fluid having electrically conducting properties has played a key role in several commercial production, for instance in the refinement of crude oil, glass and paper production, manufacturing of magnetic materials, geophysics and MHD electrical power generation. The MHD factor has a fundamental role to play in controlling the cooling rate and for achieving the desired quality of the product. Mahapatra [19] analyzed the flow nearby a stagnation point by taking into consideration the heat transfer past a stretching sheet. Furthermore, Nazar et al. [20] discussed the stagnation point flow over a stretching sheet using a micropolar fluid. Several researchers have contributed in the study of the stagnation point MHD flow in the light of various significant effects [21–25].

Moreover, an analysis of the flow using the radially stretching surfaces for the nanofluids has many significant applications in the industrial sectors, for instance, drawing of plastic films, manufacturing of glass, production of paper and refining of crude oil. In addition to this, the implementation of the nanotechnology has been an aim of the recent analysis by many scholars owing to the fact that the nanoparticles exhibit remarkable electrical, optical, chemical behavior and due to their Brownian motion and thermophoresis properties. Owing to such features, the

nanoparticles are widely used in catalysis, imaging, energy-based research, microelectronics, medical and environmental applications. These particles are composed of metals or non-metals. On top of that, latest investigations have made the infusion of nanoparticles, practicable in heat transfer fluids most notably water, diethylene glycol and propylene glycol to convert them into a more efficient category of heat transfer fluids [26]. Nanofluids are processed by the diffusion of the suspended nanoparticles in the immersed liquid (a base fluid and nanoparticles). Moreover, such fluids when compared with the conventional heat transfer fuids, have much higher rate of the thermal conduction and exhibit significant characteristics. Owing to their enhanced features, nanofluids have immense applications in the automobile industries, medical arena, power plant cooling systems, nuclear engineering and a lot more. Moreover, several research studies have been performed by considering the different aspects of the flows past a stretching sheet. Crane [27] discussed the flow by considering a stretching sheet. Pavlov [28] illustrated his findings on the MHD flow past a stretching sheet. On the contrary, Fang and Zhang [29] explored the MHD flow past a stretching sheet by examining the wall mass suction and presented the exact solution for the problem. In addition, many significant features of the MHD flow past a stretching sheet were presented and elaborated in the literature [30–33]. Motivated by the formerly findings on the non-Newtonian and Newtonain fluids, the study of stagnation point MHD flow using the Casson and Carreau nanofluids has been presented. The governing PDEs have been converted to a set of ODES through suitable similarity transformations and the numerical solution has been derived by the shooting method.

Layout of Thesis:

A brief overview of the contents of the thesis is provided below.

Chapter 2 includes some basic definitions and terminologies, which will help to understand the concepts discussed later on.

Chapter 3 provides the proposed stagnation point MHD flow using the Casson nanofluid past the radially stretching sheet. The numerical results of the governing flow equations are derived by the shooting method.

Chapter 4 extends the proposed flow discussed in Chapter 3 by using the Carreau fluid instead of the Casson fluid.

Chapter 5 provides the concluding remarks of the thesis.

References used in the thesis are mentioned in **Biblography**.

Chapter 2

Basic Definitions and Governing Equations

Some definitions, basic laws and terminologies would be discussed in the current chapter, which would be used in next chapters.

2.1 Important Definitions

Definition 2.1 (Fluid)**.** [34]

"A substance exists in three primary phases: solid, liquid, and gas. (At very high temperatures, it also exists as plasma.) A substance in the liquid or gas phase is referred to as a fluid. Distinction between a solid and a fluid is made on the basis of the substances ability to resist an applied shear (or tangential) stress that tends to change its shape. A solid can resist an applied shear stress by deforming, whereas a fluid deforms continuously under the influence of shear stress, no matter how small. In solids stress is proportional to strain, but in fluids stress is proportional

to strain rate. When a constant shear force is applied, a solid eventually stops deforming, at some fixed strain angle, whereas a fluid never stops deforming and approaches a certain rate of strain."

Definition 2.2 (Fluid Mechanics)**.** [34]

"Fluid mechanics is defined as the science that deals with the behavior of fluids at rest (fluid statics) or in motion (fluid dynamics) and the interaction of fluids with solid or other fluids at the boundaries."

Definition 2.3 (Fluid dynamics)**.** [34]

"It is the study of the motion of liquids, gases and plasmas from one place to another. Fluid dynamics has a wide range of applications like calculating force and moments on aircraft, mass flow rate of petroleum passing through pipelines, prediction of weather, etc."

Definition 2.4 (Hydrodynamics)**.** [35]

"The study of the motion of fluids that are practically incompressible such as liquids, especially water and gases at low speeds is usually referred to as hydrodynamics."

Definition 2.5 (Magnetohydrodynamics)**.** [35]

"Magnetohydrodynamics (MHD) is concerned with the flow of electrically conducting fluids in the presence of magnetic fields, either externally applied or generated within the fluid by inductive action."

Definition 2.6 (Nanofluid)**.** [35]

"A nanofluid is a fluid containing nanometer-sized particles, called nanoparticles. These fluids are engineered colloidal suspensions of nanoparticles in a base fluid.

The nanoparticles used in nanofluids are typically made of metals, oxides, carbides, or carbon nanotubes. Common base fluids include water, ethylene glycol and oil."

Definition 2.7 (Casson Fluid)**.** [1]

"Casson fluid can be defined as a shear thinning liquid which is assumed to have an infinite viscosity at zero rate of shear, a yield stress below which no flow occurs, and a zero viscosity at an infinite rate of shear."

Definition 2.8 (Carreau Fluid)**.** [36]

"Carreau fluid is a type of generalized Newtonian fluid where viscosity depends upon the shear rate. At low and high shear rates, a Carreau fluid behaves as a Newtonian fluid whereas at intermediate shear rates, a Carreau fluid behaves as a Power-law fluid. Styling gel and uncooked paste of corn starch and water are few examples of Carreau fluid."

2.2 Types of Flow

Definition 2.9 (Compressible and Incompressible Flows)**.** [34]

"A flow is classified as being compressible or incompressible, depending on the level of variation of density during flow. Incompressibility is an approximation, and a flow is said to be incompressible if the density remains nearly constant throughout. Therefore, the volume of every portion of fluid remains unchanged over the course of its motion when the flow (or the fluid) is incompressible. The densities of liquids are essentially constant, and thus the flow of liquids is typically incompressible. Therefore, liquids are usually referred to as incompressible substances. A pressure of 210 atm, for example, causes the density of liquid water at 1 atm to change

by just 1 percent. Gases, on the other hand, are highly compressible. A pressure change of just 0.01 atm, for example, causes a change of 1 percent in the density of atmospheric air."

Definition 2.10 (Steady and Unsteady Flow)**.** [34]

"The terms steady and uniform are used frequently in engineering, and thus it is important to have a clear understanding of their meanings. The term steady implies no change at a point with time. The opposite of steady is unsteady. The term uniform implies no change with location over a specified region. The terms unsteady and transient are often used interchangeably, but these terms are not synonyms. In fluid mechanics, unsteady is the most general term that applies to any flow that is not steady, but transient is typically used for developing flows. When a rocket engine is fired up, for example, there are transient effects (the pressure builds up inside the rocket engine, the flow accelerates, etc.) until the engine settles down and operates steadily. The term periodic refers to the kind of unsteady flow in which the flow oscillates about a steady mean."

Definition 2.11 (Laminar and Turbulent Flow)**.** [34]

"Some flows are smooth and orderly while others are rather chaotic. The highly ordered fluid motion characterized by smooth layers of fluid is called laminar. The word laminar comes from the movement of adjacent fluid particles together in laminates. The flow of high-viscosity fluids such as oils at low velocities is typically laminar. The highly disordered fluid motion that typically occurs at high velocities and is characterized by velocity fluctuations is called turbulent. The flow of low-viscosity fluids such as air at high velocities is typically turbulent.

The flow regime greatly influences the required power for pumping. A flow that alternates between being laminar and turbulent is called transitional."

Definition 2.12 (Viscous and Inviscid Flow)**.** [34]

"When two fluid layers move relative to each other, a friction force develops between them and the slower layer tries to slow down the faster layer. This internal resistance to flow is quantified by the fluid property viscosity, which is a measure of internal stickiness of the fluid. Viscosity is caused by cohesive forces between the molecules in liquids and by molecular collisions in gases. There is no fluid with zero viscosity, and thus all fluid flows involve viscous effects to some degree. Flows in which the frictional effects are significant are called viscous flows. However, in many flows of practical interest, there are regions (typically regions not close to solid surfaces) where viscous forces are negligibly small compared to inertial or pressure forces. Neglecting the viscous terms in such inviscid flow regions greatly simplifies the analysis without much loss in accuracy."

Definition 2.13 (Newtonian and Non-Newtonian Fluids)**.** [34]

"Fluids for which the viscosity is not independent of the rate of shear are referred as non-Newtonian and the liquids for which the viscosity is independent of the rate of shear are called Newtonian fluids."

2.3 Fluid Properties

Definition 2.14 (Heat Transfer)**.** [37] "The study of heat transfer is directed to 1-the estimation of rate of flow of energy as heat through the boundary of the system both under steady and transient conditions,

2-the determination of temperature field under stwady and transient conditions, which also will provide the information about the gradient and time rate of change of temperature at various locations and time."

Definition 2.15 (Mass Transfer)**.** [37]

"Mass transfer is the flow of molecules from one body to another when these bodies are in contact or within a system consisting of two components when the distribution of materials is not uniform. When a copper plate is placed on a steel plate, some molecules from either side will diffuse into the other side. When salt is placed in a glass and water poured over it, after sufficient time the salt molecules will diffuse into the water body. A more common example is drying of clothes or the evaporation of water spilled on the floor when water molecules diffuse into the air surrounding it. Usually mass transfer takes place from a location where the particular component is proportionately high to a location where the component is proportionately low. Mass transfer may also take place due to potentials other than concentration difference."

Definition 2.16 (Thermal Radiation)**.** [37]

"The process by which heat is transferred from a body by virtue of its temperature, without the aid of any intervening medium, is called thermal radiation. Sometimes radiant energy is taken to be transported by electromagnetic waves while at other times it is supposed to be transported by particle like photons. Radiation is found to travel at the speed of light in vacuum. The term Electromagnetic radiation encompasses many types of radiation namely short wave radiation like gamma ray, x-ray, microwave, and long wave radiation like radio wave and thermal radiation.

The cause for the emission of each type of radiation is different. Thermal radiation is emitted by a medium due to its temperature."

Definition 2.17 (Boundary Layer)**.** [37]

"Viscous effects are particularly important near the solid surfaces, where the strong interaction of the molecules of the fluid with molecules of the solid causes the relative velocity between the fluid and the solid to become almost exactly zero for a stationary surface. Therefore, the fluid velocity in the region near the wall must reduce to zero. This is called no slip condition. In that condition there is no relative motion between the fluid and the solid surface at their point of contact. It follows that the flow velocity varies with distance from the wall; from zero at the wall to its full value some distance away, so that significant velocity gradients are established close to the wall. In most cases this region is thin (compared to the typical body dimension), and it is called a boundary layer".

2.4 Conservation Laws [34]

"Several conservation laws such as the laws of conservation of mass, conservation of energy and conservation of momentum are of great use by the research community. Historically, the conservation laws are first applied to a fixed quantity of matter called a closed system or just a system, and then extended to regions in space called control volumes. The conservation relations are also called balance equations since any conserved quantity must balance during a process. We now give a brief description of the conservation of mass, momentum, and energy relations."

2.4.1 Conservation of Mass

"The conservation of mass relation for a closed system undergoing a change is expressed as m_{sys} = constant or $dm_{sys}/dt = 0$, which is a statement of the obvious that the mass of the system remains constant during a process. For a control volume (CV), mass balance is expressed in the rate form as

$$m_{in} - m_{out} = \frac{dm_{CV}}{dt}$$

where m_{in} and m_{out} are the total rates of mass flow into and out of the control volume, respectively, and dm_{CV}/dt is the rate of change of mass within the control volume boundaries. In fluid mechanics, the conservation of mass relation written for a differential control volume is usually called the continuity equation."

2.4.2 Conservation of Momentum

"The product of the mass and the velocity of a body is called the linear momentum or just the momentum of the body, and the momentum of a rigid body of mass m moving with a velocity $\overrightarrow{V}$ is $m\overrightarrow{V}$. Newtons second law states that the acceleration of a body is proportional to the net force acting on it and is inversely proportional to its mass, and that the rate of change of the momentum of a body is equal to the net force acting on the body. Therefore, the momentum of a system remains constant when the net force acting on it is zero, and thus the momentum of such systems is conserved. This is known as the conservation of momentum principle."

2.4.3 Conservation of Energy

"Energy can be transferred to or from a closed system by heat or work, and the conservation of energy principle requires that the net energy transfer to or from a system during a process be equal to the change in energy content of the system. Control volumes involve energy transfer via mass flow also, and the conservation of energy principle, also called the energy balance, is expressed as.

$$E_{in} - E_{out} = \frac{dE_{cv}}{dt}$$

where E_{in} and E_{out} are the total rates of energy transfer into and out of the control volume, respectively, and dE_{CV}/dt is the rate of change of energy within the control volume boundaries. In fluid mechanics, we usually limit our consideration to mechanical forms of energy only."

2.5 Dimensional Analysis [34]

"The dimensional analysis is a powerful tool for engineers and scientists in which the combination of dimensional variables, nondimensional variables, and dimensional constants into nondimensional parameters reduces the number of necessary independent parameters in a problem."

2.5.1 Dimensions and Units

"A dimension is the measure of a physical quantity (without numerical values), while a unit is a way to assign a number to that dimension. For example, length is

a dimension that is measured in units such as microns (μm), feet (ft), centimeters (cm), meters (m), kilometers (km), etc. Further, force has the same dimensions as mass times acceleration (by Newtons's second law). Thus, in terms of primary dimensions, dimensions of force:

$$\text{Force} = \frac{\text{Mass length}}{\text{time}^2} = \frac{mL}{t^2},$$

"

2.5.2 Dimensional Homogeneity

"There is a popular old saying that you cannot add apples and oranges. This is actually a simplified expression of a far more global and fundamental mathematical law for equations, the law of dimensional homogeneity, stated as

Every additive term in an equation must have the same dimensions.

Consider, for example, the change in total energy of a simple compressible closed system from one state and/or time(1) to another (2). The change in total energy of the system E is given by

$$\Delta E = \Delta U + \Delta KE + \Delta PE, \tag{2.1}$$

where E has three components: internal energy (U), kinetic energy (KE), and potential energy (PE). These components can be written in terms of the system mass (m); measurable quantities and thermodynamic properties at each of the two states, such as speed (V), elevation (z), and specific internal energy (u); and the known gravitational acceleration constant (g),

$\Delta U = m(u_2 - u_1)$, $\Delta KE = \frac{1}{2}m(V_2^2 - V_1^2)$, $\Delta PE = mg(Z_2 - Z_1)$. It is straightforward to verify that the left side of Eq. (2.1) and all three additive terms on the right side of above equations have the same dimensionsenergy. Using the definitions of above equations, we write the primary dimensions of each term,

$\{\Delta E\} = \{\text{Energy}\} = \{\text{Force.Length}\} \rightarrow \{\Delta E\} = \{\frac{mL^2}{t^2}\}$

$\{\Delta U\} = \{\text{Mass}\frac{\text{Energy}}{\text{Mass}}\} = \{\text{Energy}\} \rightarrow \{\Delta U\} = \{\frac{mL^2}{t^2}\}$

$\{\Delta KE\} = \{\text{Mass}\frac{\text{Length}^2}{\text{time}^2}\} \rightarrow \{\Delta KE\} = \{\frac{mL^2}{t^2}\}$

$\{\Delta PE\} = \{\text{Mass}\frac{\text{Length}}{\text{time}^2}\text{Length}\} \rightarrow \{\Delta PE\} = \{\frac{mL^2}{t^2}\}$.

If at some stage of an analysis we find ourselves in a position in which two additive terms in an equation have different dimensions, this would be a clear indication that we have made an error at some earlier stage in the analysis. In addition to dimensional homogeneity, calculations are valid only when the units are also homogeneous in each additive term. For example, units of energy in the above terms may be J, N, m, or kg, m_2/s_2, all of which are equivalent. Suppose, however, that kJ were used in place of J for one of the terms. This term would be off by a factor of 1000 compared to the other terms. It is wise to write out all units when performing mathematical calculations in order to avoid such errors."

2.5.3 Nondimensionalization of Equations

"The law of dimensional homogeneity guarantees that every additive term in an equation has the same dimensions. It follows that if we divide each term in the equation by a collection of variables and constants whose product has those same

dimensions, the equation is rendered nondimensional. If, in addition, the nondimensional terms in the equation are of order unity, the equation is called normalized. Normalization is, thus, more restrictive than nondimensionalization, even though the two terms are sometimes (incorrectly) used interchangeably. Each term in nondimensional equation is dimensionless. In the process of nondimensionalizing of an equation of motion, nondimensional parameters often appear–most of which are named after a notable scientist or engineer (e.g., the Reynolds number and the Froude number). This process is referred to by some authors as the inspectional analysis."

2.6 Dimensionless Parameters

Definition 2.18 (Skin-Friction Coefficient)**.** [38]

"It is a dimensionless number and is defined as

$$C_f = \frac{\tau_w}{2Q{w_\infty}^2},$$

where τ_w is the local wall shear stress, ρ is the fluid density and U_e is the free stream velocity (usually taken outside of the boundary layer or at the inlet). It expresses the dynamic friction resistance originating in viscous fluid flow around a fixed wall."

Definition 2.19 (Nusselt Number)**.** [38]

"It is a dimensionless number, first introduced by a German engineer Ernst Kraft

Wilhelm Nusselt and is defined as

$$Nu = \frac{\alpha L}{k},$$

where where α represents the heat transfer coefficient, L denotes the characteristic length and k is the thermal conductivity. It expresses the ratio of the total heat transfer in a system to the heat transfer by conduction. In characterizes the heat transfer by convection between a fluid and the environment close to it or, alternatively, the connection between the heat transfer intensity and the temperature field in a flow boundary layer. It expresses the dimensionless thermal transference. The physical significance is based on the idea of a fluid boundary layer in which the heat is transferred by conduction. If it is not so, the criterion loses its significance. ”

Definition 2.20 (Sherwood Number)**.** [38]

“ The Sherwood number was first introduced by an American chemical engineer, Thomas Kilgore Sherwood and is defined as .

$$Sh = \frac{BL}{D}$$

where B is the mass transfer coefficient, L denotes the characteristic length and D stands for molecular diffusivity.It expresses the ratio of the heat transfer to the molecular diffusion. It characterizes the mass transfer intensity at the interface of phases. ”

Definition 2.21 (Eckert Number)**.** [38]

"The Eckert number (Ec) is a dimensionless number used in the continuum mechanics. It expresses the relationship between a flow's kinetic energy and enthalpy, and is used to characterize the dissipation. It is defined as

$$Ec = \frac{u^2}{C_p \Delta T},$$

where u (ms^{-1}) fluid flow velocity far from body, C_p is the constant pressure local specific heat of continuum, ΔT is temperature difference. It expresses the ratio of kinetic energy to a thermal energy change."

Definition 2.22 (Prandtl Number)**.** [38]

"The Prandtl number which is a dimensionless number, named after the German physicist Ludwig Prandtl, is defined as

$$Pr = \frac{\nu}{\alpha},$$

where ν stands for the kinematic viscosity and α denotes the thermal diffusivity. This number expresses the ratio of the momentum diffusivity (viscosity) to the thermal diffusivity. It characterizes the physical properties of a fluid with convective and diffusive heat transfers. It describes, for example, the phenomena connected with the energy transfer in a boundary layer. It expresses the degree of similarity between velocity and diffusive thermal fields or, alternatively, between hydrodynamic and thermal boundary layers."

Definition 2.23 (Schmidt Number)**.** [38]

“

$$Sc = \frac{\mu}{\rho D_m} = \frac{\nu}{D_m},$$

where ν is the kinematic viscosity, D_m is mass diffusivity, μ is the dynamic viscosity of the fluid and ρ is the density of the fluid. This number expresses the ratio of the kinematic viscosity, or momentum transfer by internal friction, to the molecular diffusivity. It characterizes the relation between the material and momentum transfers in mass transfer. It provides the similarity of velocity and concentration fields in mass transfer. For example, molten materials with an equal Schmidt number have similar velocity and concentration fields. Higher Sc number values characterize slower mass exchange and higher values of dividing coefficients. This leads to higher mixing and a tendency to crack in a solidified casting. The criterion was first introduced by Schmidt in 1929.”

Definition 2.24 (Weissenberg Number)**.** [38]

“ The dimensionless Weissenberg number, formulated by German physicist Karl Weissenberg, is defined as

$$We = \frac{\rho u^2}{\tau},$$

where ρ is the fluid density, u denotes the flow velocity and τ stands for the shear stress. This number expresses the characteristic material time (relaxation time) and the shear velocity. It characterizes the velocity and time relations in rheological processes in viscoelastic shear flow. Furthermore, it also expresses the ratio of the dynamic viscoelastic force to the viscous force.”

Definition 2.25 (Biot Number)**.** [38]

“

$$Bi = \frac{h_h L}{k},$$

where h_h represents the heat transfer coefficient, L denotes the characteristic length and k is the thermal conductivity. This number expresses the ratio of the heat flow transferred by convection on a body surface to the heat flow transferred by conduction in a body. The criterion was first introduced by French physicist, Jean-Baptiste Biot. ”

Definition 2.26 (Radiation Parameter)**.** [38]

“ The dimensionless Radiation parameter is defined as

$$Rd = \frac{\epsilon \sigma^* T^3 L_h}{\lambda},$$

where ϵ is the emissivity of inner channel wall, σ^* represents the Stefan Boltzmann constant, L_h stands for the hydraulic diameter, T_f denotes the temperature of the fluid and k is the thermal conductivity. This parameter expresses the ratio of the heat transferred by radiation in a passageway to that transferred by conduction in a channel wall. It characterizes the relation between the radiation and conduction heat transfers in passageways. Alternatively, it expresses the influence of the radiation on the convective transfer.”

Chapter 3

MHD Stagnation Point Casson Nanofluid Flow over a Radially Stretching sheet

3.1 Introduction

The numerical investigation on the flow of Casson nanofluid past a radially stretching sheet close to a stagnation point along with convective boundary conditions has been taken into account. Moreover, the radiation effects and magnetic field are examined. In additon to this, the effects of heat generation/absorption are also explored. The conversion of non-linear partial differential equations describing the proposed flow problem to a set of ordinary differential equations has been carried out by employing appropriate similarity transformations. The shooting method has been employed for the numerical treatment of the proposed flow equations.

The impact of pertinent flow parameters on the non-dimensional velocity, temperature and concentration profiles has been illustrated via tables and graphs. The limiting case of the present study affirms that the obtained numerical results reflect a very good agreement with those from open literature. In this chapter, a detailed review of [39] has been provided.

3.2 Mathematical Modeling

The present model aims to investigate the laminar, incompressible and steady flow of the Casson nanofluid past a radially stretched surface in close proximity of a stagnation point. In the light of thermal radiation and heat generation/absorption, the characteristics of flow and heat transfer are examined. The coordinate system is chosen in a manner that $r-$ axis is along the flow whereas $z-$axis is perpendicular to the flow. The velocity of the outer flow is taken as U_e. Furthermore, the direction of the uniform magnetic field is chosen in such a manner that it is normal to the surface of the fluid flow. The effects of Brownian motion and thermophoresis have been elaborated. Moreover, the convective surface conditions have been taken into consideration. The constitutive equations of the Casson nanofluid model are as follow [4–9]:

$$\frac{\partial u}{\partial r}+\frac{u}{r}+\frac{\partial w}{\partial z}=0, \tag{3.1}$$

$$u\frac{\partial u}{\partial r}+w\frac{\partial u}{\partial z}=\nu_f\left(1+\frac{1}{\beta}\right)\frac{\partial^2 u}{\partial z^2}+U_e\frac{dU_e}{dr}-\frac{\sigma B_0(u-U_e)}{\rho_f}, \tag{3.2}$$

$$\begin{aligned} u\frac{\partial T}{\partial r}+w\frac{\partial T}{\partial z}=\alpha_f\frac{\partial^2 T}{\partial z^2}+\tau\left[D_B\frac{\partial C}{\partial z}\frac{\partial T}{\partial z}+\frac{D_T}{T_\infty}\left(\frac{\partial T}{\partial z}\right)^2\right]+\frac{Q_0\left(T-T_\infty\right)}{(\rho c_p)_f} \\ +\frac{\nu_f}{c_p}\left(1+\frac{1}{\beta}\right)\left(\frac{\partial u}{\partial z}\right)^2+\frac{\sigma B_0^2\left(u-U_e\right)^2}{(\rho c_p)_f}-\frac{1}{(\rho c_p)_f}\frac{\partial q_r}{\partial z}, \end{aligned} \tag{3.3}$$

$$u\frac{\partial C}{\partial r}+w\frac{\partial C}{\partial z}=D_B\frac{\partial^2 C}{\partial z^2}+\frac{D_T}{T_\infty}\frac{\partial^2 T}{\partial z^2}-C_r\left(C-C_\infty\right). \tag{3.4}$$

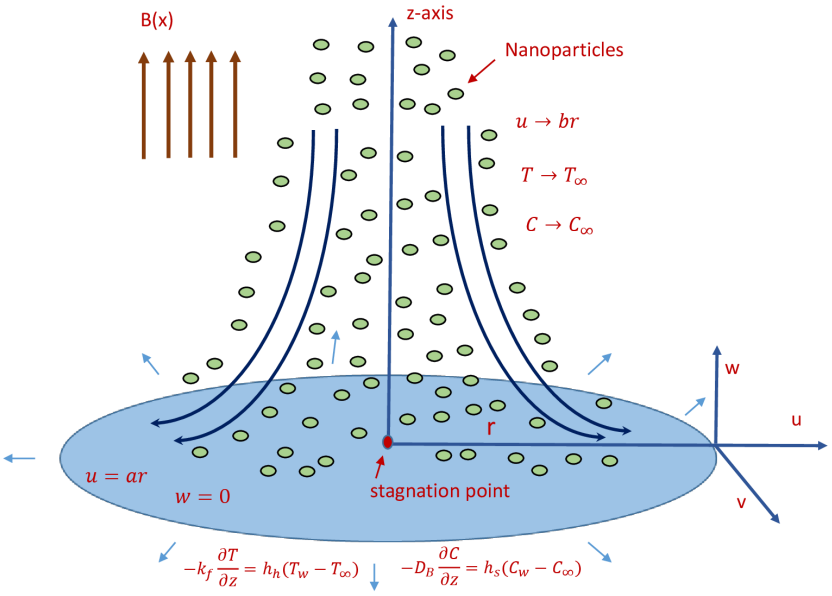

FIGURE 3.1: Schematic of physical model

The corresponding conditions at the boundary surface are

$$u=U_w=ar,\ w=0,\ -k_f\frac{\partial T}{\partial z}=h_h\left(T_f-T\right),\ D_B\frac{\partial C}{\partial z}=-h_s\left(C_f-C\right)\ \text{at}\ z=0,$$
$$u\to U_e=br,\quad T\to T_\infty,\quad C\to C_\infty\quad \text{as}\quad z\to\infty. \tag{3.5}$$

The following similarity variables are taken into consideration.

$$\eta=\sqrt{\frac{a}{\nu_f}}\,z, u=arf'\left(\eta\right), w=-2\sqrt{a\nu_f}f\left(\eta\right), \theta\left(\eta\right)=\frac{T-T_\infty}{T_f-T_\infty}, \phi\left(\eta\right)=\frac{C-C_\infty}{C_f-C_\infty}.$$

The Rosseland approximation has been considered for radiation and the formulae

for the radiative heat flux q_{r} is stated below.

$$q_r = \frac{-4\sigma^*}{3k^*}\frac{\partial T^4}{\partial z}. \tag{3.6}$$

For smaller value of temperature contrast, the temperature difference T^4 might be expanded about T_∞ using Taylor series, as follows:

$$T^4 = T_\infty^4 + \frac{4T_\infty^3}{1!}(T - T_\infty)^1 + \frac{12T_\infty^2}{2!}(T - T_\infty)^2 + \frac{24T_\infty}{3!}(T - T_\infty)^3 + ...,$$

omitting the terms having higher order, we get

$$T^4 = T_\infty^4 + \frac{4T_\infty^3}{1!}(T - T_\infty)^1.$$

Then

$$\frac{\partial T^4}{\partial z} = 4T_\infty^3\frac{\partial T}{\partial z}. \tag{3.7}$$

Using (3.7) in (3.6) and then differentiating w.r.t z, we get

$$\frac{\partial q_r}{\partial z} = -\frac{16\sigma^* T_\infty^3}{3k^*}\frac{\partial^2 T}{\partial z^2}, \tag{3.8}$$

The detailed procedure for the conversion of the partial differential equations (3.1)-(3.5) to the ordinary differential equations in the dimensionless form has been discussed below.

- $$\frac{\partial u}{\partial r} = \frac{\partial}{\partial r}(u)$$
$$= \frac{\partial}{\partial r}(arf'(\eta))$$

$$= a\frac{\partial}{\partial r}\left(rf'\left(\eta\right)\right)$$
$$= a\left(f'\left(\eta\right)\frac{\partial r}{\partial r} + r\frac{\partial f'}{\partial r}\right)$$
$$= a\left(f'\left(\eta\right) + r\frac{\partial f'}{\partial \eta}\frac{\partial \eta}{\partial r}\right)$$
$$= af'\left(\eta\right).$$

- $$\frac{u}{r} = \frac{arf'\left(\eta\right)}{r}$$
$$= af'\left(\eta\right).$$

- $$\frac{\partial w}{\partial z} = \frac{\partial}{\partial z}\left(w\right)$$
$$= \frac{\partial}{\partial z}\left(-2\sqrt{a\nu_f}f\left(\eta\right)\right)$$
$$= -2\sqrt{a\nu_f}\frac{\partial f}{\partial z}$$
$$= -2\sqrt{a\nu_f}\frac{\partial f}{\partial \eta}\frac{\partial \eta}{\partial z}$$
$$= -2\sqrt{a\nu_f}f'\left(\eta\right)\left(\sqrt{\frac{a}{\nu_f}}\right)$$
$$= -2af'\left(\eta\right).$$

Verification of the continuity equation has been carried out as:

$$\frac{\partial u}{\partial r} + \frac{u}{r} + \frac{\partial w}{\partial z} = af'\left(\eta\right) + af'\left(\eta\right) - 2af'\left(\eta\right) = 0.$$

Now equation (3.2) will be converted into the dimensionless form. The procedure includes the following conversion of different terms from dimensional to the non-dimensional form.

- $$\frac{\partial u}{\partial z} = \frac{\partial}{\partial z}\left(u\right)$$
$$= \frac{\partial}{\partial z}\left(arf'\left(\eta\right)\right)$$

$$= a\frac{\partial}{\partial z}\left(rf'\left(\eta\right)\right)$$
$$= a\left(f'\left(\eta\right)\frac{\partial r}{\partial z} + r\frac{\partial f'}{\partial z}\right)$$
$$= arf''\left(\eta\right)\left(\sqrt{\frac{a}{\nu_f}}\right)$$
$$= ar\sqrt{\frac{a}{\nu_f}}f''\left(\eta\right).$$

- $u\dfrac{\partial u}{\partial r} = \left(arf'\left(\eta\right)\right)\left(af'\left(\eta\right)\right)$
$$= a^2rf'^2\left(\eta\right).$$

- $w\dfrac{\partial u}{\partial z} = \left(-2\sqrt{a\nu_f}f\left(\eta\right)\right)\left(ar\sqrt{\frac{a}{\nu_f}}f''\left(\eta\right)\right)$
$$= -2ra^2f\left(\eta\right)f''\left(\eta\right).$$

- $\dfrac{\partial^2 u}{\partial z^2} = \dfrac{\partial}{\partial z}\left(\dfrac{\partial u}{\partial z}\right)$
$$= \frac{\partial}{\partial z}\left(ar\sqrt{\frac{a}{\nu_f}}f''\left(\eta\right)\right)$$
$$= ar\sqrt{\frac{a}{\nu_f}}\left(\frac{\partial}{\partial z}\left(f''\left(\eta\right)\right)\right)$$
$$= ar\sqrt{\frac{a}{\nu_f}}\left(\frac{\partial f''\left(\eta\right)}{\partial z}\right)$$
$$= ar\sqrt{\frac{a}{\nu_f}}\left(\frac{\partial f''\left(\eta\right)}{\partial \eta}\frac{\partial \eta}{\partial z}\right)$$
$$= ar\sqrt{\frac{a}{\nu_f}}f'''\left(\eta\right)\left(\sqrt{\frac{a}{\nu_f}}\right)$$
$$= \frac{a^2}{\nu_f}rf'''\left(\eta\right).$$

- $U_e\dfrac{dU_e}{dr} = \left(br\right)\left(\dfrac{d}{dr}\left(br\right)\right)$
$$= br\left(b\right)$$
$$= b^2r.$$

- $\left(u - U_e\right) = \left(arf'\left(\eta\right) - br\right)$
$$= ar\left(f'\left(\eta\right) - \frac{b}{a}\right).$$

The left hand side of equation (3.2) can then be written as:

$$\begin{aligned} u\frac{\partial u}{\partial r} + w\frac{\partial u}{\partial z} &= a^2 r f'^2(\eta) - 2ra^2 f(\eta) f''(\eta) \\ &= a^2 r\left(f'^2(\eta) - 2f(\eta) f''(\eta)\right). \end{aligned} \tag{3.9}$$

Likewise the right hand side of equation (3.2) is converted to the dimensionless form through the following process:

$$\begin{aligned} &\nu_f\left(1+\frac{1}{\beta}\right)\frac{\partial^2 u}{\partial z^2} + U_e\frac{dU_e}{dr} - \frac{\sigma B_0^2}{\rho}(u - U_e) \\ =\ & a^2 r\left[\left(1+\frac{1}{\beta}\right) f'''(\eta) + \frac{b^2}{a^2} - \frac{\sigma B_0^2}{a\rho}\left(f'(\eta) - \frac{b}{a}\right)\right]. \end{aligned} \tag{3.10}$$

Now using (3.9) and (3.10), equation (3.2) can be written as:

$$\left(1+\frac{1}{\beta}\right) f'''(\eta) + 2f(\eta) f''(\eta) - f'^2(\eta) - M^2\left(f'(\eta) - A\right) + A^2 = 0. \tag{3.11}$$

For converting equation (3.3) into the dimensionless form, the different terms have been treated through the similarity variable in the following way.

- $$\begin{aligned} \frac{\partial T}{\partial r} &= \frac{\partial}{\partial r}\left(\left(T_f - T_\infty\right)\theta(\eta) + T_\infty\right) \\ &= \left(T_f - T_\infty\right)\frac{\partial \theta(\eta)}{\partial r} \\ &= \left(T_f - T_\infty\right)\frac{\partial \theta(\eta)}{\partial \eta}\frac{\partial \eta}{\partial r} \\ &= \left(T_f - T_\infty\right)\frac{\partial \theta(\eta)}{\partial \eta}(0) = 0. \end{aligned}$$
- $$u\frac{\partial T}{\partial r} = ar f'(\eta)(0) = 0.$$
- $$\begin{aligned} \frac{\partial T}{\partial z} &= \frac{\partial}{\partial z}\left(\left(T_f - T_\infty\right)\theta(\eta) + T_\infty\right) \\ &= \left(T_f - T_\infty\right)\frac{\partial \theta(\eta)}{\partial z} \end{aligned}$$

$$= (T_f - T_\infty)\frac{\partial\theta(\eta)}{\partial\eta}\frac{\partial\eta}{\partial z}$$

$$= (T_f - T_\infty)\theta'(\eta)\left(\sqrt{\frac{a}{\nu_f}}\right)$$

$$= \sqrt{\frac{a}{\nu_f}}(T_f - T_\infty)\theta'(\eta).$$

- $$w\frac{\partial T}{\partial z} = \left(-2\sqrt{a\nu_f}f(\eta)\right)\left(\sqrt{\frac{a}{\nu_f}}(T_f - T_\infty)\theta'(\eta)\right)$$

$$= -2af(\eta)(T_f - T_\infty)\theta'(\eta).$$

- $$\frac{\partial^2 T}{\partial z^2} = \frac{\partial}{\partial z}\left(\frac{\partial T}{\partial z}\right)$$

$$= \frac{\partial}{\partial z}\left(\sqrt{\frac{a}{\nu_f}}(T_f - T_\infty)\theta'(\eta)\right)$$

$$= \sqrt{\frac{a}{\nu_f}}(T_f - T_\infty)\frac{\partial\theta'(\eta)}{\partial z}$$

$$= \sqrt{\frac{a}{\nu_f}}(T_f - T_\infty)\frac{\partial\theta'(\eta)}{\partial\eta}\frac{\partial\eta}{\partial z}$$

$$= \frac{a}{\nu_f}(T_f - T_\infty)\theta''(\eta).$$

- $$\frac{\partial C}{\partial z} = \frac{\partial}{\partial z}\left((C_f - C_\infty)\phi(\eta) + C_\infty\right)$$

$$= (C_f - C_\infty)\frac{\partial\phi(\eta)}{\partial z}$$

$$= (C_f - C_\infty)\frac{\partial\phi(\eta)}{\partial\eta}\frac{\partial\eta}{\partial z}$$

$$= (C_f - C_\infty)\phi'(\eta)\left(\sqrt{\frac{a}{\nu_f}}\right)$$

$$= \sqrt{\frac{a}{\nu_f}}(C_f - C_\infty)\phi'(\eta).$$

- $$\frac{\partial C}{\partial z}\frac{\partial T}{\partial z} = \frac{a}{\nu_f}(C_f - C_\infty)(T_f - T_\infty)\phi'(\eta)\theta'(\eta).$$
- $$\left(\frac{\partial T}{\partial z}\right)^2 = \frac{a}{\nu_f}(T_f - T_\infty)^2\theta'^2(\eta).$$
- $$\frac{\partial q_r}{\partial z} = -\frac{16T_\infty\sigma^*}{3k^*}\frac{\partial^2 T}{\partial z^2}$$

$$= -\frac{16T_\infty\sigma^*}{3k^*}\left(\frac{a}{\nu_f}(T_f - T_\infty)\theta''(\eta)\right)$$

$$= -\frac{16T_\infty\sigma^* a}{3k^*\nu_f}(T_f - T_\infty)\theta''(\eta).$$

- $$\left(\frac{\partial u}{\partial z}\right)^2 = \left(ar\sqrt{\frac{a}{\nu_f}}f''(\eta)\right)^2 = \frac{a^3r^2}{\nu_f}f''^2(\eta).$$

- $$(u-U_e) = (arf'(\eta) - br) = ar\left(f'(\eta) - \frac{b}{a}\right).$$

Consider the left hand side of equation (3.3) for conversion into the dimensionless form as:

$$\begin{aligned} u\frac{\partial T}{\partial r} + w\frac{\partial T}{\partial z} &= 0 + (-2a)\, f(\eta)\,(T_f - T_\infty)\,\theta'(\eta) \\ &= -2af(\eta)\,(T_f - T_\infty)\,\theta'(\eta) \\ &= -2a\,(T_f - T_\infty)\, f(\eta)\,\theta'(\eta) \\ &= \frac{-2\alpha a\,(T_f - T_\infty)}{\nu_f}\left(\frac{\nu_f}{\alpha}\right) f(\eta)\,\theta'(\eta) \\ &= \frac{-2\alpha a\,(T_f - T_\infty)}{\nu_f} Prf(\eta)\,\theta'(\eta). \end{aligned} \tag{3.12}$$

The right hand side of equation (3.3) can now be treated as follows.

$$\begin{aligned} &\alpha\frac{\partial^2 T}{\partial z^2} + \tau\left(D_B\frac{\partial C}{\partial z}\frac{\partial T}{\partial z} + \frac{D_T}{T_\infty}\left(\frac{\partial T}{\partial T}\right)^2\right) + \frac{Q_0}{\rho c_p}(T - T_\infty) - \frac{1}{\rho c_p}\frac{\partial q_r}{\partial z} \\ &+ \frac{\nu_f}{C_p}\left(1 + \frac{1}{\beta}\right)\left(\frac{\partial u}{\partial z}\right)^2 + \frac{\sigma B_0^2}{c_p\rho}(u - U_e)^2 \\ = \;& \frac{\alpha a}{\nu_f}(T_f - T_\infty)\left[\theta''(\eta) + \frac{\tau D_B}{\alpha}(C_f - C_\infty)\,\phi'(\eta)\,\theta'(\eta) + \frac{\tau D_T}{\alpha T_\infty}(T_f - T_\infty)\,\theta'^2(\eta)\right. \\ &+ \frac{Q_0\nu_f}{\rho c_p a\alpha}\theta(\eta) + \frac{16T_\infty\sigma^*}{3k^*\alpha\rho c_p}\theta''(\eta) + \left(1 + \frac{1}{\beta}\right)\frac{a^2r^2\nu_f}{\alpha c_p\,(T_f - T_\infty)}f''^2(\eta) \\ &\left.+ \frac{\sigma B_0^2 ar^2\nu_f}{\rho c_p\alpha\,(T_f - T_\infty)}\left(f'(\eta) - \frac{b}{a}\right)^2\right] \end{aligned}$$

$$
\begin{aligned}
&= \frac{\alpha a}{\nu_f}\left(T_f - T_\infty\right)\left[\theta''(\eta) + \left(\frac{\tau D_B\left(C_f - C_\infty\right)}{\nu_f}\right)\left(\frac{\nu_f}{\alpha}\right)\phi'(\eta)\,\theta'(\eta)\right.\\
&\quad + \left(\frac{\tau D_T\left(T_f - T_\infty\right)}{\nu_f T_\infty}\right)\left(\frac{\nu_f}{\alpha}\right)\theta'^2(\eta) + \left(\frac{Q_0}{\rho c_p a}\right)\left(\frac{\nu_f}{\alpha}\right)\theta(\eta)\\
&\quad + \frac{4}{3}\left(\frac{4T_\infty\sigma^*}{k^*\left(\alpha\rho c_p\right)}\right)\theta''(\eta) + \left(1+\frac{1}{\beta}\right)\left(\frac{\nu_f}{\alpha}\right)\left(\frac{(ar)^2}{c_p\left(T_f - T_\infty\right)}\right)f'''^2(\eta)\\
&\quad \left. + \left(\frac{\nu_f}{\alpha}\right)\left(\frac{\sigma B_0^2}{\rho a}\right)\left(\frac{(ar)^2}{c_p\left(T_f - T_\infty\right)}\right)\left(f'(\eta) - \frac{b}{a}\right)^2\right]\\
&= \frac{\alpha a}{\nu_f}\left(T_f - T_\infty\right)\left[\theta''(\eta) + NbPr\phi'(\eta)\,\theta'(\eta) + NtPr\theta'^2(\eta) + QPr\theta(\eta)\right.\\
&\quad \left. + \frac{4}{3}Rd\theta''(\eta) + \left(1+\frac{1}{\beta}\right)PrEcf'''^2(\eta) + M^2EcPr\left(f'(\eta) - A\right)^2\right]. \qquad (3.13)
\end{aligned}
$$

Different parameters used in the above expression have the following formulations:

$$
\begin{aligned}
&Nb = \frac{\tau D_B\left(C_f - C_\infty\right)}{\nu_f},\ Pr = \frac{\nu_f}{\alpha},\ Nt = \frac{\tau D_T\left(T_f - T_\infty\right)}{\nu_f T_\infty},\ M^2 = \frac{\sigma B_o^2}{\rho a},\\
&Q = \frac{Q_o}{\rho c_p a},\ Rd = \frac{4T_\infty\sigma^*}{k^*\left(\alpha\rho c_p\right)},\quad Ec = \frac{a^2r^2}{\alpha c_p\left(T_f - T_\infty\right)},\ A = \frac{b}{a}.
\end{aligned}
$$

Now using equation (3.12)-(3.13), the dimensionless form of equation (3.3) is:

$$
\begin{aligned}
&\theta''(\eta) + NbPr\phi'(\eta)\,\theta'(\eta) + NtPr\theta'^2(\eta) + QPr\theta(\eta) + \frac{4}{3}Rd\theta''(\eta)\\
&\quad + \left(1+\frac{1}{\beta}\right)PrEcf'''^2(\eta) + M^2EcPr\left(f'(\eta) - A\right)^2 = -2Prf(\eta)\,\theta'(\eta).\\
&\Rightarrow \left(1+\frac{4}{3}Rd\right)\theta'' + PrNb\theta'\phi' + PrNt\theta'^2 + 2Prf\theta' + \left(1+\frac{1}{\beta}\right)PrEcf'''^2\\
&\quad + QPr\theta + M^2EcPr\left(f' - A\right)^2 = 0.
\end{aligned}
$$

For converting equation (3.4) into the dimensionless form, the following procedure has been described.

- $C = \left(C_f - C_\infty\right)\phi(\eta) + C_\infty.$

- $T = (T_f - T_\infty)\,\theta(\eta) + T_\infty.$
- $$\begin{aligned}\frac{\partial C}{\partial r} &= (C_f - C_\infty)\,\frac{\partial \phi(\eta)}{\partial r} \\ &= (C_f - C_\infty)\,\frac{\partial \phi(\eta)}{\partial \eta}\frac{\partial \eta}{\partial r} \\ &= (C_f - C_\infty)\,\frac{\partial \phi(\eta)}{\partial \eta}(0) = 0.\end{aligned}$$
- $$\begin{aligned}\frac{\partial C}{\partial z} &= (C_f - C_\infty)\,\frac{\partial \phi(\eta)}{\partial z} \\ &= (C_f - C_\infty)\,\frac{\partial \phi(\eta)}{\partial \eta}\frac{\partial \eta}{\partial z} \\ &= (C_f - C_\infty)\,\phi'(\eta)\left(\sqrt{\frac{a}{\nu_f}}\right) \\ &= (C_f - C_\infty)\sqrt{\frac{a}{\nu_f}}\phi'(\eta).\end{aligned}$$
- $$\begin{aligned}w\frac{\partial C}{\partial z} &= \left(-2\sqrt{a\nu_f}f(\eta)\right)\left((C_f - C_\infty)\sqrt{\frac{a}{\nu_f}}\phi'(\eta)\right) \\ &= -2a\,(C_f - C_\infty)\,f(\eta)\,\phi'(\eta).\end{aligned}$$
- $$\begin{aligned}\frac{\partial^2 C}{\partial z^2} &= \frac{\partial}{\partial z}\left(\frac{\partial C}{\partial z}\right) \\ &= \frac{\partial}{\partial z}\left((C_f - C_\infty)\sqrt{\frac{a}{\nu_f}}\phi'(\eta)\right) \\ &= (C_f - C_\infty)\sqrt{\frac{a}{\nu_f}}\frac{\partial \phi'(\eta)}{\partial z} \\ &= (C_f - C_\infty)\sqrt{\frac{a}{\nu_f}}\frac{\partial \phi'(\eta)}{\partial \eta}\frac{\partial \eta}{\partial z} \\ &= (C_f - C_\infty)\sqrt{\frac{a}{\nu_f}}\phi''(\eta)\left(\sqrt{\frac{a}{\nu_f}}\right) \\ &= \frac{a}{\nu_f}(C_f - C_\infty)\,\phi''(\eta).\end{aligned}$$
- $$\begin{aligned}\frac{\partial T}{\partial z} &= \frac{\partial}{\partial z}\left((T_f - T_\infty)\,\theta(\eta) + T_\infty\right) \\ &= (T_f - T_\infty)\,\frac{\partial \theta(\eta)}{\partial z} \\ &= (T_f - T_\infty)\,\frac{\partial \theta(\eta)}{\partial \eta}\frac{\partial \eta}{\partial z} \\ &= (T_f - T_\infty)\,\theta'(\eta)\left(\sqrt{\frac{a}{\nu_f}}\right) \\ &= \sqrt{\frac{a}{\nu_f}}\,(T_f - T_\infty)\,\theta'(\eta).\end{aligned}$$

- $$\begin{aligned}\frac{\partial^2 T}{\partial z^2} &= \frac{\partial}{\partial z}\left(\frac{\partial T}{\partial z}\right)\\ &= \frac{\partial}{\partial z}\left(\sqrt{\frac{a}{\nu_f}}\left(T_f - T_\infty\right)\theta'(\eta)\right)\\ &= \sqrt{\frac{a}{\nu_f}}\left(T_f - T_\infty\right)\frac{\partial \theta'(\eta)}{\partial z}\\ &= \sqrt{\frac{a}{\nu_f}}\left(T_f - T_\infty\right)\frac{\partial \theta'(\eta)}{\partial \eta}\frac{\partial \eta}{\partial z}\\ &= \frac{a}{\nu_f}\left(T_f - T_\infty\right)\theta''(\eta).\end{aligned}$$

The left hand side of equation (3.4) gets the following form.

$$\begin{aligned}u\frac{\partial C}{\partial r} + w\frac{\partial C}{\partial z} &= \left(arf'(\eta)\right)(0) + \left(-2\sqrt{a\nu_f}f(\eta)\right)\left(\left(C_f - C_\infty\right)\sqrt{\frac{a}{\nu_f}}\phi'(\eta)\right)\\ &= D_B\frac{a}{\nu_f}\left(C_f - C_\infty\right)\left(-2Scf(\eta)\phi'(\eta)\right). \qquad (3.14)\end{aligned}$$

Now the right hand side of equation (3.3), can be reformed as:

$$\begin{aligned}&D_B\frac{\partial^2 C}{\partial z^2} + \frac{D_T}{T_\infty}\frac{\partial^2 T}{\partial z^2} - C_r\left(C - C_\infty\right)\\ =\ & D_B\frac{a}{\nu_f}\left(C_f - C_\infty\right)\phi''(\eta) + \frac{D_T}{T_\infty}\frac{a}{\nu_f}\left(T_f - T_\infty\right)\theta''(\eta) - C_r\left(C_f - C_\infty\right)\phi(\eta)\\ =\ & D_B\frac{a}{\nu_f}\left(C_f - C_\infty\right)\left[\phi''(\eta) + \frac{D_T}{T_\infty D_B}\frac{\left(T_f - T_\infty\right)}{\left(C_f - C_\infty\right)}\theta''(\eta) - C_r\frac{\nu_f}{aD_B}\phi(\eta)\right]\\ =\ & D_B\frac{a}{\nu_f}\left(C_f - C_\infty\right)\left[\phi''(\eta) + \frac{\tau D_T\left(T_f - T_\infty\right)}{\nu_f}\frac{\nu_f}{\tau D_B\left(C_f - C_\infty\right)}\theta''(\eta)\right.\\ &\left. - \frac{C_r}{a}\frac{\nu_f}{D_B}\phi(\eta)\right]\\ =\ & D_B\frac{a}{\nu_f}\left(C_f - C_\infty\right)\left[\phi''(\eta) + \frac{Nt}{Nb}\theta''(\eta) - \gamma Sc\,\phi(\eta)\right]. \qquad (3.15)\end{aligned}$$

From equations (3.14) and (3.15),we get

$$\phi''(\eta) + \frac{Nt}{Nb}\theta''(\eta) - \gamma Sc\,\phi(\eta) = -2Scf(\eta)\phi'(\eta)$$

$$\Rightarrow \ \phi''(\eta) + 2Scf(\eta)\phi'(\eta) + \frac{Nt}{Nb}\theta''(\eta) - \gamma Sc\,\phi(\eta) = 0. \tag{3.16}$$

The dimensionless quantities used in equation (3.16) are formulated as:

$$Sc = \frac{\nu_f}{D_B},\ \gamma = \frac{C_r}{a}. \tag{3.17}$$

The procedure for the conversion of boundary conditions into dimensionless form has been discussed below.

- $u(r,z) = ar \quad at \ \ z = 0.$

  $\Rightarrow \quad arf'(\eta) = ar \quad at \ \ \eta = 0.$

  $\Rightarrow \quad f'(\eta) = 1.$

- $w(r,z) = 0 \quad at \quad z = 0.$

  $\Rightarrow \quad -2\sqrt{a\nu_f} f(\eta) = 0 \quad at \quad \eta = 0.$

  $\Rightarrow \quad f(0) = 0.$

- $-k_f \frac{\partial T}{\partial z} = h_h (T_f - T) \quad at \ \ z = 0.$

  $\Rightarrow \quad -k_f \sqrt{\frac{a}{\nu_f}} (T_f - T_\infty)\theta'(\eta) = h_h \left[T_f - (T_f - T_\infty)\theta(\eta) - T_\infty\right] \quad at \ \ \eta = 0.$

  $\Rightarrow \quad -k_f \sqrt{\frac{a}{\nu_f}} (T_f - T_\infty)\theta'(0) = h_h (T_f - T_\infty)(1 - \theta(0)).$

  $\Rightarrow \quad \theta'(0) = -\frac{h_h}{k_f}\sqrt{\frac{\nu_f}{a}}(1 - \theta(0)).$

  $\Rightarrow \quad \theta'(0) = -Bi_1 (1 - \theta(0)).$

- $D_B \frac{\partial C}{\partial z} = -h_s (C_f - C) \quad at \ \ z = 0.$

  $\Rightarrow \quad D_B \sqrt{\frac{a}{\nu_f}} (C_f - C_\infty)\phi'(\eta) = -h_s \left[C_f - (C_f - C_\infty)\phi(\eta) - C_\infty\right] \quad at \ \ \eta = 0.$

  $\Rightarrow \quad D_B \sqrt{\frac{a}{\nu_f}} (C_f - C_\infty)\phi'(0) = -h_s (C_f - C_\infty)(1 - \phi(0)).$

$$\Rightarrow \quad \phi'(0) = -\frac{h_s}{D_B}\sqrt{\frac{\nu_f}{a}}\,(1-\phi(0))\,.$$

$$\Rightarrow \quad \phi'(0) = -Bi_2\,(1-\theta(0))\,.$$

- $u(r,z) \to br \quad at \quad z \to \infty.$

$$\Rightarrow \quad arf'(\eta) \to br \quad at \quad \eta \to \infty.$$

$$\Rightarrow \quad f'(\eta) \to \frac{b}{a} = A \quad at \quad \eta \to \infty.$$

- $T \to T_\infty \quad at \quad z \to \infty.$

$$\Rightarrow \quad (T_f - T_\infty)\,\theta(\eta) + T_\infty \to T_\infty \quad at \quad \eta \to \infty.$$

$$\Rightarrow \quad (T_f - T_\infty)\,\theta(\eta) \to T_\infty - T_\infty \quad at \quad \eta \to \infty.$$

$$\Rightarrow \quad (T_f - T_\infty)\,\theta(\eta) \to 0 \quad at \quad \eta \to \infty.$$

$$\Rightarrow \quad \theta(\eta) \to 0 \quad at \quad \eta \to \infty.$$

- $C \to C_\infty \quad at \quad z \to \infty.$

$$\Rightarrow \quad (C_f - C_\infty)\,\phi(\eta) + C_\infty \to C_\infty \quad at \quad \eta \to \infty.$$

$$\Rightarrow \quad (C_f - C_\infty)\,\phi(\eta) \to C_\infty - C_\infty \quad at \quad \eta \to \infty.$$

$$\Rightarrow \quad (C_f - C_\infty)\,\phi(\eta) \to 0 \quad at \quad \eta \to \infty.$$

$$\Rightarrow \quad \phi(\eta) \to 0 \quad at \quad \eta \to \infty.$$

Different parameters used in the above expression have the following formulations:

$$Bi_1 = \frac{h_h}{k_f}\sqrt{\frac{\nu_f}{a}},\ Bi_2 = \frac{h_s}{D_B}\sqrt{\frac{\nu_f}{a}}.$$

Finally, the ODEs describing the proposed flow problem can be re-collected in the following system.

$$\left(1+\frac{1}{\beta}\right) f''' + 2ff'' - f'^2 + A^2 - M^2\left(f' - A\right) = 0, \tag{3.18}$$

$$\left(1+\frac{4}{3}Rd\right)\theta'' + PrNb\theta'\phi' + PrNt\theta'^2 + 2Prf\theta' + \left(1+\frac{1}{\beta}\right)PrEcf''^2$$

$$+ PrEcM^2\left(f' - A\right)^2 + PrQ\theta = 0, \tag{3.19}$$

$$\phi'' + \frac{Nt}{Nb}\theta'' + Sc\left(2f\phi' - \gamma\phi\right) = 0. \tag{3.20}$$

The transformed boundary conditions are stated below.

$$\left.\begin{aligned} & f\left(0\right) = 0,\ f'\left(0\right) = 1, \\ & \theta'\left(0\right) = -Bi_1\left(1 - \theta\left(0\right)\right),\ \phi'\left(0\right) = -Bi_2\left(1 - \phi\left(0\right)\right), \\ & f' \to A,\ \theta \to 0,\ \phi \to 0 \ \text{ as } \ \eta \to \infty. \end{aligned}\right\} \tag{3.21}$$

The formulae for the dimensional form of skin-friction coefficient, Nusselt number and Sherwood number are as follows:

$$C_f = \frac{\tau_w}{\rho_f U_w^2}, \quad Nu = \frac{rq_w}{k_f\left(T_f - T_\infty\right)}, \quad Sh = \frac{rq_m}{D_B\left(C_f - C_\infty\right)}. \tag{3.22}$$

Given below are the formulae for τ_w, q_w and q_m.

$$\tau_w = \mu\left(1+\frac{1}{\beta}\right)\left(\frac{\partial u}{\partial z}\right)_{z=0}, \quad q_w = -k_f\left[\left(\frac{\partial T}{\partial z}\right) - \frac{q_r}{k_f}\right]_{z=0},$$

$$q_m = -D_B\left(\frac{\partial C}{\partial z}\right)_{z=0}. \tag{3.23}$$

The transformation of the above formulae into the dimensionless form has been carried out as:

- $$\begin{aligned}\tau_w &= \mu\left(1+\frac{1}{\beta}\right)\left(\frac{\partial u}{\partial z}\right)_{z=0}\\ &= \mu\left(1+\frac{1}{\beta}\right)\left(ar\sqrt{\frac{a}{\nu_f}}f''(0)\right)\\ &= \mu ar\sqrt{\frac{a}{\nu_f}}\left(1+\frac{1}{\beta}\right)f''(0).\end{aligned} \tag{3.24}$$
- $$\begin{aligned}q_w &= -k_f\left[\left(\frac{\partial T}{\partial z}\right)-\frac{q_r}{k_f}\right]_{z=0}\\ &= -k_f\left[\sqrt{\frac{a}{\nu_f}}(T_f-T_\infty)\theta'(0)-\left(\frac{-16\sigma^* T_\infty^3}{3k_f k^*}\sqrt{\frac{a}{\nu_f}}(T_f-T_\infty)\theta'(0)\right)\right]\\ &= -k_f\sqrt{\frac{a}{\nu_f}}(T_f-T_\infty)\left[1+\frac{4}{3}\left(\frac{4\sigma^* T_\infty^3}{k_f k^*}\right)\right]\theta'(0)\\ &= -k_f\sqrt{\frac{a}{\nu_f}}(T_f-T_\infty)\left[1+\frac{4}{3}Rd\right]\theta'(0).\end{aligned} \tag{3.25}$$
- $$\begin{aligned}q_m &= -D_B\left(\frac{\partial C}{\partial z}\right)_{z=0}\\ &= -D_B\sqrt{\frac{a}{\nu_f}}(C_f-C_\infty)\phi'(0).\end{aligned} \tag{3.26}$$

Incorporating equation (3.24), (3.25) and (3.26) in equation (3.22), we get the following dimensionless form for skin-friction coefficient, Nusselt number and Sherwood number.

- $$\begin{aligned}C_f &= \frac{\tau_w}{\rho_f U_w^2}\\ &= \frac{\mu ar\sqrt{\frac{a}{\nu_f}}\left(1+\frac{1}{\beta}\right)f''(0)}{\rho_f a^2 r^2}\\ &= \frac{1}{r}\sqrt{\frac{\nu_f}{a}}\left(1+\frac{1}{\beta}\right)f''(0)\\ &= Re^{-\frac{1}{2}}\left(1+\frac{1}{\beta}\right)f''(0).\end{aligned}$$

$$\Rightarrow \quad Re^{\frac{1}{2}} C_f = \left(1 + \frac{1}{\beta}\right) f''(0). \tag{3.27}$$

- $$\begin{aligned} Nu &= \frac{r q_w}{k_f (T_f - T_\infty)} \\ &= \frac{-r k_f \sqrt{\frac{a}{\nu_f}} (T_f - T_\infty) \left[1 + \frac{4}{3} Rd\right] \theta'(0)}{k_f (T_f - T_\infty)} \\ &= -r \sqrt{\frac{a}{\nu_f}} \left[1 + \frac{4}{3} Rd\right] \theta'(0) \\ &= -Re^{\frac{1}{2}} \left[1 + \frac{4}{3} Rd\right] \theta'(0). \end{aligned}$$

$$\Rightarrow \quad Re^{-\frac{1}{2}} Nu = -\left[1 + \frac{4}{3} Rd\right] \theta'(0). \tag{3.28}$$

- $$\begin{aligned} Sh &= \frac{r q_m}{D_B (C_f - C_\infty)} \\ &= \frac{-r D_B \sqrt{\frac{a}{\nu_f}} (C_f - C_\infty) \phi'(0)}{D_B (C_f - C_\infty)} \\ &= -r \sqrt{\frac{a}{\nu_f}} \phi'(0). \\ &= -Re^{\frac{1}{2}} \phi'(0). \end{aligned}$$

$$\Rightarrow \quad Re^{-\frac{1}{2}} Sh = -\phi'(0), \tag{3.29}$$

where $Re = \dfrac{r U_w}{\nu_f}$ elucidates the local Reynolds number and $\nu_f = \dfrac{\mu}{\rho}$ the kinematic viscosity.

3.3 Solution Methodology

In order to solve the system of ODEs (3.18)-(3.20) subject to the boundary conditions (3.21), the shooting method has been used. Primarily equation (3.18) is solved numerically and then the computed results of f, f' and f'' are used in equations (3.19)-(3.20). For the numerical treatment of equation (3.18), the missing initial condition $f''(0)$ has been denoted as s and the following notations have

been considered.

$$f = h_1, f' = h_2, f'' = h_3, \frac{\partial f}{\partial s} = h_4, \frac{\partial f'}{\partial s} = h_5, \frac{\partial f''}{\partial s} = h_6. \tag{3.30}$$

Using the above notations, equation (3.18) can be converted into a system of three first order ODEs. First three of the following ODEs correspond to (3.18) and the other three are obtained by differentiating the first three w.r.t s.

$$\begin{aligned}
h_1' &= h_2, && h_1(0) = 0,\\
h_2' &= h_3, && h_2(0) = 1,\\
h_3' &= \frac{\beta}{(1+\beta)}\left[h_2^2 + M^2(h_2 - A) - 2h_1h_3 - A^2\right], && h_3(0) = s,\\
h_4' &= h_5, && h_4(0) = 0,\\
h_5' &= h_6, && h_5(0) = 0,\\
h_6' &= \frac{\beta}{(1+\beta)}\left[\left(2h_2 + M^2\right)h_5 - 2(h_1h_6 + h_3h_4)\right], && h_6(0) = 1.
\end{aligned}$$

The RK-4 method has been used to solve the above initial value problem. In order to get the approximate numerical results, the problem's domain is considered to be bounded i.e. $[0, \eta_\infty]$, where η_∞ is chosen to be an appropriate finite positive real number in such a way that the variation in the solution for $\eta > \eta_\infty$ is ignorable. The missing condition for the above system of equations is to be chosen such that $(h_2(\eta_\infty))_s = A$. This algebraic equation has been solved by using the Newton's method governed by the following iterative formula.

$$s^{(n+1)} = s^{(n)} - \frac{\left(h_2(\eta_\infty)\right)_{s=s^{(n)}} - A}{\left(\dfrac{\partial h_2(\eta_\infty)}{\partial s}\right)_{s=s^{(n)}}}.$$

$$\Rightarrow \; s^{(n+1)} = s^{(n)} - \frac{\left(h_2(\eta_\infty)\right)_{s=s^{(n)}} - A}{\left(h_5(\eta_\infty)\right)_{s=s^{(n)}}}. \tag{3.31}$$

The stopping criteria for the shooting method is set as

$$\left|\left(h_2(\eta_\infty)\right)_{s=s^{(n)}} - A\right| < \epsilon, \tag{3.32}$$

for some very small positive number ϵ.

Now to solve equations (3.19) and (3.20) numerically, the missing initial conditions $\theta(0)$ and $\phi(0)$ have been denoted by l and m, respectively. Thereby the following notations have been taken into account.

$$\left.\begin{aligned} &\theta = y_1,\ \theta' = y_2,\ \phi = y_3,\ \phi' = y_4,\ \frac{\partial\theta}{\partial l} = y_5,\ \frac{\partial\theta'}{\partial l} = y_6,\ \frac{\partial\phi}{\partial l} = y_7,\\ &\frac{\partial\phi'}{\partial l} = y_8,\ \frac{\partial\theta}{\partial m} = y_9,\ \frac{\partial\theta'}{\partial m} = y_{10},\ \frac{\partial\phi}{\partial m} = y_{11},\ \frac{\partial\phi'}{\partial m} = y_{12}. \end{aligned}\right\} \tag{3.33}$$

Incorporating the above notations, a system of first order ODEs is achieved that is stated below.

$$y_1' = y_2, \qquad y_1(0) = l,$$

$$y_2' = \frac{-3}{3+4Rd}(PrNby_2y_4 + PrNty_2^2 + 2Prh_1y_2 + PrQy_1 + \left(1+\frac{1}{\beta}\right)PrEch_3^2 + PrEcM^2\left(h_2 - A\right)^2), \qquad y_2(0) = -Bi_1(1-l),$$

$$y_3' = y_4, \qquad y_3(0) = m,$$

$$y_4' = -\left(\frac{Nt}{Nb}\right)y_2' - Sc\left(2h_1y_4 - \gamma y_3\right), \qquad y_4(0) = -Bi_2(1-m),$$

$$
\begin{aligned}
y_5' &= y_6, && y_5(0) = 1,\\
y_6' &= \frac{-3Pr}{3+4Rd}\left((Nby_4 + 2Nty_2 + 2h_1)y_6 + Nby_2y_8 + By_5\right), && y_6(0) = Bi_1,\\
y_7' &= y_8, && y_7(0) = 0,\\
y_8' &= \frac{3NtPr}{Nb(3+4Rd)}\left(Nby_4 + 2Nty_2 + 2h_1\right)y_6 + By_5 + Nby_2y_8)\\
&\quad - 2Sch_1y_8 + Sc\gamma y_7, && y_8(0) = 0,\\
y_9' &= y_{10}, && y_9(0) = 0,\\
y_{10}' &= \frac{-3Pr}{3+4Rd}\left((Nby_4 + 2Nty_2 + 2h_1)y_{10} + Nby_2y_{12} + By_9\right), && y_{10}(0) = 1,\\
y_{11}' &= y_{12}, && y_{11}(0) = 0,\\
y_{12}' &= \frac{3NtPr}{Nb(3+4Rd)}\left((Nby_4 + 2Nty_2 + 2h_1)y_{10} + By_9 + Nby_2y_{12}\right)\\
&\quad - 2Sch_1y_{12} + Sc\gamma y_{11}, && y_{12}(0) = 0.
\end{aligned}
$$

The RK-4 method has been taken into consideration for solving the above initial value problem. For the above system of equations, the missing conditions are to be chosen such that

$$
\left(y_1(l,m)\right)_{\eta=\eta_\infty} = 0, \;\; \left(y_3(l,m)\right)_{\eta=\eta_\infty} = 0. \tag{3.34}
$$

The above algebraic equations have been solved by using the Newton's method governed by the following iterative formula:

$$
\begin{bmatrix} l^{(n+1)} \\ m^{(n+1)} \end{bmatrix} = \begin{bmatrix} l^{(n)} \\ m^{(n)} \end{bmatrix} - \left[\begin{bmatrix} \frac{\partial y_1(l,m)}{\partial l} & \frac{\partial y_1(l,m)}{\partial m} \\ \frac{\partial y_3(l,m)}{\partial l} & \frac{\partial y_3(l,m)}{\partial m} \end{bmatrix}^{-1} \begin{bmatrix} y_1 \\ y_3 \end{bmatrix} \right]_{\left(l^{(n)},\, m^{(n)},\, \eta_\infty\right)}.
$$

$$\Rightarrow \begin{bmatrix} l^{(n+1)} \\ m^{(n+1)} \end{bmatrix} = \begin{bmatrix} l^{(n)} \\ m^{(n)} \end{bmatrix} - \left[\begin{bmatrix} y_5 & y_9 \\ y_7 & y_{11} \end{bmatrix}^{-1} \begin{bmatrix} y_1 \\ y_3 \end{bmatrix} \right]_{\left(l^{(n)},\ m^{(n)},\ \eta_\infty\right)} .$$

The stopping criteria for the shooting method is set as:

$$max\{|\,(y_1(\eta_\infty)|,\ |y_3(\eta_\infty))\,|\} < \epsilon, \tag{3.35}$$

for some very small positive number ϵ. Throughout this chapter ϵ has been taken as 10^{-12} whereas η_∞ is set as 7.

3.4 Results with Discussion

In this section, the numerical results of skin-friction coefficient, Nusselt and Sherwood numbers are illustrated with tables and graphs by assuming different values of pertinent flow parameters of interest.

3.4.1 Skin-friction Coefficient, Nusselt and Sherwood Numbers

To validate the MATLAB code, the results of $-f''(0)$ and $-\theta'(0)$ are reproduced for the problem discussed by Attia [39]. Tables 3.1-3.4 reflect an excellent agreement between the results computed by the present code and those already published in the relevant articles.

Table 3.5 discloses the numerical results of skin-friction coefficient along with Nusselt and sherwood numbers for the present model in regards to a change in the values of various parameters like β, M, Rd, A, Pr, Q, Nb, Nt, Ec and Sc.

		$f''(0)$				$f''(0)$	
M	A	Attia [39]	Present	M	A	Attia [39]	Present
0	0.1	-1.1246	-1.1246	2	0.1	-2.1138	-2.1138
	0.2	-1.0556	-1.0556		0.2	-1.9080	-1.9081
	0.5	-0.7534	-0.7534		0.5	-1.2456	-1.2456
	1.0	0.0000	0.0000		1.0	0.0000	0.0000
	1.1	0.1821	0.1821		1.1	0.2691	0.2691
	1.2	0.3735	0.3735		1.2	0.5445	0.5445
	1.5	1.0009	1.0009		1.5	1.4080	1.4081
1	0.1	-1.4334	-1.4334	3	0.1	-2.9174	-2.9175
	0.2	-1.3179	-1.3179		0.2	-2.6141	-2.6141
	0.5	-0.9002	-0.9002		0.5	-1.6724	-1.6725
	1.0	0.0000	0.0000		1.0	0.0000	0.0000
	1.1	0.2070	0.2070		1.1	0.3494	0.3494
	1.2	0.4004	0.42236		1.2	0.7037	0.7038
	1.5	1.1157	1.1157		1.5	1.7954	1.7955

TABLE 3.1: Comparison of the computed values of $f''(0)$ with those given by Attia [39] when $Nt = Nb = Rd = Ec = Sc = 0$.

It has been remarked from the results that for the larger M, the skin-friction coefficient escalates whereas heat and mass transfer rates fall significantly.The higher estimation of β depreciates the skin-friction coefficient, Nusselt and Sherwood numbers. For the higher estimation of A, the skin-friction coefficient and the Nusselt number de-escalate whereas the Sherwood number climbs marginally.

		$-\theta'(0)$				$-\theta'(0)$	
Pr	A	Attia [39]	Present	Pr	A	Attia [39]	Present
0.05	0.1	0.1273	0.1669	0.5	0.1	0.4691	0.4703
	0.2	0.1421	0.1761		0.2	0.5223	0.5224
	0.5	0.1845	0.2044		0.5	0.6345	0.6345
	1.0	0.2439	0.2510		1.0	0.7699	0.7699
	1.1	0.2545	0.2599		1.1	0.7933	0.7933
	1.2	0.2632	0.2688		1.2	0.8136	0.8158
	1.5	0.2919	0.2942		1.5	0.8793	0.8793
0.1	0.1	0.1618	0.1951	1.0	0.1	0.7657	0.7656
	0.2	0.1911	0.2139		0.2	0.8152	0.8151
	0.5	0.2615	0.2679		0.5	0.9332	0.9332
	1.0	0.3343	0.3450		1.0	1.0888	1.0888
	1.1	0.3581	0.3586		1.1	1.1166	1.1165
	1.2	0.3700	0.3716		1.2	1.1408	1.1434
	1.5	0.4080	0.4081		1.5	1.2200	1.2199

TABLE 3.2: Comparison of the computed results of Nusselt number $-\theta'(0)$ with those given by Attia [39] when $Nt = Nb = Rd = Ec = Sc = 0$.

$-\theta'(0)$ with $M = 1, Pr = 0.5$		
A	Attia [39]	Present
0.1	0.4691	0.4703
0.2	0.5223	0.5224
0.5	0.6345	0.6345
1.0	0.7699	0.7699
1.1	0.7933	0.7933
1.2	0.8136	0.8158

TABLE 3.3: Comparison of the computed results of $-\theta'(0)$ with those given by Attia [39] when $Nt = Nb = Rd = Ec = Sc = 0$ and $Q = 0.1$.

β	M	A	Rd	Pr	Q	Nb	Nt	Ec	Sc	$-a_1 f''(0)$	$-a_2\theta'(0)$	$-\phi'(0)$
0.5	1.0	0.1	0.1	0.7	0.1	0.5	0.1	0.1	1.2	2.4828	0.0862	0.09398
5.0										1.5703	0.0870	0.09373
10										1.5034	0.0871	0.09371
	1.2									2.6870	0.0781	0.09312
	1.4									3.0284	0.0762	0.09302
		0.3								2.0980	0.0922	0.09301
		0.5								1.5591	0.0945	0.09200
			0.2							2.4828	0.0858	0.09396
			0.3							2.4828	0.0853	0.09395
				1.0						2.4828	0.0874	0.09411
				2.0						2.4828	0.0878	0.09475
					0.5					2.4828	0.0701	0.09448
					0.7					2.4828	-0.1018	0.09929
						0.7				2.4828	0.0862	0.09393
						0.8				2.4828	0.0861	0.09392
							0.2			2.4828	0.0862	0.09416
							0.3			2.4828	0.0379	0.09434
								0.5		2.4828	0.0379	0.09592
								1.0		2.4828	-0.0231	0.09835
									1.4	2.4828	0.0862	0.09445
									1.6	2.4828	0.0863	0.09482

TABLE 3.4: The computed results of skin-friction coefficient, Nusselt and Sherwood numbers for $\gamma = 1, Bi_1 = 0.1 = Bi_2$, where $a_1 = \left(1 + \frac{1}{\beta}\right)$ and $a_2 = \left(1 + \frac{4}{3}Rd\right)$.

γ	Bi_1	Bi_2	$-a_1 f''(0)$	$-a_2\theta'(0)$	$\phi'(0)$
1.0	0.1	0.1	2.4828	0.0761	0.1064
1.5			2.4828	0.0761	0.1073
2.0			2.4828	0.0761	0.1078
	0.2		2.4828	0.7699	0.1062
	0.3		2.4828	0.7933	0.1061
		0.2	2.4828	0.8158	0.2006
		0.3	2.4828	0.8793	0.2843

TABLE 3.5: The computed results of skin-friction coefficient, Nusselt and Sherwood numbers for $\beta = 0.5, M = 1, A = 0.1, Rd = 0.1, Pr = 0.7, Q = 0.1, Nb = 0.5, Nt = 0.1, Ec = 0.1, Sc = 1.2$, where $a_1 = \left(1 + \frac{1}{\beta}\right)$ and $a_2 = \left(1 + \frac{4}{3}Rd\right)$.

Furthermore, heat and mass transfer rates decline by assuming the larger vaues of Rd and Nb. An enhancement in the Nusselt and Sherwood numbers has been seen as Pr and Sc assume the larger values. Mass transfer rate falls by taking into account the larger values of Q, Nt and Ec whereas Sherwood number increases. Table 3.6 reflects the computed results of the Nusselt and Sherwood numbers on account of the various values of γ, Bi_1 and Bi_2. Both heat and mass transfer rates increase as the value of γ escalates. For the larger Bi_1, the Nusselt number is enhanced whereas the Sherwood number experiences an opposite behaviour.

It can be seen that a rise in Bi_2 decreases the Nusselt number but contrary to this the mass transfer rate climbs significantly. Tables 3.7-3.8 portray the intervals I_f, I_θ and I_ϕ where from the missing initial conditions $f''(0)$, $\theta'(0)$ and $\phi'(0)$ respectively can be chosen. It is noteworthy that the intervals mentioned offer a

considerable flexibility for the choice of initial guesses.

β	M	A	Rd	Pr	Q	Nb	Nt	Ec	Sc	I_f	I_θ	I_ϕ
0.5	1	0.1	0.1	0.7	0.1	0.5	0.1	0.1	1.2	[-1, 2.5]	[-1.9, 170]	[-1.9, 170]
5.0										[-1.4, -0.9]	[-1.9, 160]	[-1.9, 160]
10										[-1.4, -1.3]	[-1.3, 160]	[-1.3, 160]
	1.2									[-0.7, 0]	[0, 150]	[0, 150]
	1.4									[-0.9,-0.8]	[-0.5, 200]	[-0.5, 200]
		0.3								[-1, 2.5]	[-6, 220]	[-6, 200]
		0.5								[-0.9, -0.2]	[-0.5, 250]	[-0.5, 250]
			0.2							[-0.9, 0.8]	[-2, 190]	[-2, 190]
			0.3							[-0.9, 1]	[-2, 200]	[-2, 200]
				1.0						[-1, 2.5]	[-1, 140]	[-1, 140]
				2.0						[-1, 2.5]	[-1, 100]	[-1, 100]
					0.5					[-1, 2.5]	[-0.8, 160]	[-0.8, 160]
					0.7					[-1, 2.5]	[-1, 150]	[-1, 150]
						0.7				[-1, 2.5]	[-1, 140]	[-1, 140]
						0.8				[-1, 2.5]	[-1, 180]	[-1, 180]
							0.2			[-1, 2.5]	[-2, 150]	[-2, 150]
							0.3			[-1, 2.5]	[-2, 170]	[-2, 170]
								0.5		[-1, 2.5]	[-2, 170]	[-2, 170]
								1.0		[-1, 2.5]	[-3, 170]	[-3, 170]
									1.4	[-1, 2.5]	[-3, 170]	[-3, 170]
									1.6	[-1, 2.5]	[-2, 140]	[-2, 140]

TABLE 3.6: The intervals for the initial guesses for the missing initial conditions when $\gamma = 1, Bi_1 = 0.1 = Bi_2$.

γ	Bi_1	Bi_2	I_f	I_θ	I_ϕ
1.0	0.1	0.1	[-1, 2.5]	[-0.3, 10]	[-0.2, 10]
1.5			[-1, 2.5]	[-0.07, 8]	[-0.09, 9]
2.0			[-1, 2.5]	[-0.07, 10]	[-0.09, 10]
	0.2		[-1, 2.5]	[-0.13, 10]	[-0.09, 10]
	0.3		[-1, 2.5]	[-0.13, 19]	[-0.09, 15]
		0.2	[-1, 2.5]	[-0.07, 10]	[-0.17, 10]
		0.3	[-1, 2.5]	[-0.07, 10]	[-0.25, 10]

TABLE 3.7: The intervals for the initial guesses for the missing initial conditions when $\beta = 0.5, M = 1, A = 0.1, Rd = 0.1, Pr = 0.7, Q = 0.1, Nb = 0.5, Nt = 0.1, Ec = 0.1, Sc = 1.2$.

3.4.2 The Velocity, Temperature and Concentration Profiles

Figures 3.2-3.4 present the impact of the magnetic parameter on the velocity, temperature and concentration distributions. The larger estimation of M decelerate the velocity and escalate the temperature and concentration of the fluid. This stems from the fact that an opposing force is generated by the magnetic field, generally referred as the Lorentz force, which depresses the motion of the fluid resulting in a decrement in the momentum boundary layer thickness and heightens the thermal and concentration boundary layer thickness.

Figures 3.5-3.7 are delineated to show the effect of A on the velocity, temperature and concentration distributions. An enhancement in the flow velocity has been observed for $A > 1$. On the other hand, the velocity reduces for the case

$A < 1$. Also, both the temperature and concentration profiles decrease when A assumes the larger value. As the value of A heightens, the heat transfer from the sheet to the fluid becomes smaller and as a result, the temperature falls significantly. Furthermore, the thermal boundary layer thickness is reduced. Moreover, the concentration boundary layer thickness also shows a declining behaviour.

Figures 3.8-3.10 are framed to delineate the effect of Casson parameter on the velocity, temperature and concentration fields. The velocity profile shows an increasing trend by increasing β. Additionally, the velocity boundary layer thickness undergoes a decrement as β assumes the larger value. This stems from the fact that the plasticity of the Casson fluid increases for the smaller β and leads to an enhancement in the momentum boundary layer thickness. Also, the temperature distribution can be seen to rise for the increasing values of β. Further to this, the thermal boundary thickness is strengthened. A rise in the nanoparticle volume fraction has been observed for the higher estimation of β and the concentration boundary layer thickness is enhanced.

Figures 3.11-3.12 are framed to delineate the outcome of Pr on the temperature and concentration distributions. Since Pr is directly proportionate to the viscous diffusion rate and inversely related to the thermal diffusivity, so the thermal diffusion rate suffers a reduction for the larger estimation of Pr and subsequently, the temperature of the fluid drops significantly. Moreover, a decrement in the thermal boundary layer thickness has been noted. However, the nanoparticle volume fraction of the fluid can be remarked to escalates for the higher values of Pr. In addition to that, an increment can be seen in the concentration boundary layer

thickness.

The outcome of Ec on the velocity and temperature profiles has been characterized through Figures 3.13-3.14. Physically, the Eckert number depicts the relation between the kinetic energy of the fluid particles and the boundary layer enthalpy. The kinetic energy of the fluid particles rises as Ec assumes the larger values. Hence, the velocity and temperature of the fluid climbs marginally and therefore, the associated momentum and thermal boundary layer thickness are enhanced.

Figures 3.15-3.16 elucidate the effect of the radiation parameter Rd and the heat generation or absorption parameter Q on the temperature distributions. Since the heat transfer climbs marginally for the higher estimation of Rd, thereby an increment in the temperature of the fluid and the thermal boundary layer has been noticed. However, as the value of Q rises, more heat is generated causing an increment in the temperature and the thermal boundary layer thickness. On the other hand, as the value of Q de-escalates , the heat absorbed results in a decrement in the temperature and the associated thermal boundary layer thickness.

Figures 3.17-3.18 delineate the outcome of Sc and γ on the concentration fields. The concentration of the fluid depicts a decreasing behaviour as Sc assumes the higher value. This behaviour stems from the fact that the Schmidt number and mass diffusion rate have inverse relation, therefore, for the larger Sc, the process of the mass diffusivity slows down and thus, the concentration falls and the concentration boundary layer thickness is reduced. Furthermore, the chemical reaction

parameter also has a similar effect on the concentration profile. The larger values of γ result in a decrement in the chemical molecular diffusion and hence, the concentration of the fluid de-escalates and the associated concentration boundary layer thickness is reduced.

Figures 3.19-3.20 interpret the impact of the thermophoresis parameter on the temperature and concentration distributions. Both the temperature and concentration escalate by taking larger values of Nt into account. In addition to this, an increment in the associated thermal and concentration boundary layer has been noticed.

Figures 3.21-3.22 display the influence of the Brownian motion parameter on the temperature and concentration distributions. The temperature profile climbs marginally for the larger values of Nb. This happens due to the reason that as the value of Nb rises, the movement of the nanoparticles enhances significantly which triggers the kinetic energy of the nanoparticles and eventually, the temperature enhances and the thermal boundary layer thickness is magnified. On the other hand, the concentration of the fluid falls as Nb assumes the higher values. Also, the concentration boundary layer thickness is depressed.

The impact of the thermal Biot number on the temperature distribution and the concentration Biot number on the nanoparticle volume fraction has been portrayed by Figures 3.23-3.24. It is remarkable that the temperature can be observed as an increasing function of Bi_1 and the concentration of the fluid also enhances as Bi_2 heightens. Further to this, the associated thermal and concentration boundary

layer thickness are enhanced.

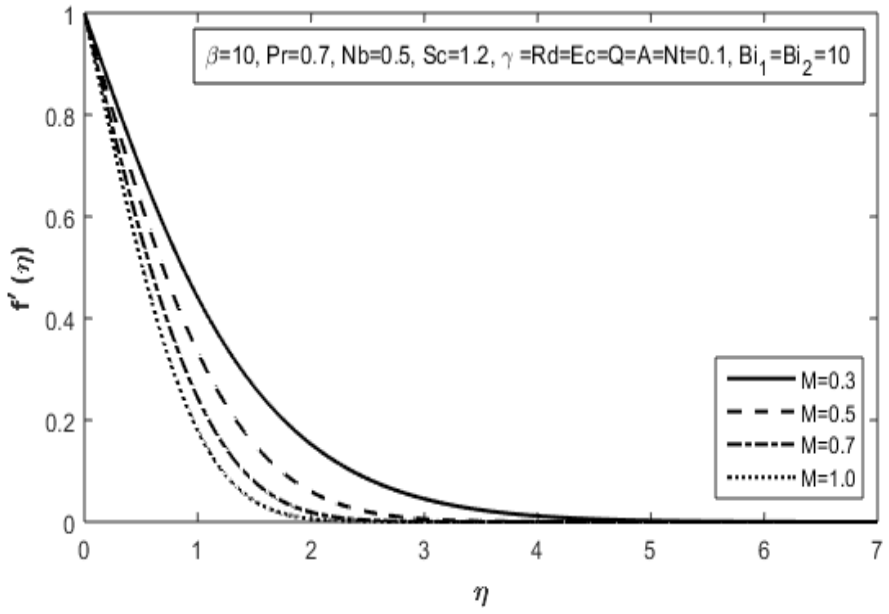

FIGURE 3.2: Effect of M on $f'(\eta)$

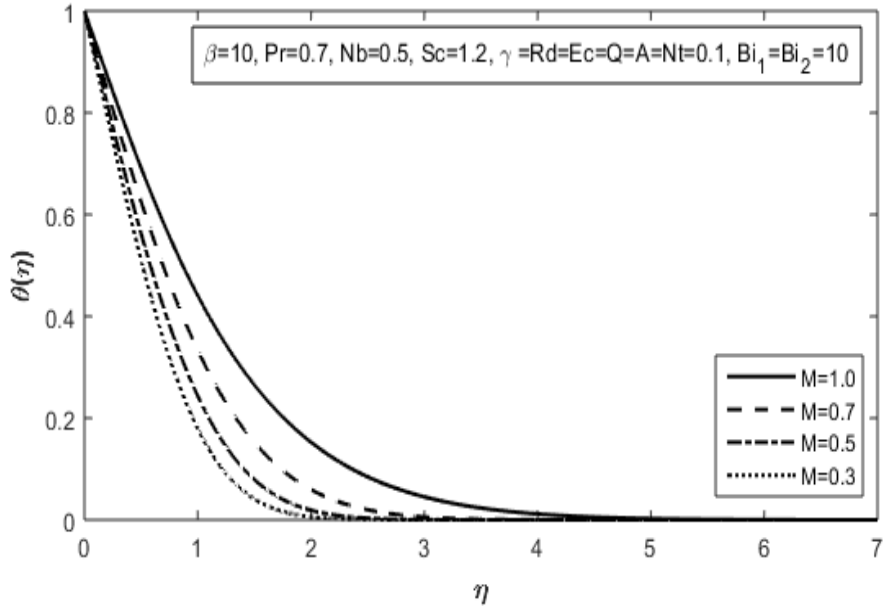

FIGURE 3.3: Effect of M on $\theta(\eta)$

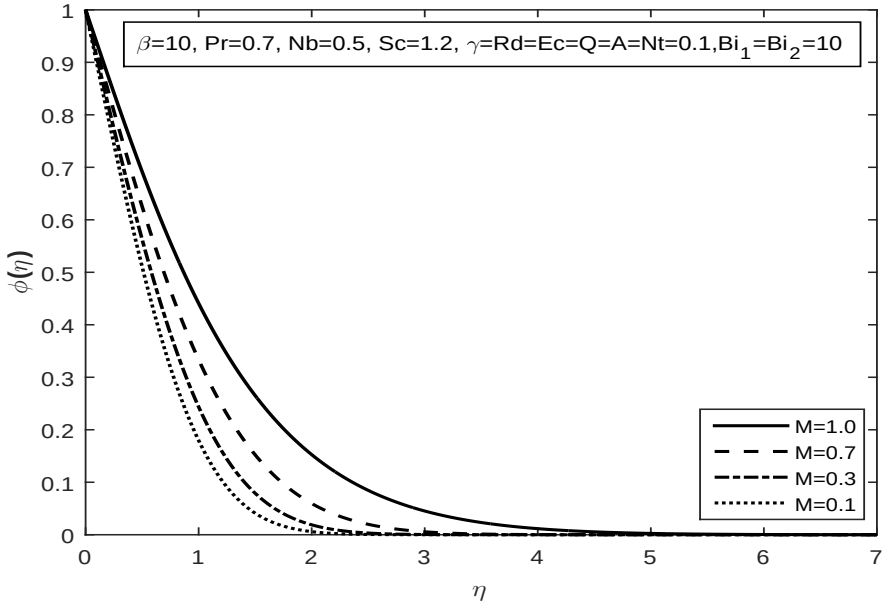

FIGURE 3.4: Effect of M on $\phi(\eta)$

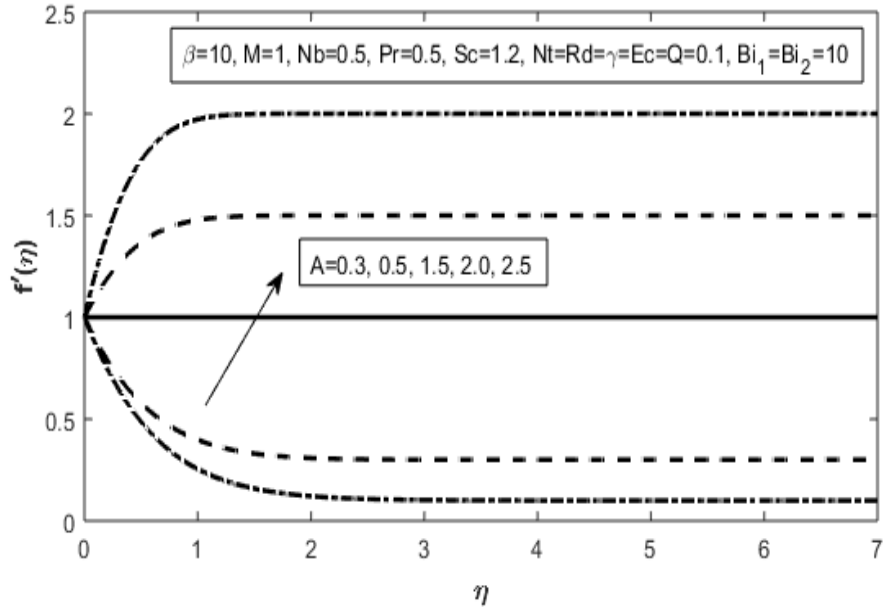

FIGURE 3.5: Effect of A on $f^{'}(\eta)$

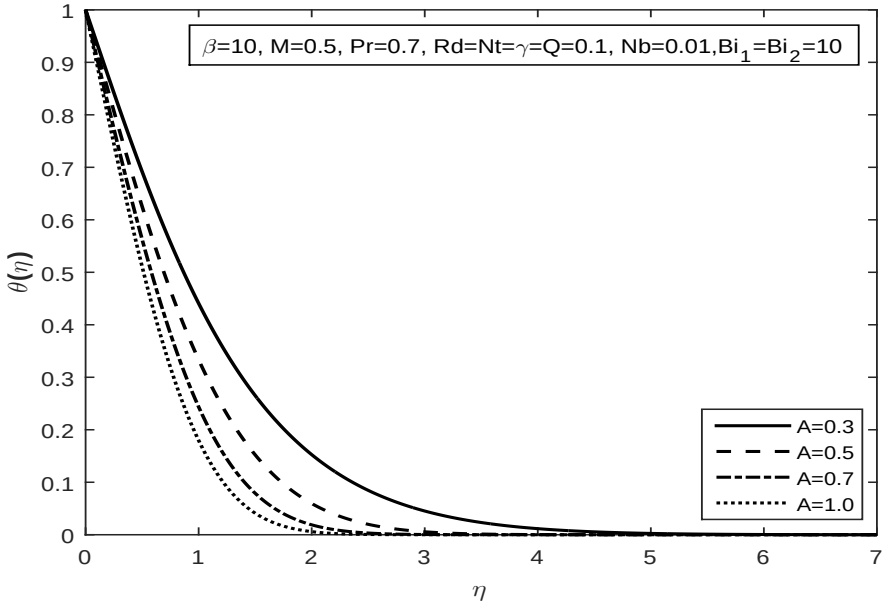

FIGURE 3.6: Effect of A on $\theta(\eta)$

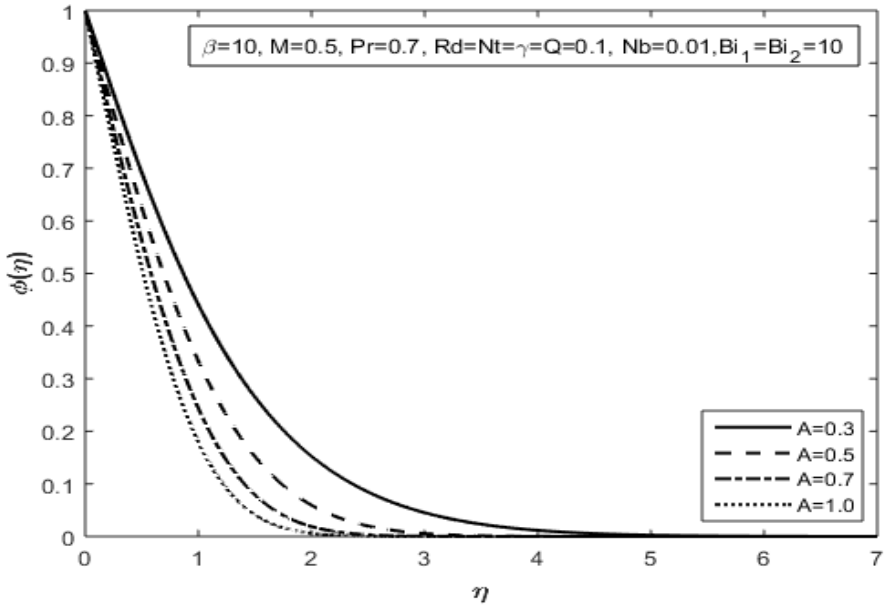

FIGURE 3.7: Effect of A on $\phi(\eta)$

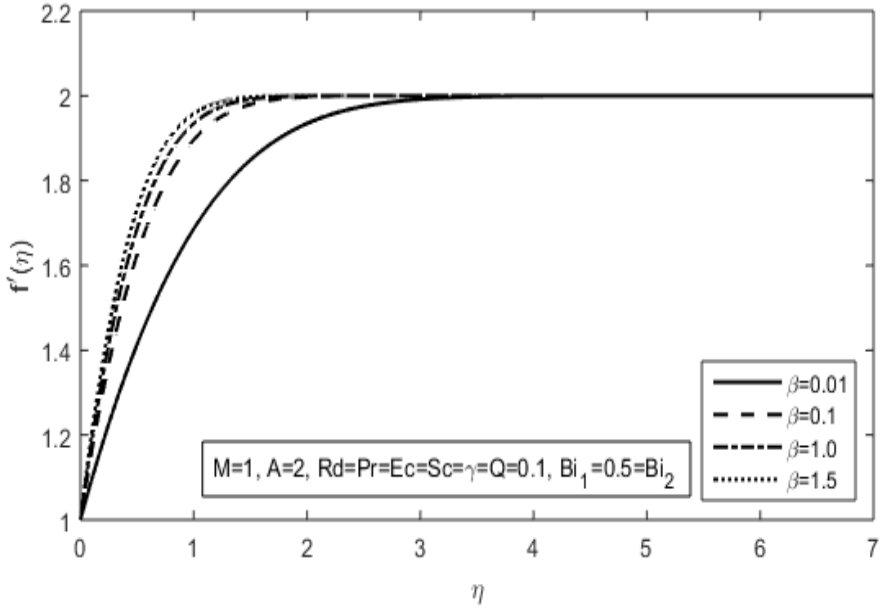

FIGURE 3.8: Effect of β on $f'(\eta)$

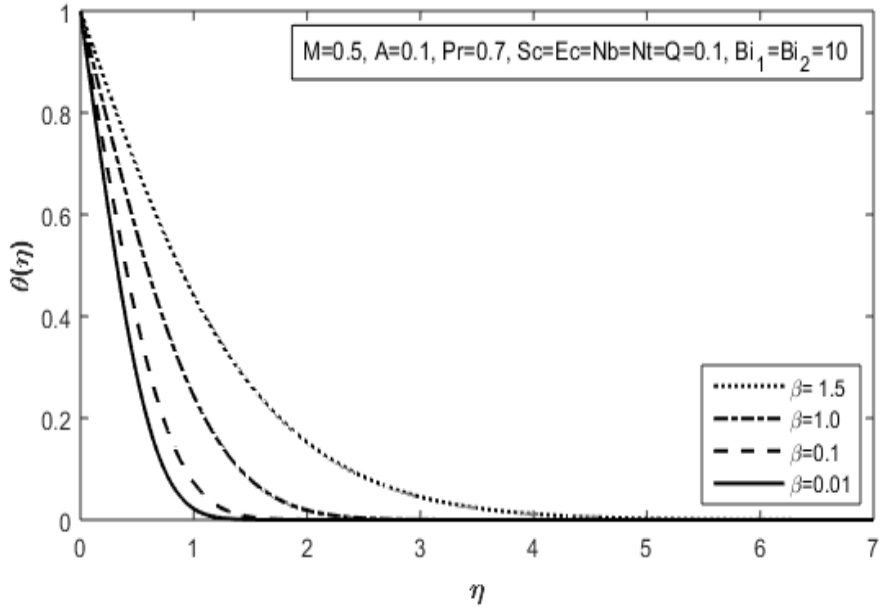

FIGURE 3.9: Effect of β on $\theta(\eta)$

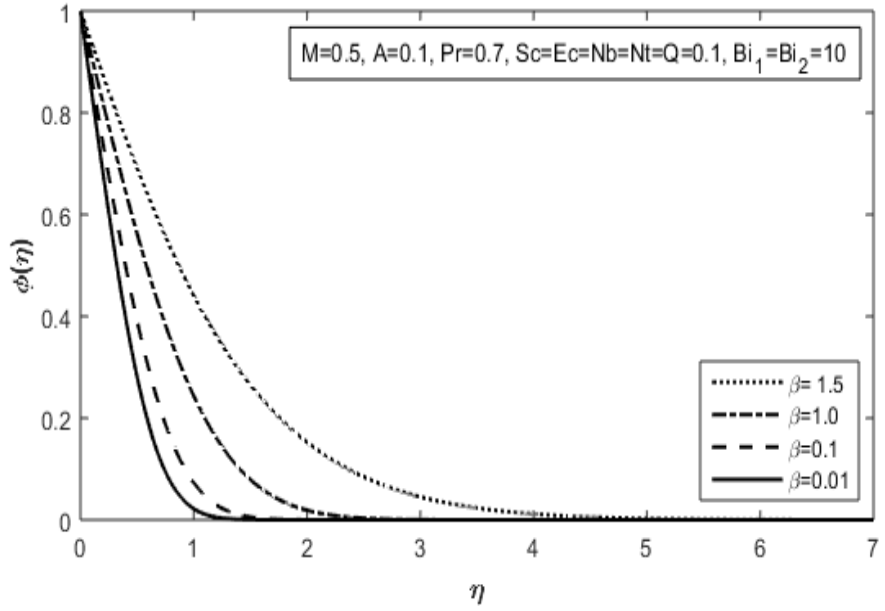

FIGURE 3.10: Effect of β on $\phi(\eta)$

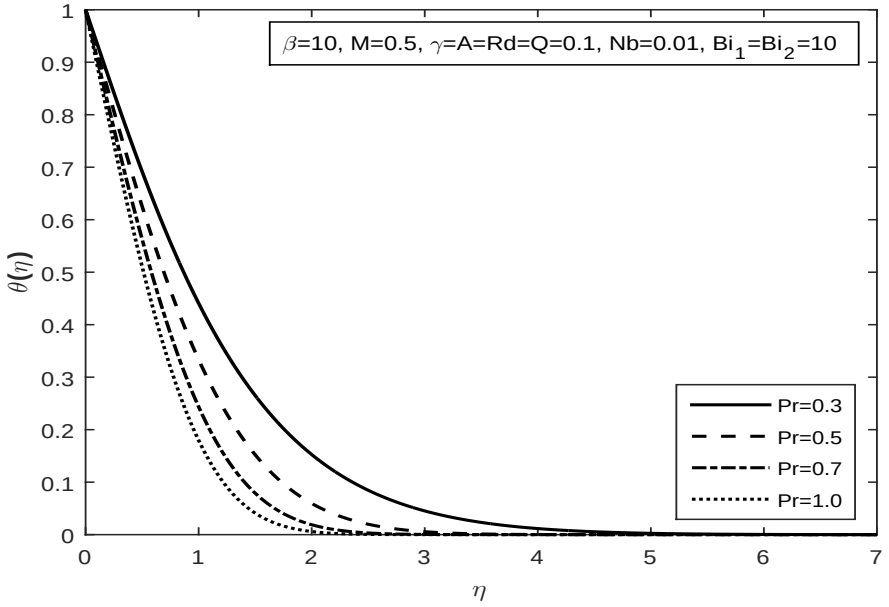

FIGURE 3.11: Effect of Pr on $\theta(\eta)$

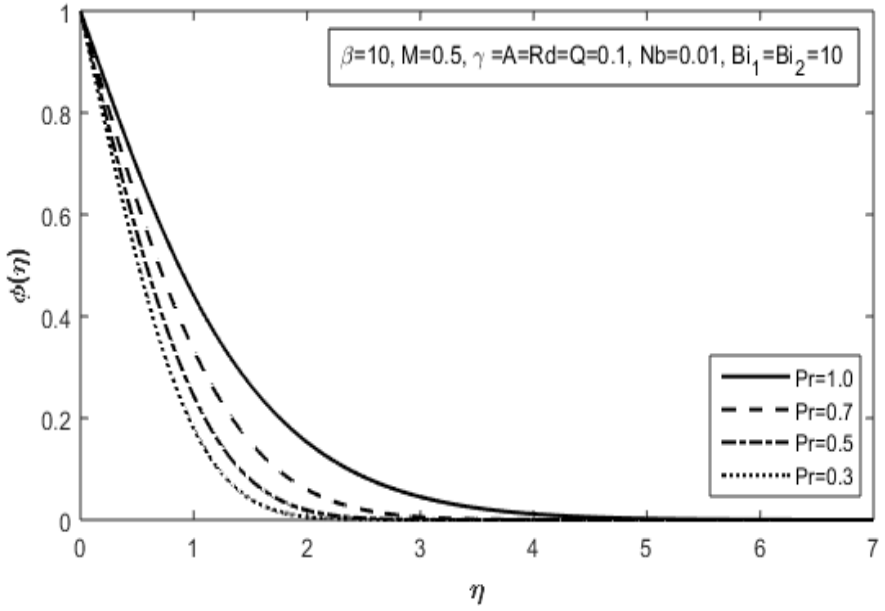

FIGURE 3.12: Effect of Pr on $\phi(\eta)$

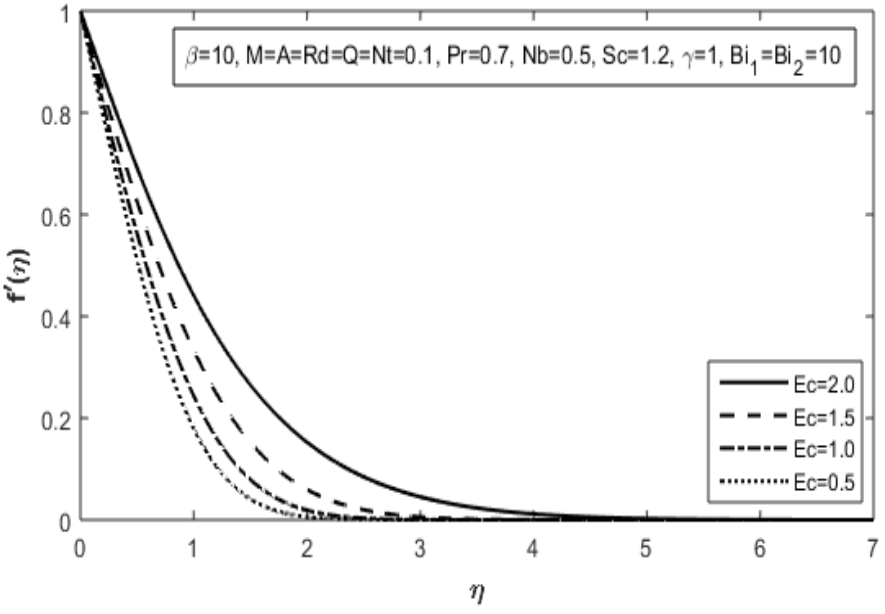

FIGURE 3.13: Effect of Ec on $f'(\eta)$

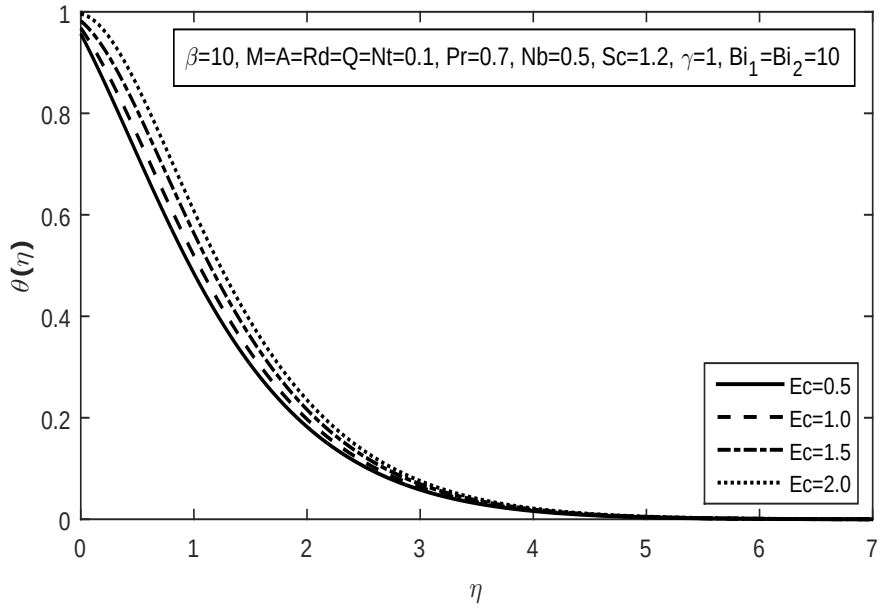

FIGURE 3.14: Effect of Ec on $\theta(\eta)$

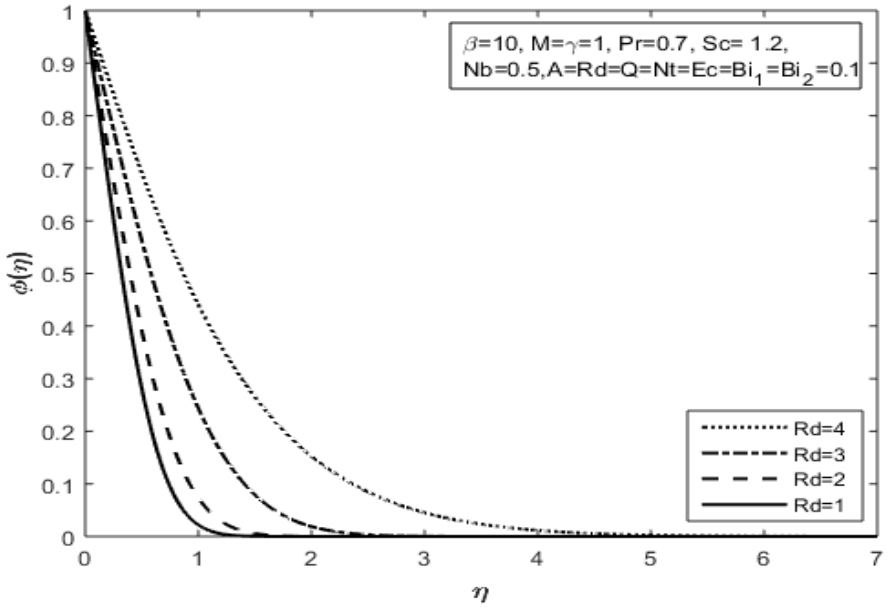

FIGURE 3.15: Effect of Rd on $\theta(\eta)$

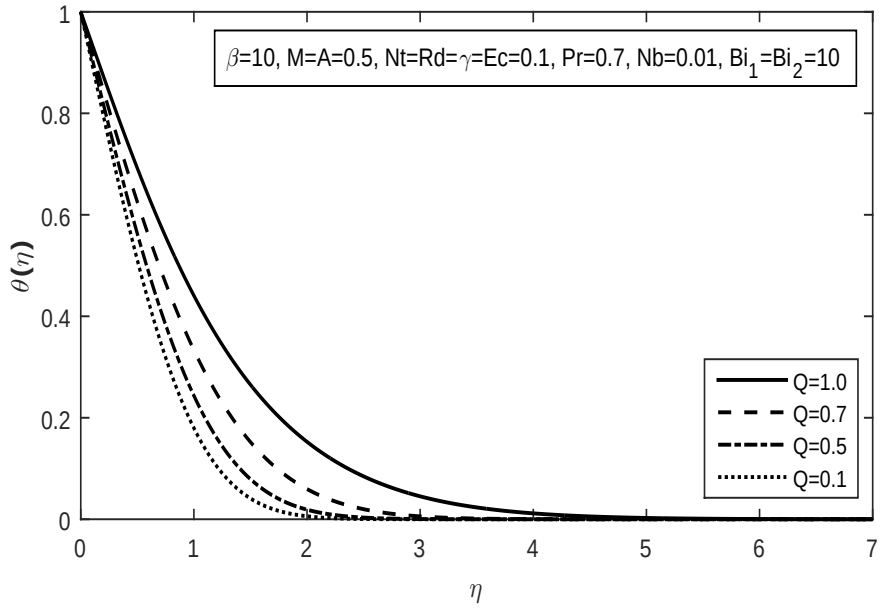

FIGURE 3.16: Effect of Q on $\theta(\eta)$

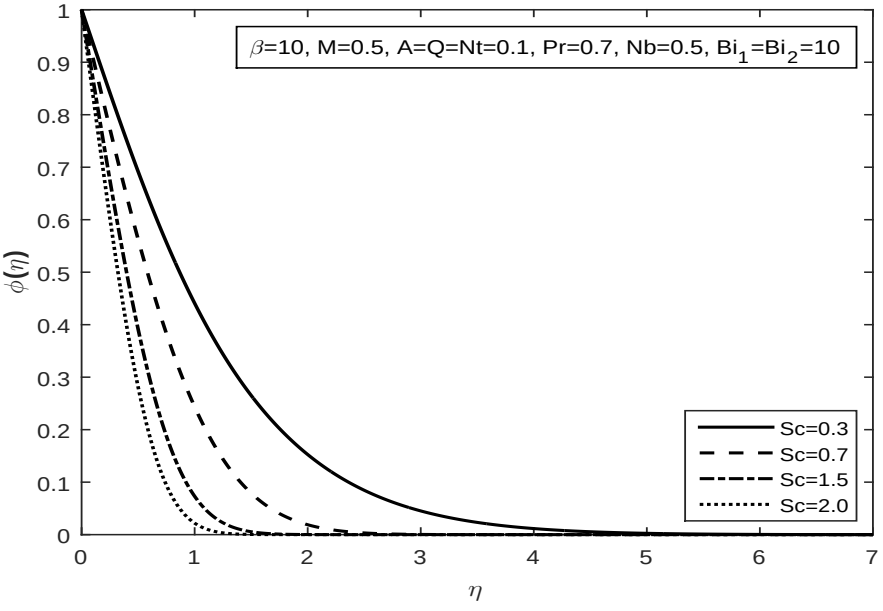

FIGURE 3.17: Effect of Sc on $\phi(\eta)$

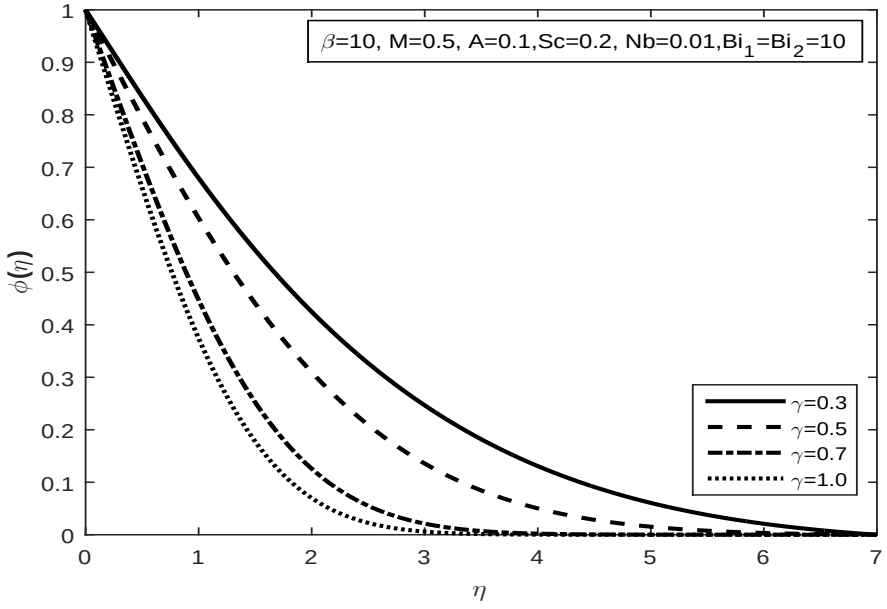

FIGURE 3.18: Effect of γ on $\phi(\eta)$

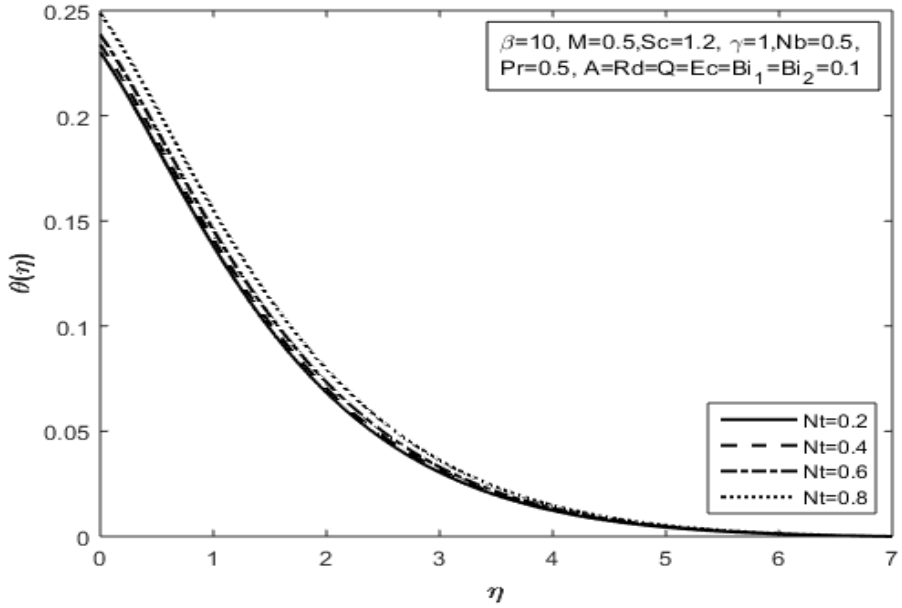

FIGURE 3.19: Effect of Nt on $\theta(\eta)$

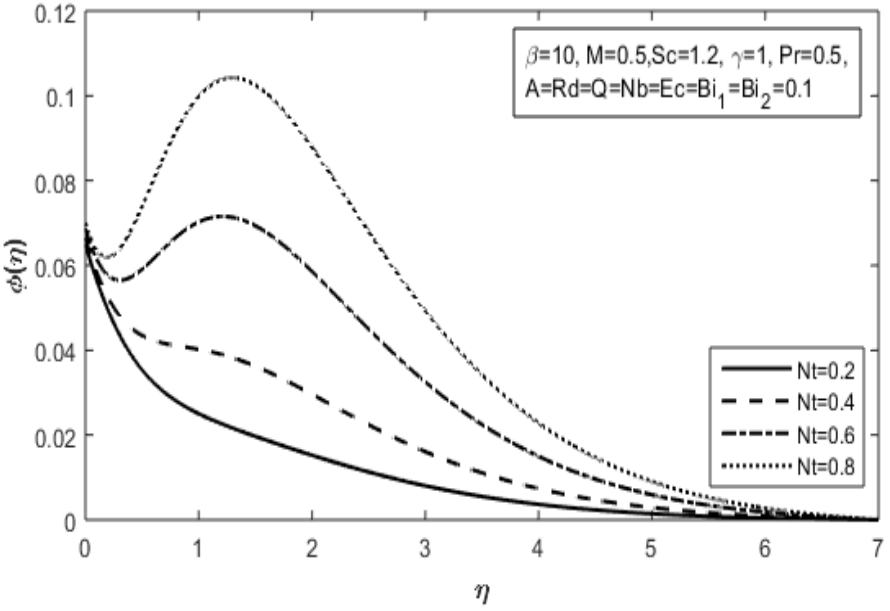

FIGURE 3.20: Effect of Nt on $\phi(\eta)$

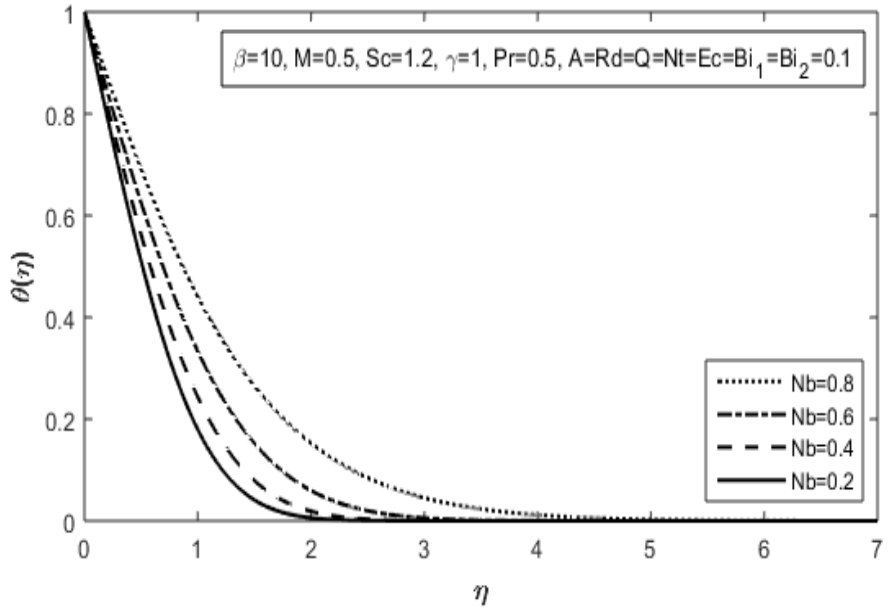

FIGURE 3.21: Effect of Nb on $\theta(\eta)$

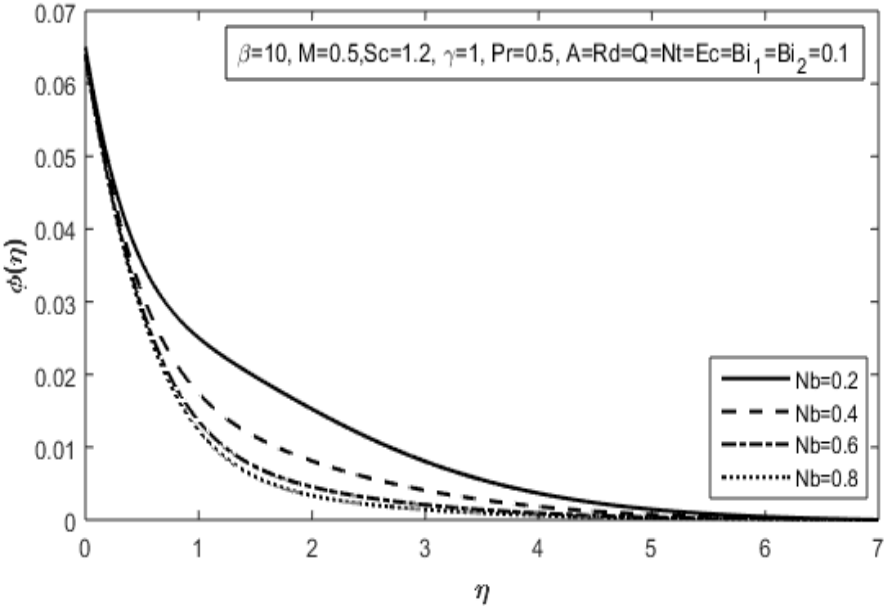

FIGURE 3.22: Effect of Nb on $\phi(\eta)$

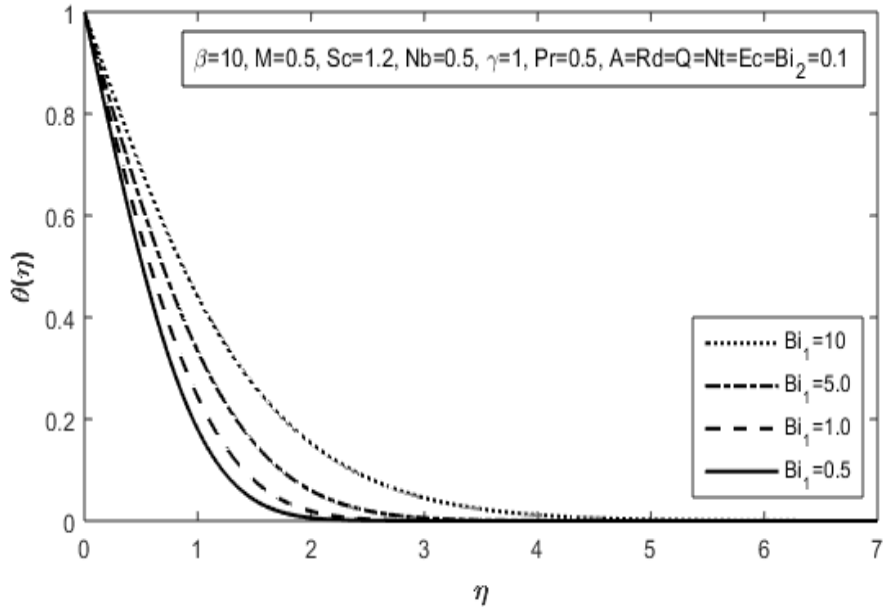

FIGURE 3.23: Effect of Bi_1 on $\theta(\eta)$

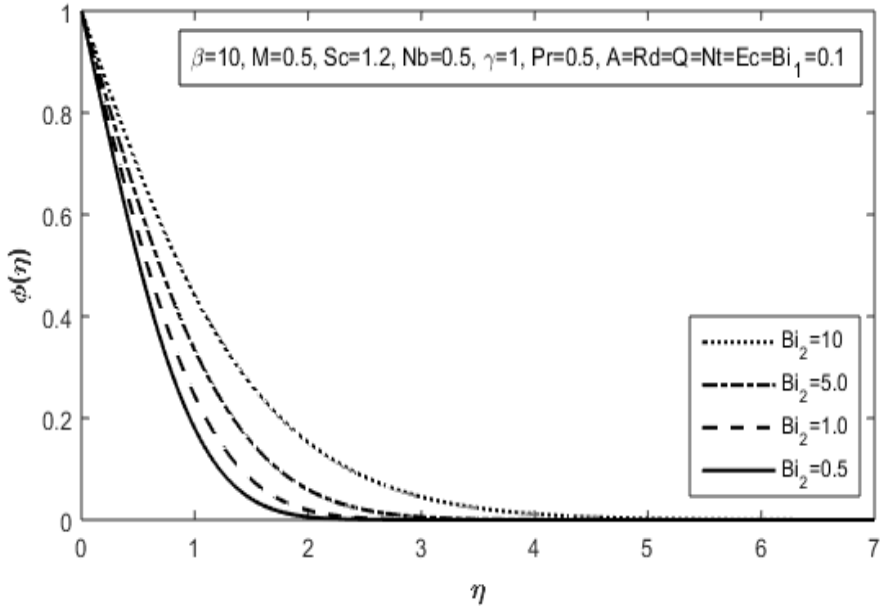

FIGURE 3.24: Effect of Bi_2 on $\phi(\eta)$

Chapter 4

MHD Stagnation Point Carreau Nanofluid Flow over a Radially Stretching Sheet

4.1 Introduction

The numerical investigation on the flow of Carreau nanofluid past a radially stretching sheet close to a stagnation point along with convective boundary conditions has been taken into account. Moreover, the radiation effects and magnetic field are examined. In addition to this, the effects of heat generation/absorption are also explored. The conversion of non-linear partial differential equations describing the proposed flow problem to a set of ordinary differential equations has been carried out by employing appropriate similarity transformations. The numerical solution of the proposed flow equations is derived by the shooting method.

The impact of pertinent flow parameters on the non-dimensional velocity, temperature and concentration profiles has been illustrated via tables and graphs. The limiting case of the present study affirms that the obtained numerical results reflect a very good agreement with those from open literature.

4.2 Mathematical Modeling

The present model aims to investigate the laminar, incompressible and steady flow of the Carreau nanofluid past a radially stretched surface nearby a stagnation point. In the light of the thermal radiation and heat generation/absorption, the characteristics of flow and heat transfer have been examined. The coordinate system is chosen in such a way that $r-$ axis is along the flow whereas $z-$axis is perpendicular to the flow. The velocity of the outer flow is taken as U_e. Furthermore, the direction of the uniform magnetic field is chosen in such a manner that it is normal to the surface of the fluid flow. The effects of Brownian motion and thermophoresis have been elaborated. Moreover, the convective surface conditions have been taken into consideration. The geometry of the problem is similar to that discussed in chapter 3. The constitutive equations of the Carreau nanofluid model are as follow [36]:

$$\frac{\partial u}{\partial r}+\frac{u}{r}+\frac{\partial w}{\partial z}=0, \tag{4.1}$$

$$u\frac{\partial u}{\partial r}+w\frac{\partial u}{\partial z}=\nu_f\frac{\partial^2 u}{\partial z^2}\left[1+\Gamma^2\left(\frac{\partial u}{\partial z}\right)^2\right]^{\frac{n-1}{2}}+\nu_f\left(n-1\right)\Gamma^2\frac{\partial^2 u}{\partial z^2}\left(\frac{\partial u}{\partial z}\right)^2 \left[1+\tau^2\left(\frac{\partial u}{\partial z}\right)^2\right]^{\frac{n-3}{2}}+U_e\frac{dU_e}{dr}-\frac{\sigma B_0(u-U_e)}{\rho_f}, \tag{4.2}$$

$$u\frac{\partial T}{\partial r}+w\frac{\partial T}{\partial z}=\alpha_f\frac{\partial^2 T}{\partial z^2}+\tau\left[D_B\frac{\partial C}{\partial z}\frac{\partial T}{\partial z}+\frac{D_T}{T_\infty}\left(\frac{\partial T}{\partial z}\right)^2\right]+\frac{Q_0\left(T-T_\infty\right)}{(\rho c_p)_f}$$
$$\left(\frac{\partial u}{\partial z}\right)^2+\frac{\sigma B_0^2\left(u-U_e\right)^2}{(\rho c_p)_f}-\frac{1}{(\rho c_p)_f}\frac{\partial q_r}{\partial z}, \tag{4.3}$$

$$u\frac{\partial C}{\partial r}+w\frac{\partial C}{\partial z}=D_B\frac{\partial^2 C}{\partial z^2}+\frac{D_T}{T_\infty}\frac{\partial^2 T}{\partial z^2}-C_r\left(C-C_\infty\right). \tag{4.4}$$

The corresponding conditions at the boundary surface are

$$u=U_w=ar,\ w=0,\ -k_f\frac{\partial T}{\partial z}=h_h\left(T_f-T\right),\ D_B\frac{\partial C}{\partial z}=-h_s\left(C_f-C\right)\quad\text{at}\quad z=0,$$
$$u\to U_e=br,\quad T\to T_\infty,\quad C\to C_\infty\ \text{ as }\ z\to\infty. \tag{4.5}$$

The following similarity variables are taken into consideration.

$$\eta=\sqrt{\frac{a}{\nu_f}}\,z, u=arf'\left(\eta\right), w=-2\sqrt{a\nu_f}f\left(\eta\right), \theta\left(\eta\right)=\frac{T-T_\infty}{T_f-T_\infty}, \phi\left(\eta\right)=\frac{C-C_\infty}{C_f-C_\infty}. \tag{4.6}$$

The Rosseland approximation has been considered for the radiation. For smaller value of temperature contrast, the temperature difference T^4 might be expanded about T_∞ using Taylor series and ignoring the higher order terms, the formulae for the radiative heat flux q_r is stated below.

$$\frac{\partial q_r}{\partial z}=-\frac{16\sigma^* T_\infty^3}{3k^*}\frac{\partial^2 T}{\partial z^2}. \tag{4.7}$$

The detailed procedure for the verification of the continuity equation (4.1) has been discussed in Chapter 3.

Now equation (4.2) will be converted into the dimensionless form. The left hand

side of equation (4.2) can be written as:

$$\begin{aligned} u\frac{\partial u}{\partial r} + w\frac{\partial u}{\partial z} &= a^2 r f'^2(\eta) - 2ra^2 f(\eta) f''(\eta) \\ &= a^2 r\left(f'^2(\eta) - 2f(\eta) f''(\eta)\right). \end{aligned} \tag{4.8}$$

Furthermore, the first and second expressions on the right hand side of equation (4.2) have been transformed into the dimensionless form as stated below.

$$\begin{aligned} & \nu_f \frac{\partial^2 u}{\partial z^2}\left[1+\Gamma^2\left(\frac{\partial u}{\partial z}\right)^2\right]^{\frac{n-1}{2}} + \nu_f (n-1)\Gamma^2 \frac{\partial^2 u}{\partial z^2}\left(\frac{\partial u}{\partial z}\right)^2\left[1+\Gamma^2\left(\frac{\partial u}{\partial z}\right)^2\right]^{\frac{n-3}{2}} \\ = \;& \nu_f \frac{a^2}{\nu_f} r f'''(\eta)\left[1+\Gamma^2\frac{a^3 r^2}{\nu_f} f''^2(\eta)\right]^{\frac{n-1}{2}} \\ & + \nu_f (n-1)\Gamma^2 \frac{a^2}{\nu_f} r f'''(\eta)\frac{a^3 r^2}{\nu_f} f''^2(\eta)\left[1+\Gamma^2\frac{a^3 r^2}{\nu_f} f''^2(\eta)\right]^{\frac{n-3}{2}} \\ = \;& a^2 r f'''(\eta)\left(\left[1+\Gamma^2\frac{a^3 r^2}{\nu_f} f''^2(\eta)\right]^{\frac{n-1}{2}}\right. \\ & \left. + (n-1)\Gamma^2\frac{a^3 r^2}{\nu_f} f''^2(\eta)\left[1+\Gamma^2\frac{a^3 r^2}{\nu_f} f''^2(\eta)\right]^{\frac{n-3}{2}}\right) \\ = \;& a^2 r f'''(\eta)\left(\left[1+We^2 f''^2(\eta)\right]^{\frac{n-1}{2}} + (n-1)We^2 f''^2(\eta)\left[1+We^2 f''^2(\eta)\right]^{\frac{n-3}{2}}\right) \\ = \;& a^2 r f'''(\eta)\left[1+We^2 f''^2(\eta)\right]^{\frac{n-3}{2}}\left(\frac{\left[1+We^2 f''^2(\eta)\right]^{\frac{n-1}{2}}}{\left[1+We^2 f''^2(\eta)\right]^{\frac{n-3}{2}}} + (n-1)We^2 f''^2(\eta)\right) \\ = \;& a^2 r f'''(\eta)\left[1+We^2 f''^2(\eta)\right]^{\frac{n-3}{2}}\left(\left[1+We^2 f''^2(\eta)\right]^{\left(\frac{n-1}{2}-\frac{n-3}{2}\right)}\right. \\ & \left. + (n-1)We^2 f''^2(\eta)\right) \\ = \;& a^2 r f'''(\eta)\left[1+We^2 f''^2(\eta)\right]^{\frac{n-3}{2}}\left(\left[1+We^2 f''^2(\eta)\right]^{\frac{n-1-n+3}{2}}\right. \\ & \left. + (n-1)We^2 f''^2(\eta)\right) \\ = \;& a^2 r f'''(\eta)\left[1+We^2 f''^2(\eta)\right]^{\frac{n-3}{2}}\left(\left[1+We^2 f''^2(\eta)\right] + (n-1)We^2 f''^2(\eta)\right) \\ = \;& a^2 r f'''(\eta)\left[1+We^2 f''^2(\eta)\right]^{\frac{n-3}{2}}\left(1+We^2 f''^2(\eta) + nWe^2 f''^2(\eta) - We^2 f''^2(\eta)\right) \\ = \;& a^2 r f'''(\eta)\left[1+We^2 f''^2(\eta)\right]^{\frac{n-3}{2}}\left[1+nWe^2 f''^2(\eta)\right]. \end{aligned} \tag{4.9}$$

On the similar note, conversion of the remaining terms of the right hand side of equation (4.2) into the dimensionless form has been stated below.

$$\begin{aligned} & U_e\frac{dU_e}{dr} - \frac{\sigma B_0^2}{\rho}\left(u - U_e\right) \\ = \; & b^2 r - \frac{\sigma B_0^2}{\rho}\left(ar\left(f'\left(\eta\right) - \frac{b}{a}\right)\right) \\ = \; & b^2 r - \frac{\sigma a r B_0^2}{\rho}\left(f'\left(\eta\right) - \frac{b}{a}\right) \\ = \; & a^2 r\left[\frac{b^2}{a^2} - \frac{\sigma B_0^2}{a\rho}\left(f'\left(\eta\right) - \frac{b}{a}\right)\right]. \end{aligned} \tag{4.10}$$

Now using equations (4.9) and (4.10), the right hand side of equation (4.2) can be written as:

$$\begin{aligned} & \nu_f\frac{\partial^2 u}{\partial z^2}\left[1 + \Gamma^2\left(\frac{\partial u}{\partial z}\right)^2\right]^{\frac{n-1}{2}} + \nu_f\left(n-1\right)\Gamma^2\frac{\partial^2 u}{\partial z^2}\left(\frac{\partial u}{\partial z}\right)^2\left[1 + \tau^2\left(\frac{\partial u}{\partial z}\right)^2\right]^{\frac{n-3}{2}} \\ & + U_e\frac{dU_e}{dr} - \frac{\sigma B_0(u - U_e)}{\rho_f} \\ = \; & a^2 r f'''\left(\eta\right)\left[1 + We^2 f''^2\left(\eta\right)\right]^{\frac{n-3}{2}}\left[1 + nWe^2 f''^2\left(\eta\right)\right] \\ & + a^2 r\left(A^2 - M^2\left(f'\left(\eta\right) - A\right)\right) \\ = \; & a^2 r\left(\left[1 + We^2 f''^2\left(\eta\right)\right]^{\frac{n-3}{2}}\left[1 + nWe^2 f''^2\left(\eta\right)\right] f'''\left(\eta\right) + A^2 - M^2\left(f'\left(\eta\right) - A\right)\right) \end{aligned} \tag{4.11}$$

The detailed procedure for the conversion of equations (4.3)-(4.4) and boundary conditions into the dimensionless form is similar to that discussed in chapter 3. Finally, the ODEs describing the proposed flow problem can be re-collected in the

following system.

$$\left[1+nWe^2\left(f''\right)^2\right]\left[1+We^2\left(f''\right)^2\right]^{\frac{n-3}{2}} f'''+2ff''-f'^2+A^2$$
$$-M^2\left(f'-A\right)=0, \tag{4.12}$$
$$\left(1+\frac{4}{3}Rd\right)\theta''+PrNb\theta'\phi'+PrNt\theta'^2+2Prf\theta'+PrQ\theta$$
$$+PrEcM^2\left(f'-A\right)^2=0, \tag{4.13}$$
$$\phi''+\frac{Nt}{Nb}\theta''+Sc\left(2f\phi'-\gamma\phi\right)=0. \tag{4.14}$$

The transformed boundary conditions are stated below.

$$\left.\begin{aligned} &f\left(0\right)=0,\ f'\left(0\right)=1,\\ &\theta'\left(0\right)=-Bi_1\left(1-\theta\left(0\right)\right),\ \phi'\left(0\right)=-Bi_2\left(1-\phi\left(0\right)\right),\\ &f'\to A,\ \theta\to 0,\ \phi\to 0\ \text{ as }\ \eta\to\infty. \end{aligned}\right\} \tag{4.15}$$

The dimensional form of skin-friction coefficient, Nusselt number and Sherwood number is formulated as follows:

$$C_f=\frac{\tau_w}{\rho_f U_w^2},\ Nu=\frac{rq_w}{k_f\left(T_f-T_\infty\right)},\ Sh=\frac{rq_m}{D_B\left(C_f-C_\infty\right)}. \tag{4.16}$$

Given below are the formulae for τ_w, q_w and q_m.

$$\tau_w=\mu\left(\frac{\partial u}{\partial z}\right)_{z=0}\left[1+\Gamma^2\left(\frac{\partial u}{\partial z}\right)^2\right]^{\frac{n-1}{2}}_{z=0},\ q_w=-k_f\left[\left(\frac{\partial T}{\partial z}\right)-\frac{q_r}{k_f}\right]_{z=0},$$
$$q_m=-D_B\left(\frac{\partial C}{\partial z}\right)_{z=0}. \tag{4.17}$$

The transformation of the above formulae into the dimensionless form has been carried out as:

- $$\begin{aligned}\tau_w &= \mu\left(\frac{\partial u}{\partial z}\right)_{z=0}\left[1+\Gamma^2\left(\frac{\partial u}{\partial z}\right)^2\right]_{z=0}^{\frac{n-1}{2}} \\ &= \mu\left(ar\sqrt{\frac{a}{\nu_f}}f''(0)\right)\left[1+\Gamma^2\frac{a^3r^2}{\nu_f}f''^2(0)\right]^{\frac{n-1}{2}} \\ &= \mu ar\sqrt{\frac{a}{\nu_f}}f''(0)\left[1+We^2f''^2(0)\right]^{\frac{n-1}{2}}. \end{aligned} \tag{4.18}$$
- $$\begin{aligned}q_w &= -k_f\left[\left(\frac{\partial T}{\partial z}\right)-\frac{q_r}{k_f}\right]_{z=0} \\ &= -k_f\left[\sqrt{\frac{a}{\nu_f}}(T_f-T_\infty)\theta'(0)-\left(\frac{-16\sigma^*T_\infty^3}{3k_fk^*}\sqrt{\frac{a}{\nu_f}}(T_f-T_\infty)\theta'(0)\right)\right] \\ &= -k_f\sqrt{\frac{a}{\nu_f}}(T_f-T_\infty)\left[1+\frac{4}{3}\left(\frac{4\sigma^*T_\infty^3}{k_fk^*}\right)\right]\theta'(0) \\ &= -k_f\sqrt{\frac{a}{\nu_f}}(T_f-T_\infty)\left[1+\frac{4}{3}Rd\right]\theta'(0). \end{aligned} \tag{4.19}$$
- $$\begin{aligned}q_m &= -D_B\left(\frac{\partial C}{\partial z}\right)_{z=0} \\ &= -D_B\sqrt{\frac{a}{\nu_f}}(C_f-C_\infty)\phi'(0). \end{aligned} \tag{4.20}$$

Incorporating equation (4.28), (4.29) and (4.30) in equation (4.26), we get the following dimensionless form for skin-friction coefficient, Nusselt number and Sherwood number.

- $$\begin{aligned}C_f &= \frac{\tau_w}{\rho_f U_w^2} \\ &= \frac{\mu ar\sqrt{\frac{a}{\nu_f}}f''(0)\left[1+We^2f''^2(0)\right]^{\frac{n-1}{2}}}{\rho_f a^2r^2} \\ &= \frac{1}{r}\sqrt{\frac{\nu_f}{a}}f''(0)\left[1+We^2f''^2(0)\right]^{\frac{n-1}{2}} \\ &= Re^{-\frac{1}{2}}f''(0)\left[1+We^2f''^2(0)\right]^{\frac{n-1}{2}}. \end{aligned}$$

$$\Rightarrow \quad Re^{\frac{1}{2}}C_f = f''(0)\left[1+We^2 f''^2(0)\right]^{\frac{n-1}{2}}. \tag{4.21}$$

- $$\begin{aligned} Nu &= \frac{rq_w}{k_f(T_f-T_\infty)} \\ &= \frac{-rk_f\sqrt{\frac{a}{\nu_f}}(T_f-T_\infty)\left[1+\frac{4}{3}Rd\right]\theta'(0)}{k_f(T_f-T_\infty)} \\ &= -r\sqrt{\frac{a}{\nu_f}}\left[1+\frac{4}{3}Rd\right]\theta'(0) \\ &= -Re^{\frac{1}{2}}\left[1+\frac{4}{3}Rd\right]\theta'(0). \end{aligned}$$

$$\Rightarrow \quad Re^{-\frac{1}{2}}Nu = -\left[1+\frac{4}{3}Rd\right]\theta'(0).$$

- $$\begin{aligned} Sh &= \frac{rq_m}{D_B(C_f-C_\infty)} \\ &= \frac{-rD_B\sqrt{\frac{a}{\nu_f}}(C_f-C_\infty)\phi'(0)}{D_B(C_f-C_\infty)} \\ &= -r\sqrt{\frac{a}{\nu_f}}\phi'(0) \\ &= -Re^{\frac{1}{2}}\phi'(0). \end{aligned}$$

$$\Rightarrow \quad Re^{-\frac{1}{2}}Sh = -\phi'(0), \tag{4.22}$$

where $Re = \dfrac{rU_w}{\nu_f}$ elucidates the local Reynolds number and $\nu_f = \dfrac{\mu}{\rho}$ the kinematic viscosity.

4.3 Solution Methodology

In order to solve the system of ODEs (4.22)-(4.24) subject to the boundary conditions (4.25), the shooting method has been used. Primarily equation (4.22) is solved numerically and then the computed results of f, f' and f'' are used in equations (4.23)-(4.24). For the numerical treatment of equation (4.22), the missing initial condition $f''(0)$ has been denoted as s and the following notations have

been considered.

$$f = h_1, f' = h_2, f'' = h_3, \frac{\partial f}{\partial s} = h_4, \frac{\partial f'}{\partial s} = h_5, \frac{\partial f''}{\partial s} = h_6 \tag{4.23}$$

Using the above notations, equation (4.22) can be converted into a system of three first order ODEs. First three of the following ODEs correspond to (4.22) and the other three are obtained by differentiating the first three w.r.t s.

$$\begin{aligned}
h_1' &= h_2, && h_1(0) = 0,\\
h_2' &= h_3, && h_2(0) = 1,\\
h_3' &= \frac{h_2^2 + M^2(h_2 - A) - 2h_1h_3 - A^2}{(1 + nWe^2h_3^2)(1 + We^2h_3^2)^{\frac{n-3}{2}}}, && h_3(0) = s,\\
h_4' &= h_5, && h_4(0) = 0,\\
h_5' &= h_6, && h_5(0) = 0,\\
h_6' &= \frac{1}{(1 + nWe^2h_3^2)^2 (1 + We^2h_3^2)^{n-3}} \\
&\Bigg[\left[1 + nWe^2h_3^2\right] \left[1 + We^2h_3^2\right]^{\frac{n-3}{2}} \left[\left(2h_2 + M^2\right) h_5 - 2\left(h_1h_6 + h_3h_4\right)\right] \\
&- \left(h_2^2 + M^2(h_2 - A) - 2h_1z_3 - A^2\right) \left[1 + We^2h_3^2\right]^{\frac{n-5}{2}} (2We^2h_3h_6) \\
&\left(\frac{n-3}{2}\left[1 + nWe^2h_3^2\right] + n\left[1 + We^2h_3^2\right]^{-1}\right)\Bigg], && h_6(0) = 1.
\end{aligned}$$

The RK-4 method has been used to solve the above initial value problem. In order to get the approximate numerical results, the problem's domain is considered to be bounded i.e. $[0, \eta_\infty]$, where η_∞ is chosen to be an appropriate finite positive real number in such a way that the variation in the solution for $\eta > \eta_\infty$ is ignorable. The missing condition for the above system of equations is to be chosen such that $(h_2(\eta_\infty))_s = A$. This algebraic equation has been solved by using the Newton's

method governed by the following iterative formula.

$$s^{(n+1)} = s^{(n)} - \frac{\left(h_2(\eta_\infty)\right)_{s=s^{(n)}} - A}{\left(\frac{\partial h_2(\eta_\infty)}{\partial s}\right)_{s=s^{(n)}}}.$$

$$\Rightarrow \; s^{(n+1)} = s^{(n)} - \frac{\left(h_2(\eta_\infty)\right)_{s=s^{(n)}} - A}{\left(h_5(\eta_\infty)\right)_{s=s^{(n)}}}. \tag{4.24}$$

The stopping criteria for the shooting method is set as

$$\left|\left(h_2(\eta_\infty)\right)_{s=s^{(n)}} - A\right| < \epsilon, \tag{4.25}$$

for some very small positive number ϵ.

For the numerical treatment of equations (4.23) and (4.24), the similar procedure has been followed as discussed in Chapter 3.

4.4 Results with Discussions

In this section, the numerical values of skin-friction coefficient, Nusselt and Sherwood numbers are illustrated by tables and graphs by assuming various values of different physical parameters of interest.

4.4.1 Skin-friction Coefficient, Nusselt and Sherwood Numbers

To validate the MATLAB code, the values of $-f''(0)$ and $-\theta'(0)$ are reproduced for the problem discussed by Dianchen et al. [36]. Table 4.1 reflects a very good

agreement between the results computed by the present code and those of Dianchen et al. [36].

Tables 4.2-4.3 disclose the numerical results of the skin-friction coefficient, Nusselt and sherwood numbers for the present model in regards to a change in the values of various parameters like n, We, A, M, Rd, Pr, Q, Nb, Nt, Ec, Sc, γ, Bi_1 and Bi_2.

	$f''(0)$ with $We = 0, n = 1$	
M^2	Dianchen et al.[36]	Present
0.0	-1.173720	-1.173733759
0.5	-1.365814	-1.365815468
1.0	-1.535709	-1.535710609
2.0	-1.830490	-1.870040277
3.0	-2.084846	-2.3083441658

TABLE 4.1: Comparison of the present results of $f''(0)$ with those reported by Dianchen et al. [36].

For the larger values of n and A, the skin-friction coefficient depresses whereas the heat and mass transfer rates climb marginally. The skin-friction coefficient, Nusselt and Sherwood numbers are enhanced as We assumes the higher values. A rise in the value of M depreciates the Nusselt number whereas the skin-friction coefficient and Sherwood number increase significantly. Both the Nusselt and Sherwood numbers increase with an escalation in the value of Rd, Sc and γ.

As the value of Q, Pr and Bi_1 rise, the Nusselt number is enhanced whereas

the Sherwood number shows a declining behaviour. A decrement in the heat and mass transfer rates has been observed for the higher estimation of of Nb, Ec and

n	We	A	M	Rd	Pr	Nb	Nt	Q	Ec	$-a_1 f''(0)$	$-a_2\theta'(0)$	$-\phi'(0)$
1.5	0.05	0.1	1.0	0.1	0.7	0.5	0.1	0.1	0.1	1.4382	0.093158	0.093391
2.0										1.4296	0.093161	0.093392
2.5										1.4274	0.093163	0.093393
	2.0									3.1754	0.094621	0.093585
	4.0									4.5149	0.095321	0.093697
		0.2								1.3216	0.094145	0.093459
		0.3								1.1928	0.094389	0.093538
			1.2							1.5573	0.093791	0.093858
			1.4							1.6879	0.091504	0.093960
				0.2						1.4382	0.102877	0.093406
				0.3						1.4382	0.112401	0.093409
					1.0					1.4382	0.096244	0.093348
					2.0					1.4382	0.100356	0.093279
						0.6				1.4382	0.093109	0.093424
						0.7				1.4382	0.093059	0.093447
							0.2			1.4382	0.093065	0.093214
							0.3			1.4382	0.092969	0.093042
								1.0		1.4382	0.105005	0.093307
								2.0		1.4382	0.111079	0.093031
									0.5	1.4382	0.083702	0.093799
									1.0	1.4382	0.071850	0.094308

TABLE 4.2: The computed results of skin-friction coefficient, Nusselt and Sherwood numbers for $Sc = 1.2, \gamma = 1, Bi_1 = 0.1 = Bi_2$, where $a_1 = \left[1 + We^2 f''^2\,(0)\right]^{\frac{n-1}{2}}$ and $a_2 = \left(1 + \frac{4}{3}Rd\right)$.

Sc	γ	Bi_1	Bi_2	$-a_1 f''(0)$	$-a_2\theta'(0)$	$\phi'(0)$
1.2	1.0	0.1	0.1	1.4382	0.093158	0.093391
1.4				1.4382	0.093172	0.093909
1.6				1.4382	0.093183	0.094323
	1.5			1.4382	0.093182	0.094194
	2.0			1.4382	0.093199	0.094756
		0.2		1.4382	0.160826	0.093193
		0.3		1.4382	0.212083	0.093043
			0.2	1.4382	0.092941	0.175524
			0.3	1.4382	0.092747	0.248316

TABLE 4.3: The computed results of skin-friction coefficient, Nusselt and Sherwood numbers for $n = 1.5, We = 0.05, M = 1, A = 0.1, Rd = 0.1, Pr = 0.7, Q = 0.1, Nb = 0.5, Nt = 0.1, Ec = 0.1$, where $a_1 = \left[1 + We^2 f''^2\,(0)\right]^{\frac{n-1}{2}}$ and $a_2 = \left(1 + \frac{4}{3}Rd\right)$.

Sc	γ	Bi_1	Bi_2	J_f	J_θ	J_ϕ
1.2	1.0	0.1	0.1	[-1.4, -1.3]	[-1, 150]	[-1, 150]
1.4				[-1.4, -1.3]	[1, 150]	[1, 150]
1.6				[-1.4, -1.3]	[1, 150]	[1, 150]
	1.5			[-1.4, -1.3]	[1, 130]	[1, 130]
	2.0			[-1.4, -1.3]	[1, 50]	[1, 50]
		0.2		[-1.4, -1.3]	[1, 100]	[1, 100]
		0.3		[-1.4, -1.3]	[1, 110]	[1, 110]
			0.2	[-1.4, -1.3]	[1, 120]	[1, 120]
			0.3	[-1.4, -1.3]	[1, 130]	[1, 130]

TABLE 4.4: The intervals for the initial guesses for the missing initial conditions when $n = 1.5, We = 0.05, M = 1, A = 0.1, Rd = 0.1, Pr = 0.7, Q = 0.1, Nb = 0.5, Nt = 0.1, Ec = 0.1$.

n	We	A	M	Rd	Pr	Nb	Nt	Q	Ec	J_f	J_θ	J_ϕ
1.5	0.05	0.1	1.0	0.1	0.7	0.5	0.1	0.1	0.1	[-1.4, -1.3]	[-1, 150]	[-1, 150]
2.0										[-1.4, -1.3]	[-1, 150]	[-1, 150]
2.5										[-1.4, -1.3]	[-1, 160]	[-1, 160]
	2.0									[-0.9, -0.8]	[-1, 165]	[-1, 165]
	4.0									[-0.7,-0.6]	[-1, 175]	[-1, 175]
		0.2								[-1.3, -1.2]	[-1, 180]	[-1, 180]
		0.3								[-1.2, -1]	[-1, 195]	[-1, 195]
			1.2							[-1.5, -1.4]	[-1, 150]	[-1, 150]
			1.4							[-1.6, -1.5]	[-1, 150]	[-1, 150]
				0.2						[-1.4, -1.3]	[1, 160]	[1, 160]
				0.3						[-1.4, -1.3]	[1, 160]	[1, 160]
					1.0					[-1.4, -1.3]	[1, 170]	[1, 170]
					2.0					[-1.4, -1.3]	[1, 130]	[1, 130]
						0.6				[-1.4, -1.3]	[1, 90]	[1, 90]
						0.7				[-1.4, -1.3]	[1, 140]	[1, 140]
							0.2			[-1.4, -1.3]	[1, 120]	[1, 120]
							0.3			[-1.4, -1.3]	[1, 160]	[1, 160]
								1.0		[-1.4, -1.3]	[1, 150]	[1, 150]
								2.0		[-1.4, -1.3]	[1, 140]	[1, 140]
									0.5	[-1.4, -1.3]	[1, 120]	[1, 120]
									1.0	[-1.4, -1.3]	[1, 160]	[1, 160]

TABLE 4.5: The intervals for the initial guesses for the missing initial conditions when $\gamma = 1, Bi_1 = 0.1 = Bi_2$.

Bi_2, the heat transfer rate falls, however, the mass transfer rate rises. Tables 4.4-4.5 portray the intervals J_f, J_θ and J_ϕ where from the missing initial conditions $f''(0)$, $\theta'(0)$ and $\phi'(0)$ respectively can be chosen. It is noteworthy that the intervals mentioned offer a considerable flexibility for the choice of initial guesses.

4.4.2 The Velocity, Temperature and Concentration Profiles

The graphs illustrated in this section show the behaviour of the velocity, temperature and concentration for the present model in regards to a change in the values of various parameters like n, We, A, M, Rd, Pr, Q, Nb, Nt, Ec, Sc, γ, Bi_1 and Bi_2.

Figures 4.2-4.4 are framed to delineate the impact of n on the velocity, temperature and concentration profiles. The velocity, temperature and concentration distributions can be seen to depress as the larger values of n are taken into account. In addition, a decrement has been observed in the momentum, thermal and concentration boundary layer thickness.

The effect of the Weissenberg number on the velocity, temperature and concentration fields has been displayed through Figures 4.5-4.7. The velocity can be seen to decerates while the temperature and concentration escalate for the higher estimation of We, that bring about a decrement in the momentum boundary layer thickness whereas an escalation in the thermal and concentration boundary layer thickness has been noticed.

Figures 4.8-4.10 are sketched to show the impact of A on the velocity, temperature and concentration distributions. An enhancement in the flow velocity has been observed for $A > 1$. On the other hand, the velocity de-escalates for the case $A < 1$. Also, both the temperature and concentration profiles decrease when A assumes the larger value. As the value of A heightens, the heat transfer from the sheet to the fluid becomes smaller and as a result, the temperature falls. Furthermore, the thermal boundary layer thickness is reduced. Moreover, the concentration boundary layer thickness also shows a declining behaviour.

Figures 4.11-4.13 present the impact of the magnetic parameter on the velocity, temperature and concentration profiles. The higher values of M decelerate the velocity and increase the temperature and concentration of the fluid. This stems from the fact that an opposing force is generated by the magnetic field, generally referred as the Lorentz force, which depresses the motion of the fluid resulting in a decrement in the momentum boundary layer thickness and heightens the thermal and concentration boundary layer thickness.

Figures 3.11-3.12 are framed to delineate the effect of Pr on the temperature and concentration distributions. Since Pr is directly proportionate to the viscous diffusion rate and inversely related to the thermal diffusivity, so the thermal diffusion rate suffers a reduction for the larger estimation of Pr and subsequently, the temperature of the fluid drops significantly. Moreover, a decrement in the thermal boundary layer thickness has been noted. However, the nanoparticle volume fraction of the fluid can be remarked to escalates for the higher values of Pr. In

addition to that, an increment can be seen in the concentration boundary layer thickness.

The outcome of Ec on the velocity and temperature profiles has been characterized through Figures 3.13-3.14. Physically, the Eckert number depicts the relation between the kinetic energy of the fluid particles and the boundary layer enthalpy. The kinetic energy of the fluid particles rises as Ec assumes the larger values. Hence, the velocity and temperature of the fluid climb marginally and therefore, the associated momentum and thermal boundary layer thickness are enhanced.

Figures 3.15-3.16 elucidate the effect of the radiation parameter Rd and the heat generation or absorption parameter Q on the temperature distributions. Since the heat transfer climbs marginally for the higher estimation of Rd, thereby an increment in the temperature of the fluid and the thermal boundary layer has been noticed. However, as the value of Q rises, more heat is generated causing an increment in the temperature and the thermal boundary layer thickness. On the other hand, as the value of Q de-escalates , the heat absorbed results in a decrement in the temperature and the associated thermal boundary layer thickness.

Figures 3.17-3.18 delineate the effect of Sc and γ on the concentration fields. The concentration of the fluid depicts a decreasing behaviour as Sc assumes the higher value. This behaviour stems from the fact that the Schmidt number and mass diffusion rate have inverse relation, therefore, for the larger Sc, the process of the mass diffusivity slows down and thus, the nanoparticle volume fraction falls and

the concentration boundary layer thickness is reduced. Furthermore, the chemical reaction parameter also has a similar effect on the concentration profile. The larger values of γ result in a decrement in the chemical molecular diffusion and hence, the concentration of the fluid de-escalates and the associated concentration boundary layer thickness is reduced.

Figures 4.22-4.23 interpret the impact of the thermophoresis parameter on the temperature and concentration distributions. Both the temperature and concentration escalate by taking larger values of Nt into account. In addition to this, an increment in the associated thermal and concentration boundary layer thickness has been noticed.

Figures 3.21-3.22 display the influence of the Brownian motion parameter on the temperature and concentration distributions. The temperature profile climbs marginally for the larger values of Nb. This happens due to the reason that as the value of Nb rises, the movement of the nanoparticles enhances significantly which triggers the kinetic energy of the nanoparticles resulting in an escalation in the temperature and the thermal boundary layer thickness. On the other hand, the concentration of the fluid falls as Nb assumes the higher values. Also, the concentration boundary layer thickness is depressed.

The effect of the thermal Biot number on the temperature distribution and the concentration Biot number on the nanoparticle volume fraction has been portrayed by Figures 4.26-4.27. It is remarkable that the temperature can be observed as an increasing function of Bi_1 and the concentration of the fluid also enhances as Bi_2

heightens. Further to this, the associated thermal and concentration boundary layer thickness are enhanced.

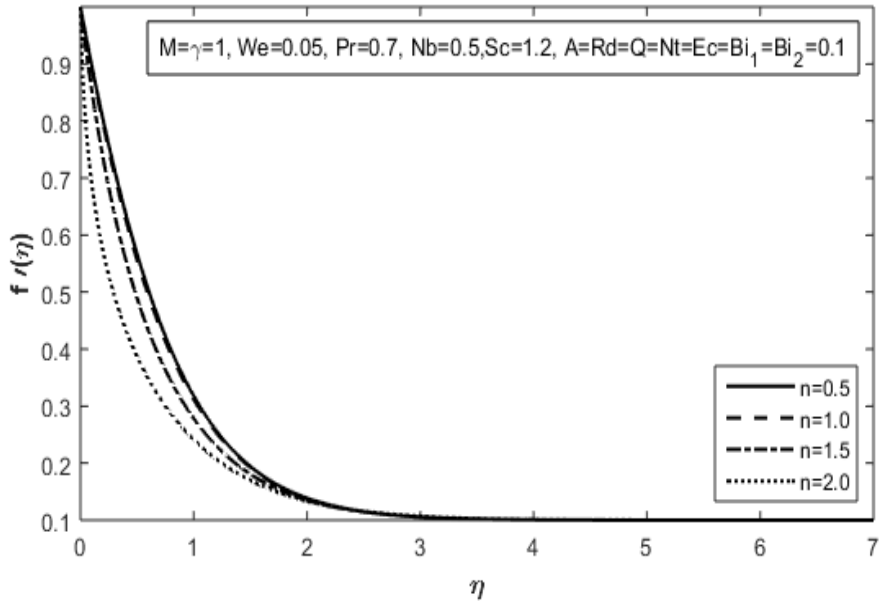

FIGURE 4.1: Effect of n on $f'(\eta)$

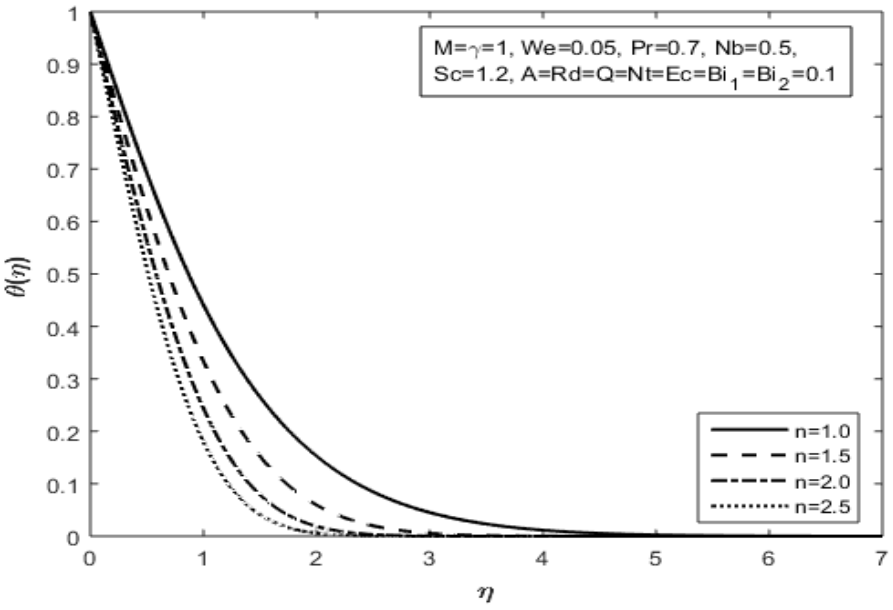

FIGURE 4.2: Effect of n on $\theta(\eta)$

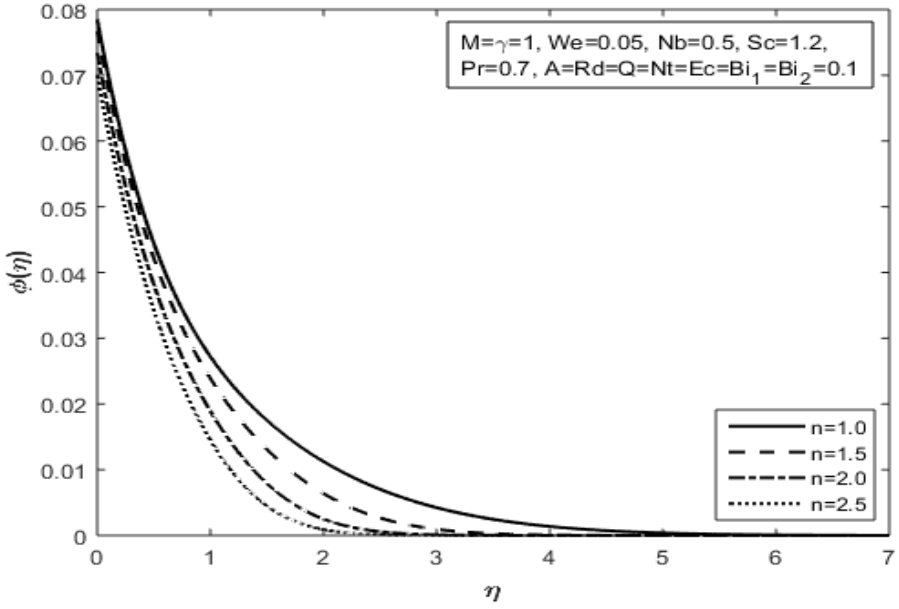

FIGURE 4.3: Effect of n on $\phi(\eta)$

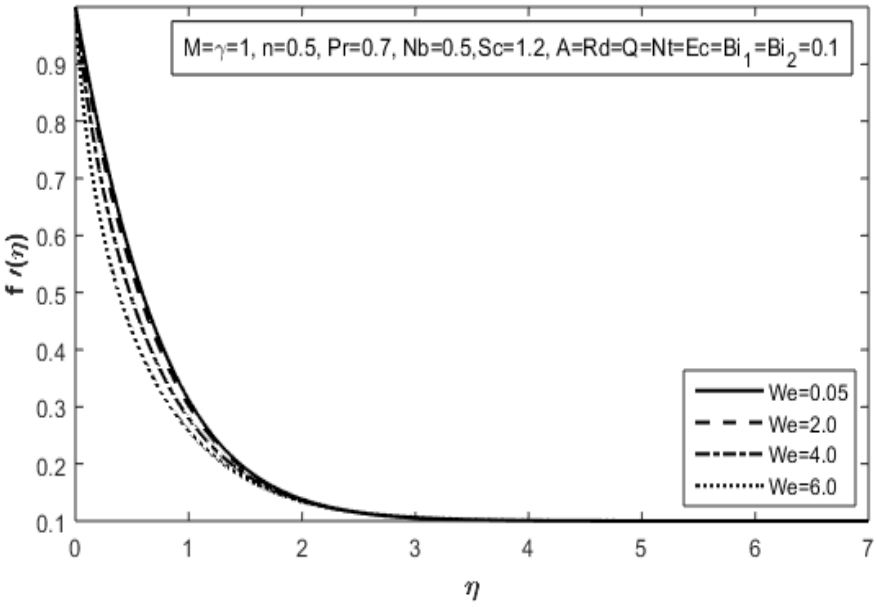

FIGURE 4.4: Effect of We on $f'(\eta)$

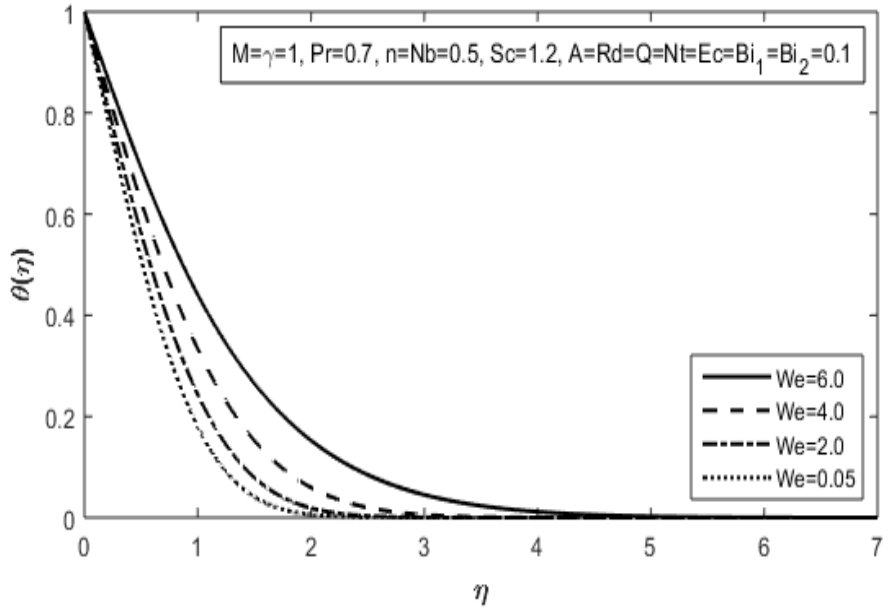

FIGURE 4.5: Effect of We on $\theta(\eta)$

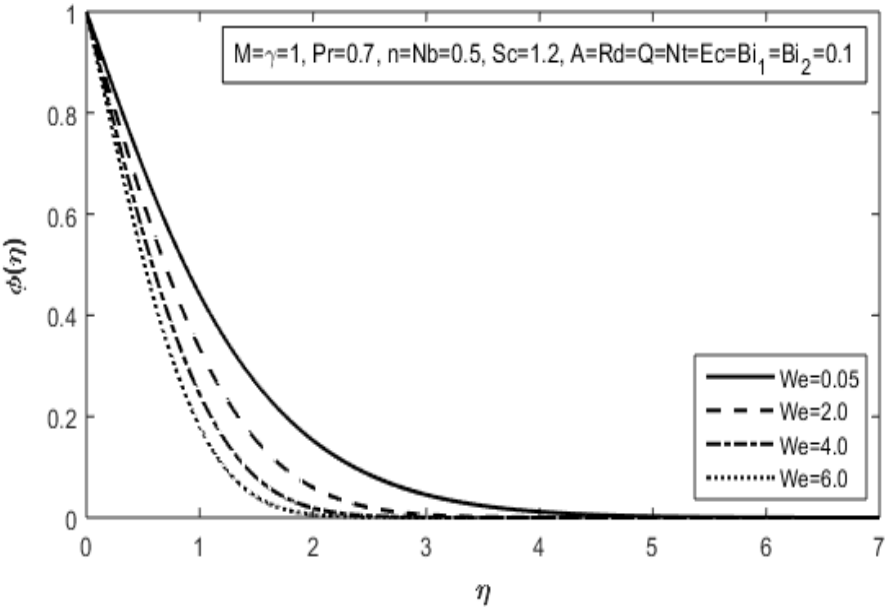

FIGURE 4.6: Effect of We on $\phi(\eta)$

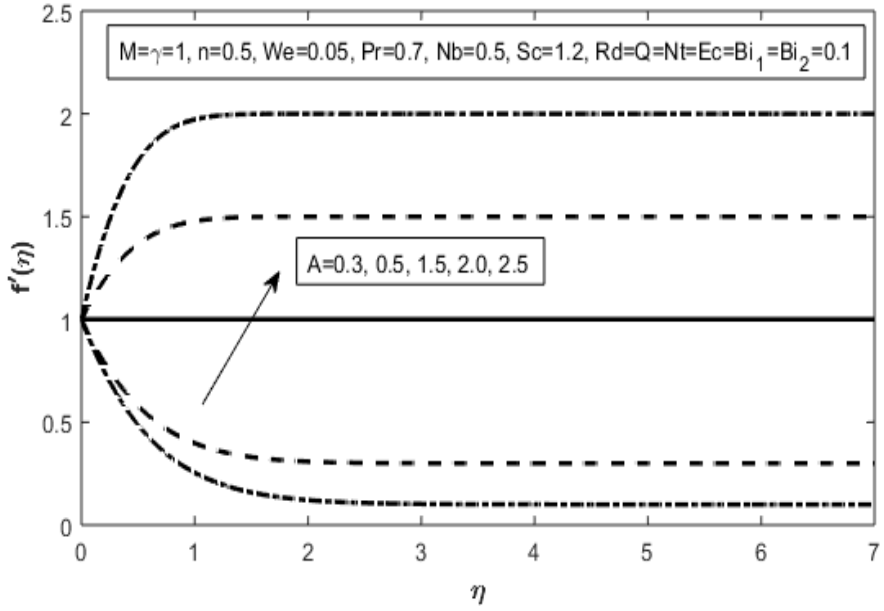

FIGURE 4.7: Effect of A on $f'(\eta)$

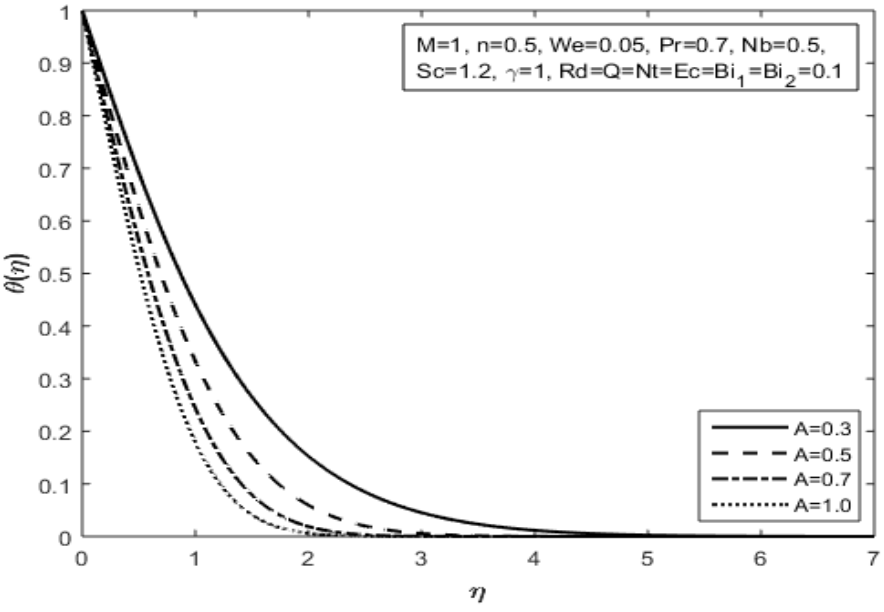

FIGURE 4.8: Effect of A on $\theta(\eta)$

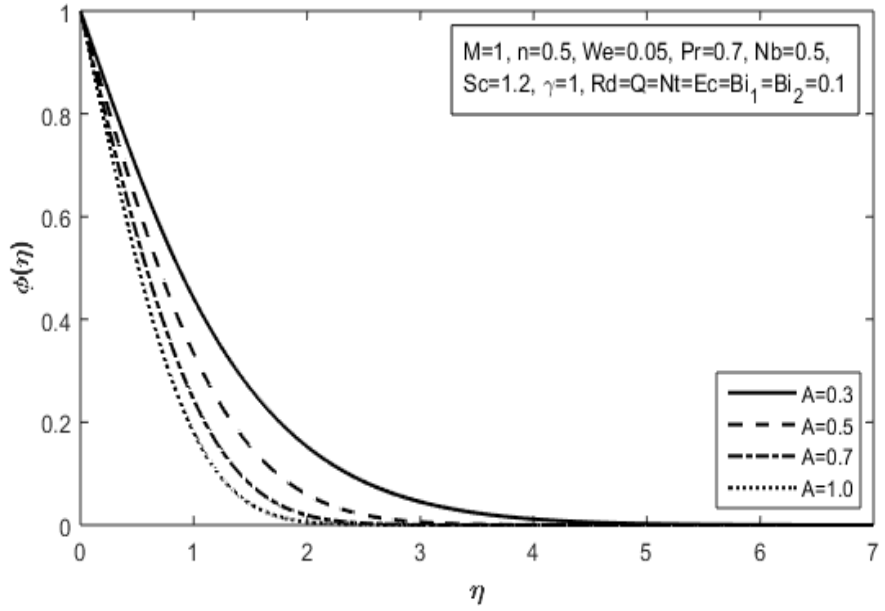

FIGURE 4.9: Effect of A on $\phi(\eta)$

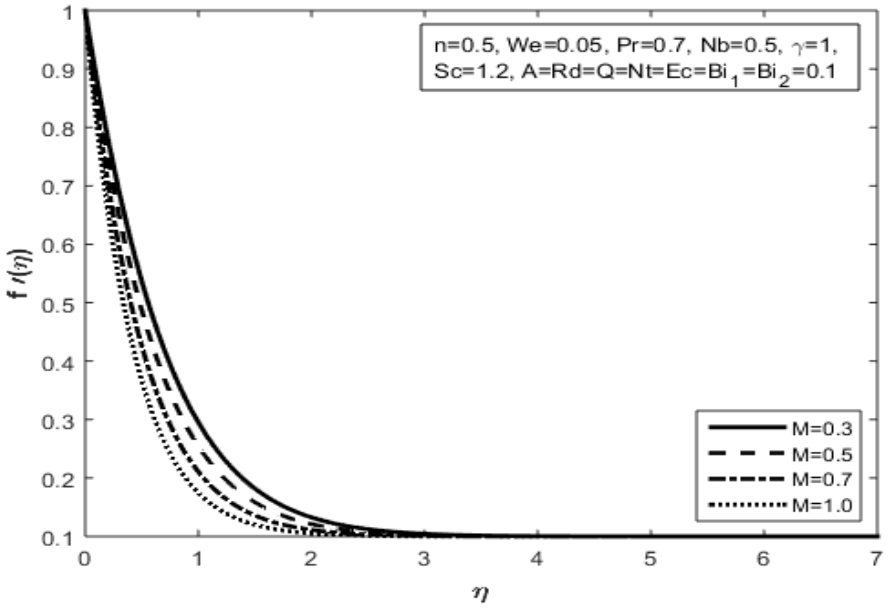

FIGURE 4.10: Effect of M on $f'(\eta)$

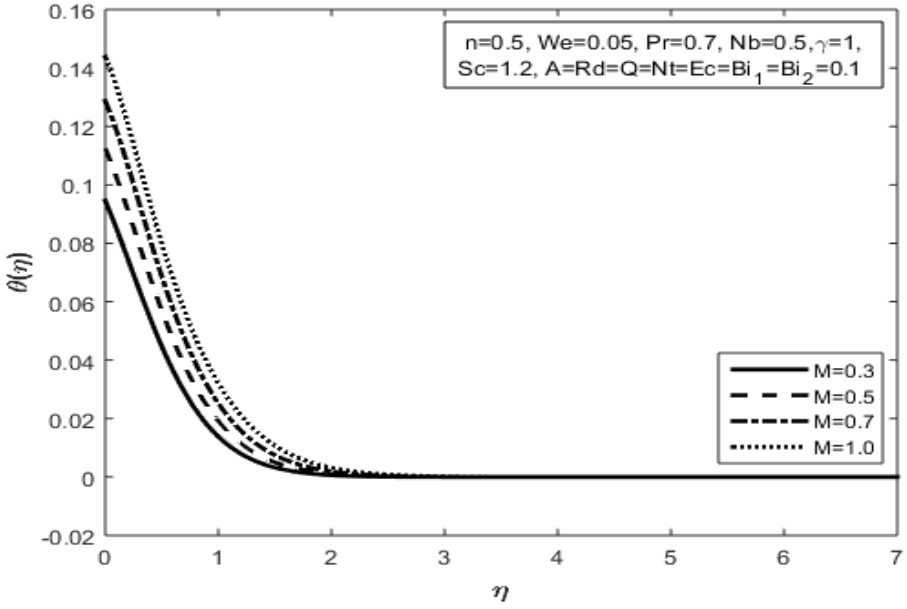

FIGURE 4.11: Effect of M on $\theta(\eta)$

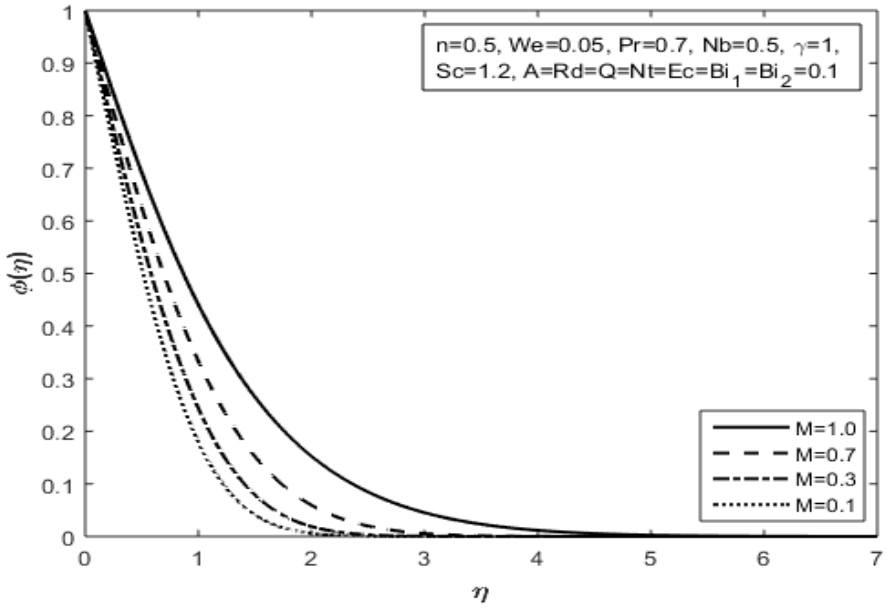

FIGURE 4.12: Effect of M on $\phi(\eta)$

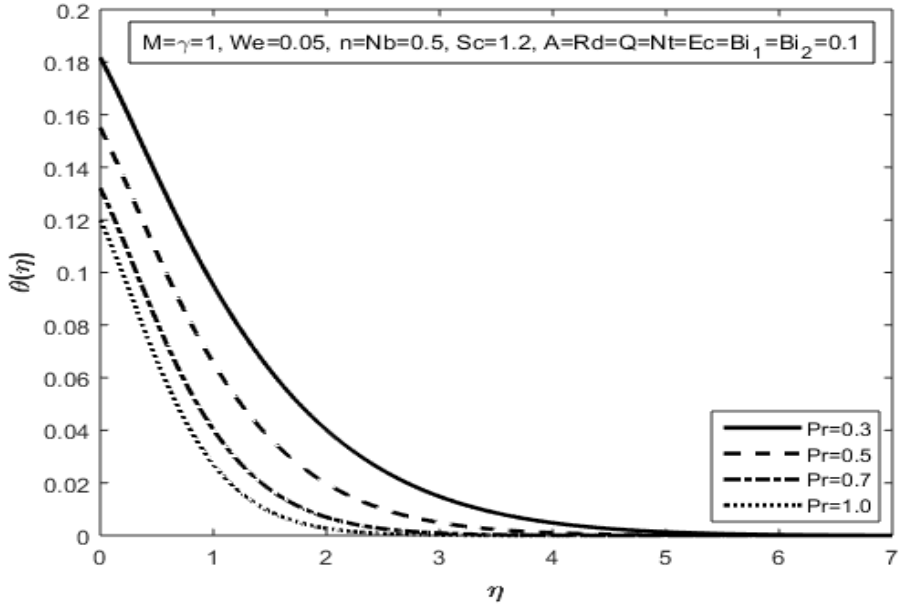

FIGURE 4.13: Effect of Pr on $\theta(\eta)$

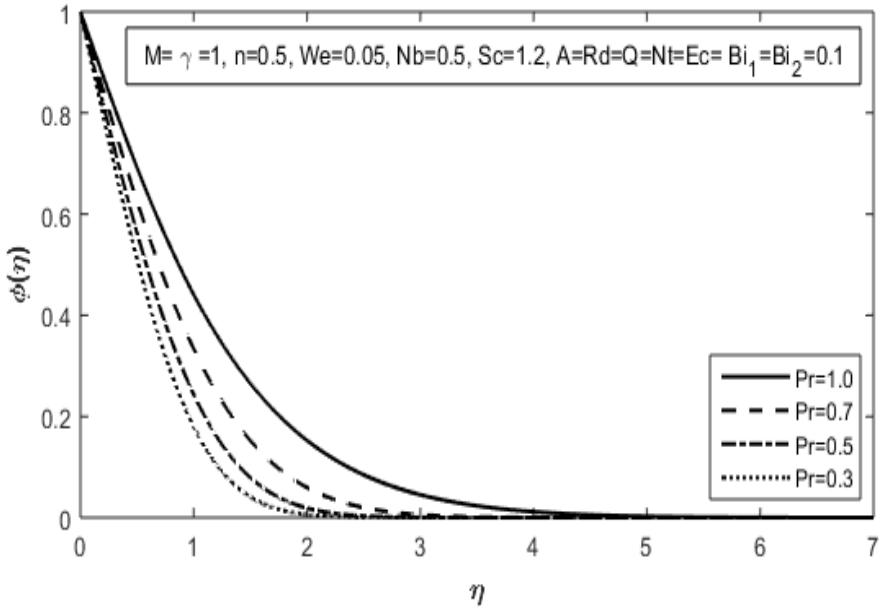

FIGURE 4.14: Effect of Pr on $\phi(\eta)$

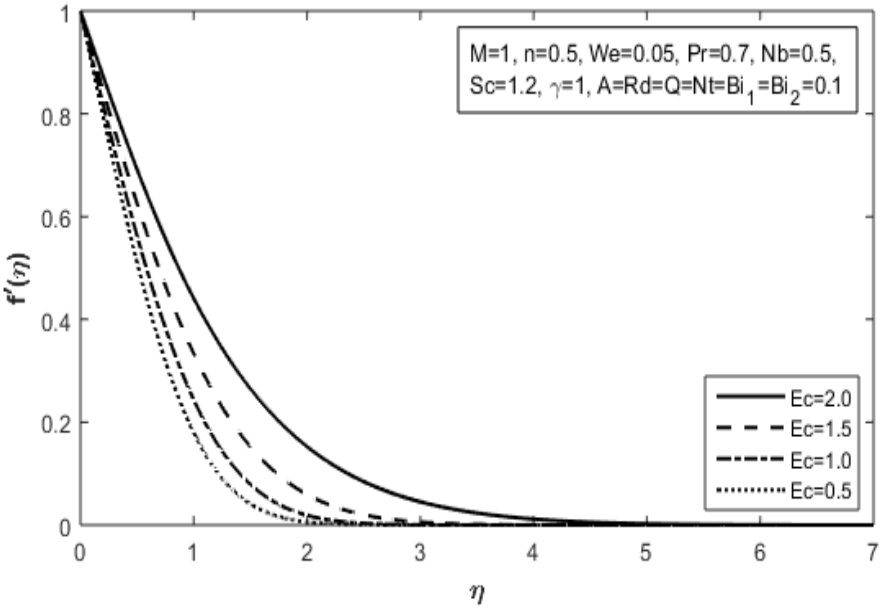

FIGURE 4.15: Effect of Ec on $f'(\eta)$

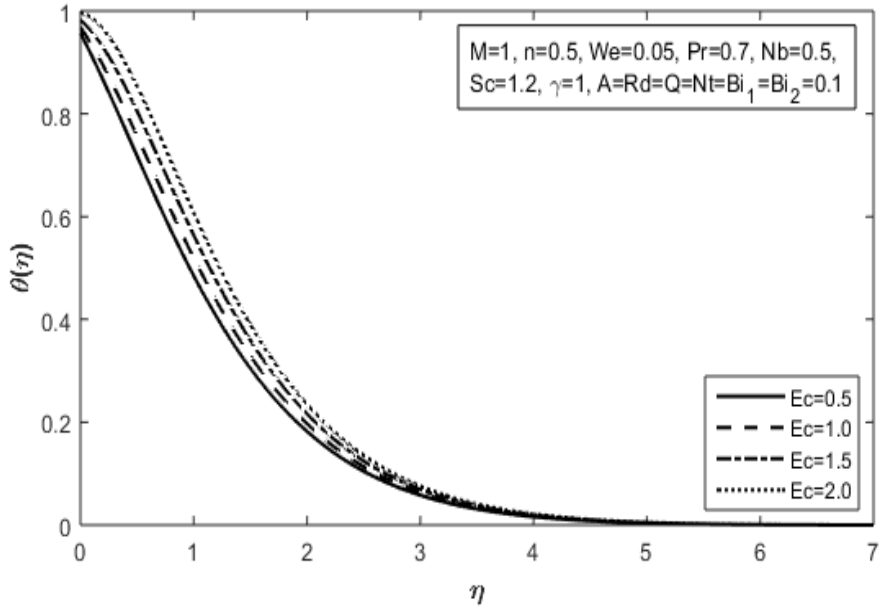

FIGURE 4.16: Effect of Ec on $\theta(\eta)$

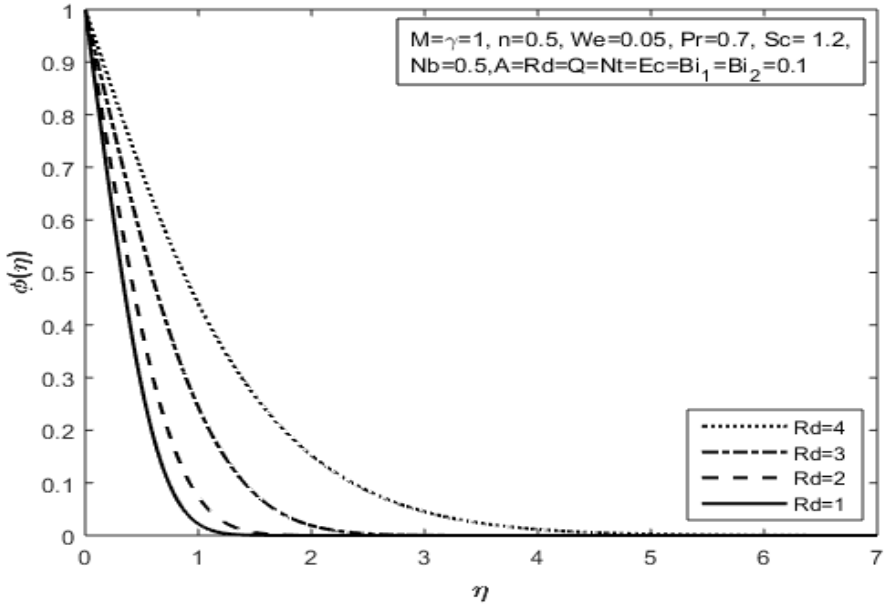

FIGURE 4.17: Effect of Rd on $\theta(\eta)$

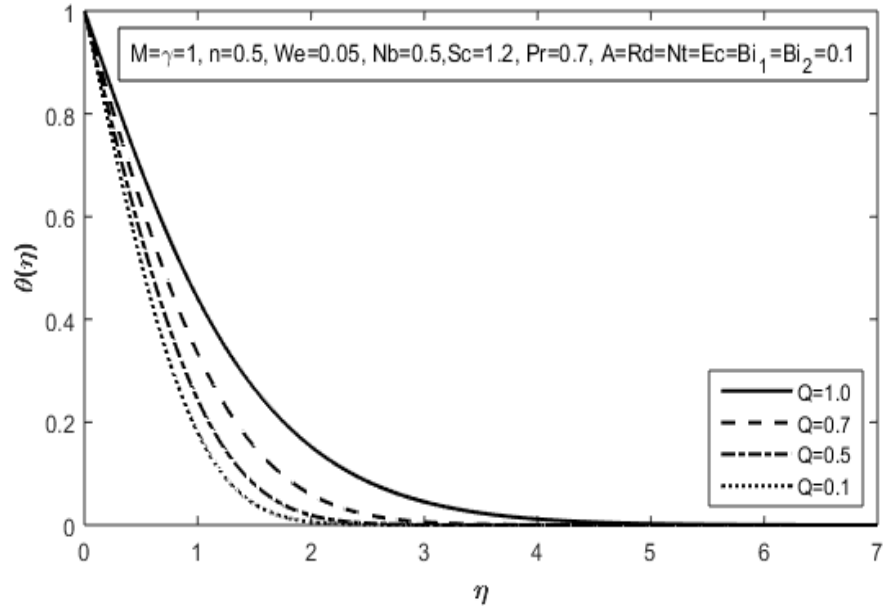

FIGURE 4.18: Effect of Q on $\theta(\eta)$

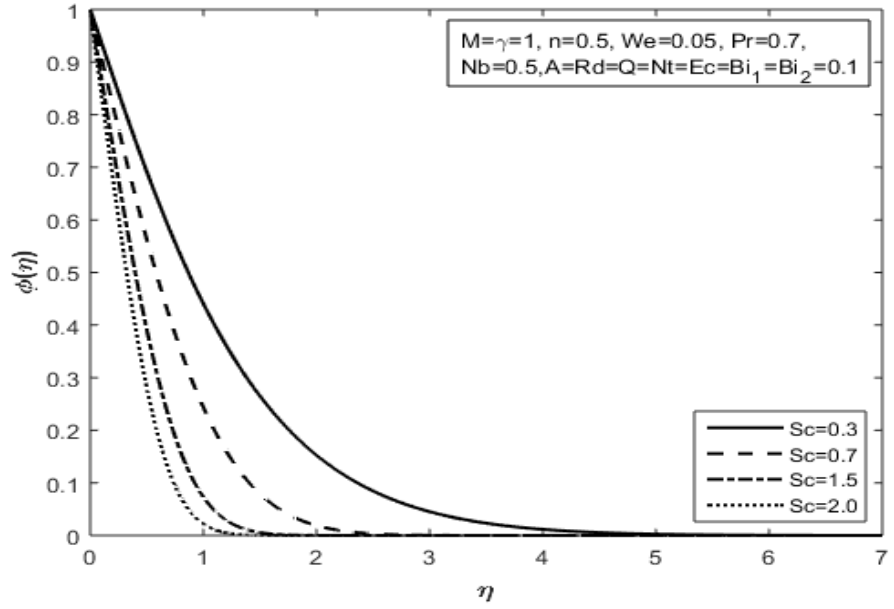

FIGURE 4.19: Effect of Sc on $\phi(\eta)$

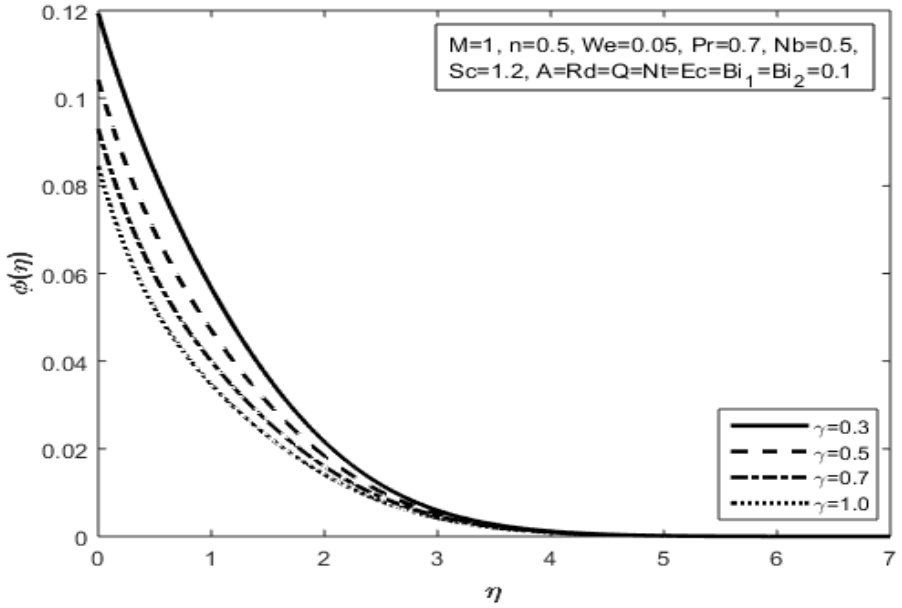

FIGURE 4.20: Effect of γ on $\phi(\eta)$

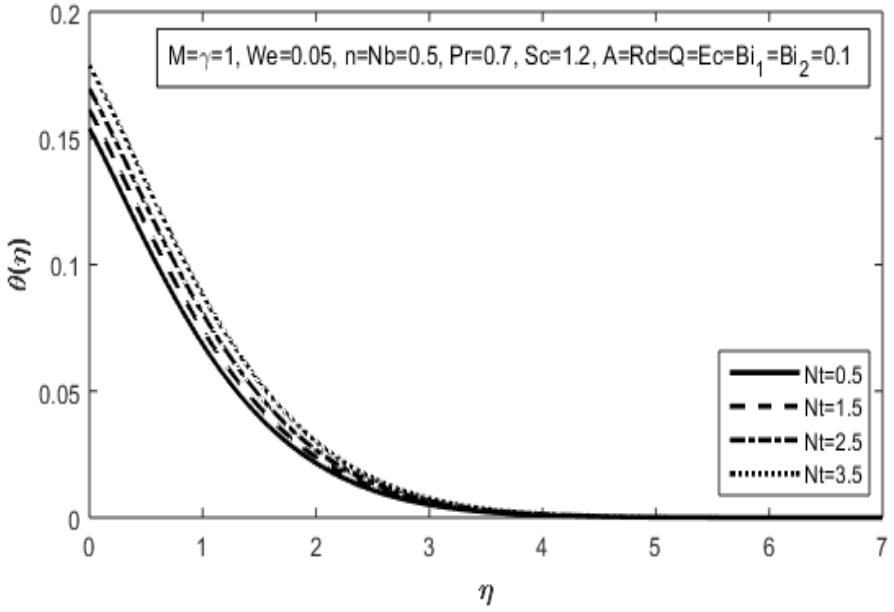

FIGURE 4.21: Effect of Nt on $\theta(\eta)$

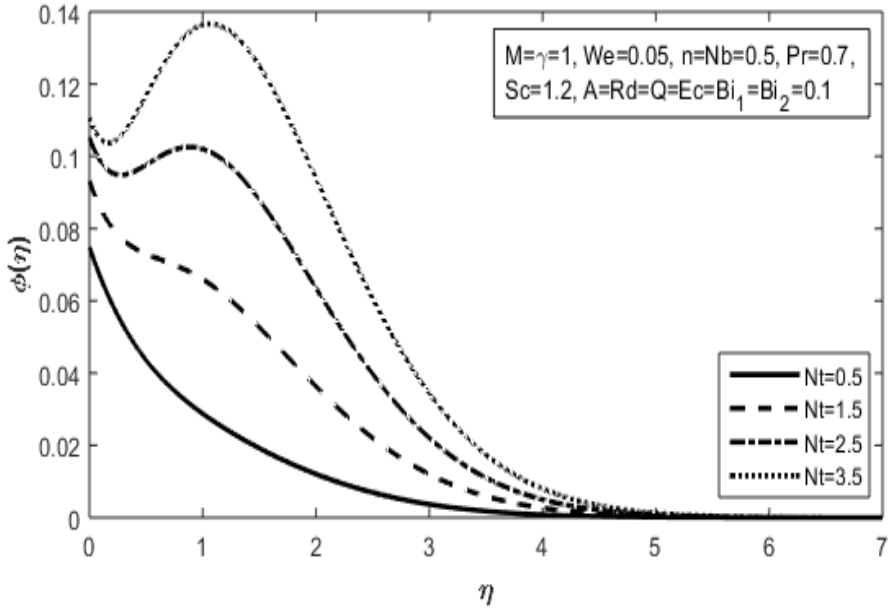

FIGURE 4.22: Effect of Nt on $\phi(\eta)$

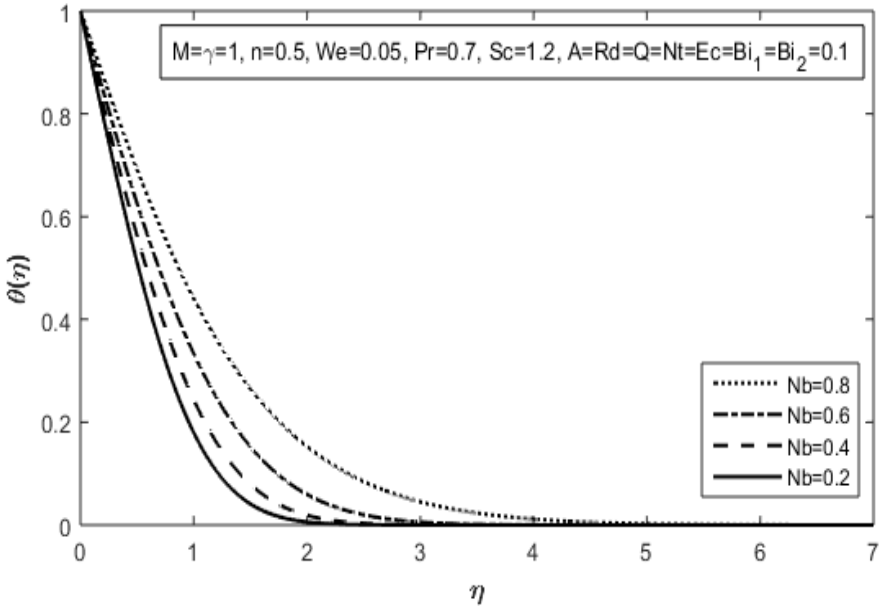

FIGURE 4.23: Effect of Nb on $\theta(\eta)$

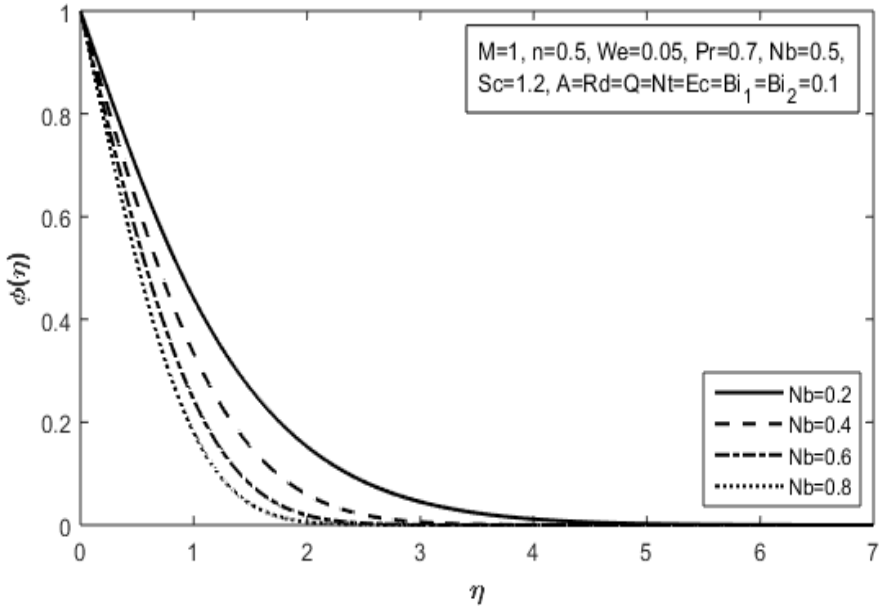

FIGURE 4.24: Effect of Nb on $\phi(\eta)$

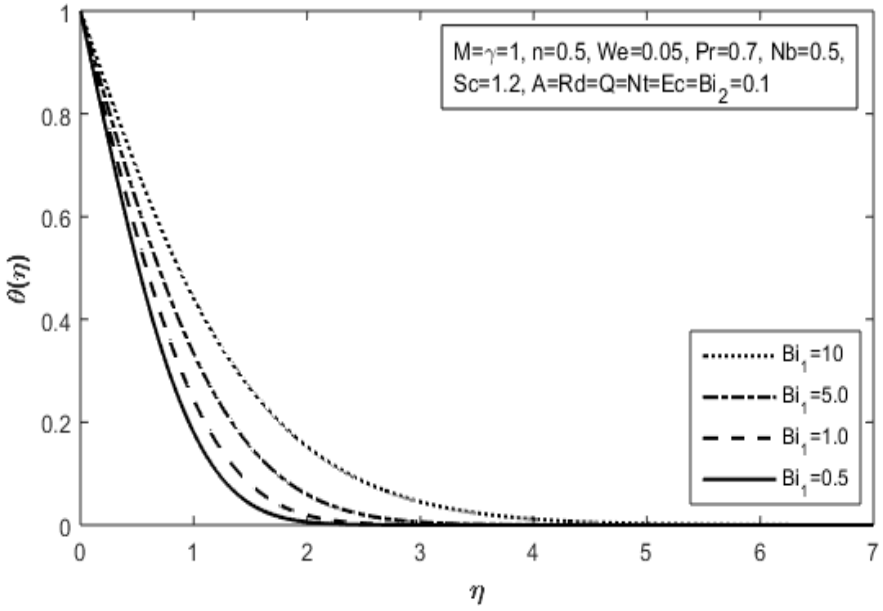

FIGURE 4.25: Effect of Bi_1 on $\theta(\eta)$

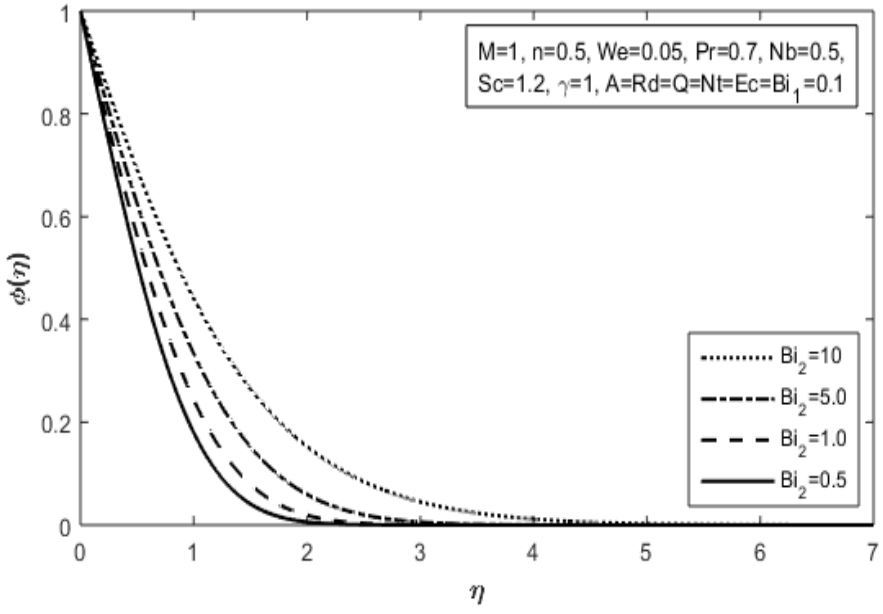

FIGURE 4.26: Effect of Bi_2 on $\phi(\eta)$

Chapter 5

Conclusion

The numerical investigation of the MHD flow nearby a stagnation point over a radially stretching sheet using the Casson and Carreau nanofluids has been presented in this thesis. Moreover, the radiation effects and magnetic field are examined. In additon to this, the effects of heat generation/absorption are also explored. The conversion of non-linear partial differential equations describing the proposed flow problem to a set of ordinary differential equations has been carried out by employing appropriate similarity transformations. The shooting method is employed for the numerical treatment. The impact of pertinent flow parameters on the non-dimensional velocity, temperature and concentration profiles has been illustrated in tabular and graphical forms. The conclusions drawn from the numerical results are summarized below.

- The magnetic parameter decelerates the velocity whereas an opposite trend has been observed for the temperature and concentration fields by considering the Casson fluid. A similar finding has been observed for the Carreau fluid.

- For the Casson fluid, the higher estimation of the Casson parameter escalates the velocity, temperature and concentration profiles.

- The temperature falls whereas the concentration escalates for the larger estimation of the Prandtl number in view of the Casson and Carreau fluids.

- The Eckert number accelerates the velocity and the temperature profile climbs marginally for the Casson fluid. Moreover, An identical outcome has been concluded for the Carreau fluid.

- The heat and mass transfer rates climb significantly as the value of thermophoresis parameter escalates, by considering the Casson and Carreau fluids into account.

- For the Casson and Carreau fluids, the heat transfer rate escalates for the radiation paramter.

Bibliography

[1] R. K. Dash, K. N. Mehta, and G. Jayaraman, "Casson fluid flow in a pipe filled with a homogeneous porous medium," *International Journal of Engineering Science*, vol. 34, no. 10, pp. 1145–1156, 1996.

[2] J. Venkatesan, D. S. Sankar, K. Hemalatha, and Y. Yatim, "Mathematical analysis of Casson fluid model for blood rheology in stenosed narrow arteries," *Journal of Applied Mathematics*, vol. 2013, pp. 1–11, 2013.

[3] T. Hayat, S. A. Shehzad, S. A. Alsaedi, and M. S. Alhothuali, "Mixed convection stagnation point flow of Casson fluid with convective boundary conditions," *Chinese Physics Letters*, vol. 29, no. 11, p. 114704, 2012.

[4] S. Mukhopadhyay, P. R. De, K. Bhattacharyya, and G. Layek, "Casson fluid flow over an unsteady stretching surface," *Ain Shams Engineering Journal*, vol. 4, no. 4, pp. 933–938, 2013.

[5] S. Mukhopadhyay, "Casson fluid flow and heat transfer over a nonlinearly stretching surface," *Chinese Physics B*, vol. 22, no. 7, p. 074701, 2013.

[6] S. Nadeem, R. U. Haq, N. S. Akbar, and Z. Khan, "MHD three-dimensional Casson fluid flow past a porous linearly stretching sheet," *Alexandria Engineering Journal*, vol. 52, no. 4, pp. 577–582, 2013.

[7] A. Khalid, I. Khan, A. Khan, and S. Shafie, "Unsteady MHD free convection flow of Casson fluid past over an oscillating vertical plate embedded in a porous medium," *Engineering Science and Technology, an International Journal*, vol. 18, no. 3, pp. 309–317, 2015.

[8] M. I. Khan, M. Waqas, T. Hayat, and A. Alsaedi, "A comparative study of Casson fluid with homogeneous-heterogeneous reactions," *Journal of Colloid and Interface science*, vol. 498, pp. 85–90, 2017.

[9] Z. Shah, S. Islam, H. Ayaz, and S. Khan, "Radiative heat and mass transfer analysis of micropolar nanofluid flow of Casson fluid between two rotating parallel plates with effects of hall current," *Journal of Heat Transfer*, vol. 141, no. 2, p. 022401, 2019.

[10] T. Hayat, N. Saleem, and N. Ali, "Effect of induced magnetic field on peristaltic transport of a Carreau fluid," *Communications in Nonlinear Science and Numerical Simulation*, vol. 15, no. 9, pp. 2407–2423, 2010.

[11] R. Ellahi, A. Riaz, S. Nadeem, and M. Ali, "Peristaltic flow of Carreau fluid in a rectangular duct through a porous medium," *Mathematical problems in Engineering*, vol. 2012, 2012.

[12] N. S. Akbar, S. Nadeem, and Z. H. Khan, "Numerical simulation of peristaltic flow of a Carreau nanofluid in an asymmetric channel," *Alexandria Engineering Journal*, vol. 53, no. 1, pp. 191–197, 2014.

[13] T. Hayat, F. M. Abbasi, B. Ahmad, and A. Alsaedi, "Peristaltic transport of Carreau-Yasuda fluid in a curved channel with slip effects," *PloS one*, vol. 9, no. 4, p. e95070, 2014.

[14] S. Suneetha and K. Gangadhar, "Thermal radiation effect on MHD stagnation point flow of a Carreau fluid with convective boundary condition," *Open Science Journal of Mathematics and Application*, vol. 3, no. 5, p. 121, 2015.

[15] C. Sulochana, G. P. Ashwinkumar, and N. Sandeep, "Transpiration effect on stagnation-point flow of a Carreau nanofluid in the presence of thermophoresis and Brownian motion," *Alexandria Engineering Journal*, vol. 55, no. 2, pp. 1151–1157, 2016.

[16] M. Khan and M. Azam, "Unsteady heat and mass transfer mechanisms in MHD Carreau nanofluid flow," *Journal of Molecular Liquids*, vol. 225, pp. 554–562, 2017.

[17] M. Waqas, M. Alsaedi, S. A. Shehzad, T. Hayat, and S. Asghar, "Mixed convective stagnation point flow of Carreau fluid with variable properties," *Journal of the Brazilian Society of Mechanical Sciences and Engineering*, vol. 39, no. 8, pp. 3005–3017, 2017.

[18] T. Hayat, I. Ullah, B. Ahmad, and A. A, "Radiative flow of Carreau liquid in presence of newtonian heating and chemical reaction," *Results in Physics*, vol. 7, pp. 715–722, 2017.

[19] T. R. Mahapatra and A. S. Gupta, "Heat transfer in stagnation-point flow towards a stretching sheet," *Heat and Mass transfer*, vol. 38, no. 6, pp. 517–521, 2002.

[20] R. Nazar, N. Amin, D. Filip, and L. Pop, "Stagnation point flow of a micropolar fluid towards a stretching sheet," *International Journal of Non-Linear Mechanics*, vol. 39, no. 7, pp. 1227–1235, 2004.

[21] A. Raptis, C. Perdikis, and H. S. Takhar, "Effect of thermal radiation on MHD flow," *Applied Mathematics and computation*, vol. 153, no. 3, pp. 645–649, 2004.

[22] A. Ishak, Jafar, R. A. Nazar, and L. Pop, "MHD stagnation point flow towards a stretching sheet," *Physica A: Statistical Mechanics and its Applications*, vol. 388, no. 17, pp. 3377–3383, 2009.

[23] N. S. Akbar, S. Nadeem, R. U. Haq, and Z. H. Khan, "Radiation effects on MHD stagnation point flow of nanofluid towards a stretching surface with convective boundary condition," *chinese Journal of aeronautics*, vol. 26, no. 6, pp. 1389–1397, 2013.

[24] R. U. Haq, S. Nadeem, Z. H. Khan, and N. S. Akbar, "Thermal radiation and slip effects on MHD stagnation point flow of nanofluid over a stretching sheet," *Physica E: Low-dimensional Systems and Nanostructures*, vol. 65, pp. 17–23, 2015.

[25] M. Farooq, M. I. Khan, M. Waqas, T. Hayat, A. Alsaedi, and M. I. Khan, "MHD stagnation point flow of viscoelastic nanofluid with non-linear radiation effects," *Journal of molecular liquids*, vol. 221, pp. 1097–1103, 2016.

[26] S. U. S. Choi, "Enhancing thermal conductivity of fluids with nanoparticles," Argonne National Lab., IL (United States), Tech. Rep., 1995.

[27] L. J. Crane, "Flow past a stretching plate," *Zeitschrift für angewandte Mathematik und Physik ZAMP*, vol. 21, no. 4, pp. 645–647, 1970.

[28] K. B. Pavlov, "Magnetohydrodynamic flow of an incompressible viscous fluid caused by deformation of a plane surface," *Magnitnaya Gidrodinamika*, vol. 4, no. 1, pp. 146–147, 1974.

[29] T. Fang and J. Zhang, "Closed-form exact solutions of MHD viscous flow over a shrinking sheet," *Communications in Nonlinear Science and Numerical Simulation*, vol. 14, no. 7, pp. 2853–2857, 2009.

[30] H. I. Andersson, K. H. Bech, and B. S. Dandapat, "Magnetohydrodynamic flow of a power-law fluid over a stretching sheet," *International Journal of Non-Linear Mechanics*, vol. 27, no. 6, pp. 929–936, 1992.

[31] K. Bhattacharyya and G. C. Layek, "Chemically reactive solute distribution in MHD boundary layer flow over a permeable stretching sheet with suction or blowing," *Chemical Engineering Communications*, vol. 197, no. 12, pp. 1527–1540, 2010.

[32] K. Bhattacharyya, "Effects of radiation and heat source/sink on unsteady MHD boundary layer flow and heat transfer over a shrinking sheet with suction/injection," *Frontiers of Chemical Science and Engineering*, vol. 5, no. 3, pp. 376–384, 2011.

[33] H. Tabaei, M. A. Moghimi, A. Kimiaeifar, and M. A. Moghimi, "Homotopy analysis and differential quadrature solution of the problem of free-convective magnetohydrodynamic flow over a stretching sheet with the hall effect and mass transfer taken into account," *Journal of applied mechanics and technical physics*, vol. 52, no. 4, p. 624, 2011.

[34] Y. A. Cengel and J. M. Cimbala, "Fluid mechanics," p. 931, 2006.

[35] S. Molokov, R. Moreau, and H. K. Moffatt, "Magnetohydrodynamics, historical evolution and trends," *Book*, p. p 407, 2006.

[36] D. Lu, M. Ramzan, N. U. Huda, J. D. Chung, and U. Farooq, "Nonlinear radiation effect on MHD Carreau nanofluid flow over a radially stretching surface with zero mass flux at the surface," *Scientific reports*, vol. 8, no. 1, p. 3709, 2018.

[37] C. P. Kothandaraman, "Fundamentals of heat and mass transfer," p. 712, 2006.

[38] J. Kunes., "Dimensionless physical quantities in science and engineering," *Book*, p. p 441, 2012.

[39] H. A. Attia, "Axisymmetric stagnation point flow towards a stretching surface in the presence of a uniform magnetic field with heat generation," *Tamkang J. Sci. Eng.*, vol. 10(1), p. 1116, 2007.